DISSERTATION

PERSISTENT BOVINE VIRAL DIARRHEA VIRUS INFECTION IN THE BOVINE FETUS: MORPHOGENESIS OF SKELETAL LESIONS AND INNATE IMMUNE RESPONSE

Submitted by

Brett Thomas Webb

Department of Biomedical Sciences

In partial fulfillment of the requirements

For the Degree of Doctor of Philosophy

Colorado State University

Fort Collins, Colorado

Summer 2012

Doctoral Committee:

Advisor: Thomas R. Hansen
Co-Advisor: Robert W. Norrdin

Natalia P. Smirnova,
Hana Van Campen
Gary L. Mason

ABSTRACT

PERSISTENT BOVINE VIRAL DIARRHEA VIRUS INFECTION IN THE BOVINE FETUS: MORPHOGENESIS OF SKELETAL LESIONS AND INNATE IMMUNE RESPONSE

Introduction. The effects of transplacental viral infections on the developing fetus are dependent upon complex interactions between feto-placental and maternal immune responses and the stage of fetal development at which the infection occurs. Bovine viral diarrhea virus **(**BVDV) has the ability to cross the placenta and infect the fetus. Infection early in gestation with non-cytopathic (ncp) BVDV leads to persistent infection (PI) due to the development of virus-specific immunotolerance, which results in life-long viremia and detrimental developmental consequences for many organ systems. PI with BVDV has been associated with osteopetrosis, other long bone lesions, and fractures in fetuses and calves. This study was undertaken to characterize the morphogenesis of fetal long bone lesions; determine the effects of PI on biomechanical properties of fetal femora; and delineate the temporal development of the fetal and placental innate immune responses during the establishment of PI.

Materials and Methods. Forty-six BVDV-naïve pregnant Hereford heifers, approximately 18 months old, were inoculated either with non-cytopathic BVDV type 2 containing media or media alone on day 75 of gestation to produce PI and

control fetuses, respectively, which were collected via Cesarean section on the following days of gestation: 82 (peak of maternal viremia), 89 (beginning of maternal seroconversion, acute stage of fetal infection), 97 (Maternal seroconversion and aviremia, fetal viremia), 192 (chronic stage of fetal persistent infection), and 245 (chronic stage of fetal persistent infection, near term).

Results. ***Experiment I: The morphogenesis of fetal skeletal lesions****.* Radiographic and histomorphometric abnormalities were first detected on day 192, at which age PI fetal long bone metaphyses contained focal densities (4/7 fetuses) and multiple, alternating (cyclic) transverse radiodense bands (3/7 fetuses). Day 245 fetuses were similarly affected. Histomorphometric analysis of proximal tibial metaphyses from day 192 fetuses revealed transverse zones with increased calcified cartilage core (Cg.V/BV, %) and trabecular bone (BV/TV, %) volumes in regions corresponding to radiodense bands ($P<0.05$). Numbers of tartrate resistant acid phosphatase positive osteoclasts (N.Oc/BS, #/mm^2) and bone perimeter occupied by osteoclasts (Oc.S/BS, %) were both decreased ($P<0.05$). Mineralizing surface (MS/BS, %), a measure of tissue level bone formation activity, was reduced in PI fetuses ($P<0.05$).

Experiment II: The effect of PI on the biomechanical properties and composition of fetal femora. PI fetuses had femora with smaller mid-diaphyseal diameters and lower cortical porosity than controls. There were no differences between PI and Control fetuses in cortical thickness ratio, ash density nor calcium or phosphorous content; however, cortical thickness ratio decreased with fetal age. Although differences in elastic modulus (PI vs Control and day 192

vs day 245) and ultimate stress (day 192 vs day 245) were identified, cortical thickness ratio largely accounted for these observed differences.

Experiment III: Fetal and Placental innate immune response to PI. Fetal viremia was confirmed starting on day 89. Significant up-regulation of mRNA encoding cytosolic dsRNA sensors - *RIG-I* and *MDA5* - was detected on days 82 -192. Detection of viral dsRNA by cytosolic sensors leads to the stimulation of ISGs, which was reflected in significant up-regulation of *ISG15* mRNA in fetal blood on days 89, 97, and 192. No difference in *IFN-*α and *IFN-*β mRNA concentration was found in fetal blood or caruncular tissue, while a significant increase in both *IFN-*α and *IFN-*β mRNA was seen in cotyledons from PI fetuses on day192.

Conclusions. It is concluded that PI with BVDV induces cyclic abnormal trabecular modeling, which is secondary to reduced numbers of osteoclasts. The factors responsible for these temporal changes are unknown but may be related to the time required for osteoclast differentiation from precursor cells. However, fetal infection with BVDV did not significantly impair inherent biomechanical properties of fetal bone but rather resulted in decreased periosteal apposition rates, which manifest as altered cortical geometry. Differences in cortical geometry disproportionally affect the error associated with calculation of stress and strain by classical beam theory equations and, therefore, critical assumptions necessary for use of these equations are not satisfactorily met when comparing samples differing solely in mid-diaphyseal diameter. Furthermore, fetuses respond to early gestational ncp BVDV infection by

induction of the type I IFN pathway, resulting in chronic up-regulation of ISGs. Cotyledonary tissue contributes to up-regulation of ISGs by increased production of IFNs. The innate immune response might partially curtail viral replication in PI fetuses, but is unable to eliminate the virus in the absence of a virus-specific adaptive immune response.

ACKNOWLEDGEMENTS

I would like to acknowledge my advisors, Thomas Hansen and Robert Norrdin, and my graduate committee members, Natalia Smirnova, Hana Van Campen and Gary Mason for the investment of time each has given in order to teach me how to perform research, publish findings and attain funding. I thank each of you for your considerable contributions to my education and professional development over the past years. Lastly, I would like to thank my wife Teckla.

DEDICATION

This dissertation is dedicated to Dr. Robert W. Norrdin who not only cultivated my interest in skeletal pathology but has been kind enough to share his vast knowledge of the field with me.

TABLE OF CONTENTS

LIST OF KEYWORDS

Biomechanical, Bone, Bovine viral diarrhea virus, Cattle, Fetus, Immune response, Interferon, Persistent infection, Placenta, Transplacental exposure, Viruses.

CHAPTER I.

LITERATURE REVIEW

Introduction

BVDV, a small (12.5 kb genome) positive sense RNA virus, is a member of the genus *Pestivirus* in the Family *Flaviviridae.* Since its discovery in the late 1940s, BVDV has become the most economically important viral disease of cattle with monetary losses to the U.S. cattle industry exceeding $400 million annually (Fray et al., 2000a; Gunn et al., 2004; Houe, 1999). BVDV has arguably received more attention in terms of research effort than any single disease agent affecting cattle. A recent PubMed search, using the term “bovine viral diarrhea” revealed more than 3,400 manuscripts devoted to understanding the impact, pathogenesis, epidemiology and control of BVDV. In nature, BVDV occurs as two biotypes: noncytopathic (ncp) and cytopathic (cp). Ncp strains are exceedingly more common, likely due to their ability to cause persistent infection (PI) in contrast to cytopathic strains, which lack this ability.

Historical Perspectives

A novel disease of cattle, later proven to be caused by infection with BVDV, was first described in 1946 by two individual groups working independently (Childs, 1946; Olafson et al., 1946). The two reports appear to describe the same disease although the morbidity and mortality differed widely

between the reports. Olafson et al. (1946) reported that most animals within a given herd, irrespective of age were affected but only 3-4 % of those died (Olafson et al., 1946). In contrast Childs (1946) reported that only a few, primarily young animals were affected and most cases appeared to be fatal (Childs, 1946). While this discrepancy certainly could be due to differences in BVDV strain virulence it is also possible that most of the acute infections were asymptomatic, and thus went unnoticed by Childs (1946) or that herds evaluated by these two groups differed significantly in the number of PI animals leading to increased incidence of fatal mucosal disease in the cases described by Childs (1946) and thus explaining the reported differences in mortality and morbidity. It is clear, in retrospect, that both of these reports contain descriptions of two similar but distinct manifestations of BVDV infection, both viral diarrhea and animals which presented with severe disease grossly characterized by mucosal erosions and ulcers causing the latter condition to be dubbed mucosal disease by Ramsey and Chivers in 1953 (Ramsey, 1953). Although a viral etiology was strongly suspected (Olafson et al., 1946) initial isolates of BVDV were noncytopathic strains and thus undetectable in cell culture. Cytopathic variants were later isolated in 1957 (Underdahl, 1957). Viruses obtained from animals with viral diarrhea and those obtained from cases of mucosal disease were shown to be similar serologically, and produced diarrhea in experimentally infected animals, however neither virus was able to reproduce fatal mucosal disease (Gillespie, 1961).

The presence of abortions in many BVDV outbreaks in both the USA and Great Britain lead to the suspicion that BVDV was capable of transplacental infection resulting in abortion (Dow, 1960; Olafson et al., 1946). Although the relationship between BVDV and abortion was formally hypothesized in 1968 (Kahrs, 1968) it was not confirmed until fetal infection was reproduced experimentally (Caraso, 1971; Kahrs, 1973). Investigation of transplacental infection and the effects of such infection on the developing fetus would lead to considerable progress in understanding the pathogenesis of mucosal disease and BVDV epidemiology.

From experimental fetal infections it became clear that the result of transplacental infection was determined by the stage of gestation in which the infection occurred; infection early in gestation lead to abortion or stillbirth, infection late in gestation lead to precolostral seropositive fetuses which outwardly appeared normal, whereas when infection occurred prior to 120 days of gestation the virus persisted postnatally (Malmquist, 1968; Thompson, 1963). These initial studies lead to the discovery of PI; the mechanism which enabled fetuses to become PI (immunotolerance) was documented along with an important observation that only immunotolerant, PI fetuses developed mucosal disease (Leiss, 1974). Although significant progress in understanding the pathogenesis of BVDV and the effect on the developing fetus was made in the subsequent decade, the etiology of mucosal disease remained elusive until it was reproduced experimentally by Brownlie et al in 1984 (Brownlie, 1984).

The Pathogenesis of Transplacental Infection

The pathogenesis of transplacental BVDV infection has been an area of consistent study since the original transplacental infection studies (Caraso, 1971; Kahrs, 1973) performed in the early 1970s. The effects of transplacental infection, particularly PI, on developing fetuses include lesions in the musculoskeletal (brachygnathia, growth arrest lines, growth retardation lattices, osteopetrosis; reviewed in CHAPTER II and CHAPTER III) (Constable et al., 1993; Espinasse, 1986; Nuss et al., 2005; O' Connor, 1993; O'Toole, 2006; Scruggs, 1995; Webb et al., 2012), integumentary (hypotrichosis, alopecia, perivascular dermatitis) (Brown, 1975; Larsson, 1991), ocular (microphthalmia, cataracts, retinal degeneration, optic neuritis) (Brown, 1975), cardiopulmonary (pulmonary hypoplasia, myocarditis), and immune systems (thymic aplasia and atrophy, pulmonary lymphoid hyperplasia), although those within the central nervous system (cerebellar hypoplasia, hydrancephaly, hydrocephalus, hypomyelinogenesis, mircoencephaly) have been studied much more extensively (Bielefeldt-Ohmann, 1995; Brock, 2004; Montgomery, 2008; Ridpath, 2010).

Transplacental infection of the fetus occurs almost exclusively in seronegative cattle as maternal antibodies are effective in preventing establishment of virus in the fetoplacental unit (Brownlie et al., 1998). There is considerable variation in the manifestation of transplacental infection which appears to be caused by variations in biologic properties of the virus (pathogenicity), biotype, and stage of gestation at time of infection (Kelling, 2007) and only ncpBVDV are capable of causing PI (Brownlie et al., 1989; Coria and

McClurkin, 1978; Harding et al., 2002). There is controversy surrounding the mechanism and route by which BVDV reaches the fetus. Historically, infection of the placenta was thought be a prerequisite for fetal infection (Caraso, 1971) and has been offered as an explanation for the apparent resistance of early term (<30 Days) fetuses to infection because the placenta is not well formed at this stage (Whitmore, 1981). However, work by Fredriksen et al. (1999) suggests that virus reaches the fetus via the hematogenous route and that infection of the placenta therefore occurs in a 'retrograde' manner (Fredriksen, 1999).

During acute infection of susceptible cattle, maternal viremia is evident beginning at 2 days post infection (Kelling, 2007) and peaks at 7 days post infection (Smirnova et al., 2008). Viral RNA and antigen does not appear in the fetus until around 14 days post maternal infection (Fredriksen, 1999); Chapter IV, Figure 14) which precedes antigen in the placenta by 2-8 days. Given the ruminant epitheliochorial placental structure (Leiser and Kaufmann, 1994; Leiser et al., 1997), direct hematogenous spread of virus to the fetus during maternal viremia would require either the virus itself or resultant maternal immune response to induce placental damage sufficient to cause mixing of maternal and fetal blood or alternatively, employ a specialized viral strategy that would mediate efficient viral transport across the placenta. To date there is no indication that the latter occurs. Purportedly, lesions in the placentomes following experimental infections of cattle are minor in nature or absent (Done et al., 1980; Kendrick, 1971). This contrasts sharply with the moderate to severe, often necrotizing placentitis caused by inoculation of pregnant ewes (Parsonson, 1979; Snowdon,

1975) and goats (Lamm et al., 2009) with bovine BVDV strains. The expedience with which BVDV reaches the ovine fetus (~72 hours) (Swasdipan et al., 2002) may suggest that in the case of cattle, placental damage, albeit not severe or potentially not even evident on the light microscopic level, is sufficient to enable hematogenous spread of BVDV to the bovine fetus.

The acute phase of PI with BVDV has received relatively less attention than the pathogenesis of acute BVDV infection in postnatal animals which closely mirror that of transient infections in late term fetuses. In the acute phase of PI, following hematogenous spread of virus to the fetus, there is evidence that vimentin positive (mesenchymal) cells, possibly endothelial cells, are the primary site of virus replication (Fredriksen, 1999). Not surprisingly these virus infected cells occur in organs that filter large quantities of blood, the liver and lung (Fredriksen, 1999). Initial viral infection of these cells is followed by virus dissemination in CD45 positive mononuclear cells, likely cells of the monocyte-macrophage linage, to nearly all organs including the intestine, brain, spleen and thymus (Bielefeldt-Ohmann et al., 2012; Bielefeldt-Ohmann et al., 2008; Fredriksen, 1999). The mechanism of transplacental spread of virus to the fetus of PI dams appears to differ slightly (Fredriksen et al., 1999).

Fetal viremia peaks sometime between 22 days and 119 days post maternal infection and then appears to decrease considerably later in the stage of PI (~120 days post maternal infection) and stabilize until term (CHAPTER IV, Figure 14). The exact reason for the decline in the level of viremia is unclear but may be related to a partially effective innate immune response (CHAPTER IV).

Subtle microscopic lesions within the vasculature occur in the brain of infected fetuses as early as 14 days post maternal infection (Bielefeldt-Ohmann et al., 2012) and within the long bone metaphysis (21 days post maternal infection) (Webb et al., 2012), but florid histologic and gross lesions do not appear until much later in the stage of infection (~120 day post infection) when lesions of the central nervous system (microcavitation, etc) and skeletal system (described in Chapter II) are predominate findings (Bielefeldt-Ohmann, 1995; Bielefeldt-Ohmann et al., 2012; Bielefeldt-Ohmann et al., 2008; Montgomery, 2008; Webb et al., 2012). Although a plethora of lesions have been associated with transplacental infection with BVDV many are difficult to reproduce experimentally (cerebellar hypoplasia) (Bielefeldt-Ohmann, 1995).

There appears to be not only considerable differences in the manifestations of infection between ncpBVDV strains but also considerable differences within controlled experimental infections using the same virus strain. Most importantly, there is little understanding of the molecular mechanisms responsible for a majority of these lesions given that the infecting viral strain is noncytopathic in nature and reportedly is quite successful in preventing apoptosis in infected cells (Schweizer and Peterhans, 2001; Zhang et al., 1996). Certainly one possibility is that the mechanism of injury is immunologically mediated and with the lack of a measurable adaptive immune response may suggest that the innate immune response to PI may be responsible (reviewed in CHAPTER IV). A single mechanism is also unlikely to be responsible as reduced cellular function in virus infected cells likely contributes as well (Kaariainen, 1984).

The fetal immune response to PI and the exact mechanisms surrounding the development of immunotolerance have been subjects of debate and research efforts concentrated on these subjects have given rise to additional questions that further underscore the lack of current understanding. Since the first description of immunotolerance to BVDV, following maternal infection prior to (~120 days) (Leiss, 1974), numerous studies have added to our understanding of the underlying mechanisms (Collen and Morrison, 2000; Coria and McClurkin, 1978). It has been shown that PI animals have complete T cell tolerance to the infecting virus strain which is highly specific in nature such that the animal can respond to the virus when a mutation results in a change of only one amino acid (Collen and Morrison, 2000).

Complete T cells tolerance should ablate any T cell dependent antibody production, however the question remains whether or not an attenuated B cell response leads to antibody production in PI animals. BVDV specific antibodies are however present in a subset of PI cattle which strongly suggests that BVDV-specific antibody production occurs (Collins, 1999). One study documented co-localization of BVDV antigen and immunoglobulin, consistent with immune complexes, deposited within the germinal centers of PI lymph nodes, suggesting that antibody is produced (Fray et al., 2000b). Other explanations for antibody production would entail placentitis resulting in crossover of maternal antibody or generation of virus quasispecies. The latter explanation is more attractive given the reported absence of placental lesions following transplacental infection and the presence of antibody in older PI animals (Collins, 1999; Done et al., 1980;

Fredriksen, 1999; Kendrick, 1971). Apparently BVDV suffers from genomic instability arising from a multitude of different mechanisms which result in recombination (Meyers et al., 1992), point mutations (Hamers et al., 2001), deletions, duplications and recombination with host mRNA (Meyers and Thiel, 1996). Production of viral quaisispecies may be the end result of these events and it has been proposed that quasispecies differing antigenicly from the original infecting strain are the impetus for antibody production in PI animals (Collins, 1999).

Although our understanding of the immunology of PI has dramatically increased over the past few decades adequate explanations for the ability of ncpBVDV to cause PI have proven elusive. Certainly immunotolerance to the infecting strain is central to this mechanism, but additional pestivirus specific characteristics must be involved to explain why other viruses, such as Blue tongue virus, Akabane, Wesselsbron virus (also a Flavivirus), Bovine herpesvirus 1, and Bovine parvovirus, which are capable of causing transplacental infection in early gestation do not result in PI to those viruses. Inhibition of type I interferon production by ncpBVDV has been implicated as one of the major mechanisms responsible (Peterhans et al., 2003; Schweizer et al., 2006) but there is evidence that refutes this hypothesis (Shoemaker et al., 2009; Smirnova et al., 2008) (CHAPTER IV).

Postnatal effects of transplacental infection

The postnatal effects of transplacental infections have received relatively little attention and a majority of the work has focused on PI animals (Houe, 1993; Loneragan et al., 2005). The results of these studies compellingly show a predisposition to comorbid disease and increased mortality in PI cattle (Houe, 1993; Loneragan et al., 2005). Numerous factors have been suggested to explain this including reduced microbial killing ability and chemotaxis (Welsh et al., 1995), inhibition of interferon production (Schweizer and Peterhans, 2001), and overall reduced cellular function (Kaariainen, 1984). Interestingly, fetuses infected after approximately 120 days of gestation and born seropositive to BVDV, had a two-fold increase in risk of serious calfhood diseases (Muñoz-Zanzi et al., 2003). Many if not all of the mechanisms/factors hypothesized to be responsible for 'immune deficits' in PI animals hinge on the presence of BVDV itself and therefore are clearly inappropriate to explain the similar postnatal effects observed in fetuses transiently infected with BVDV, which clear the virus *in utero*. Muñoz-Zanzi et al. (2003) clearly show that the potential impact, on an individual animal basis, of transient transplacental infections (incidence 9.6%) far surpass the impact of PI (0.5%). Thus, from a production standpoint, even by eliminating PI animals, approximately 10% of the herd could still have a predisposition to disease. The potential economic impacts on the cattle industry are immense. While the mechanisms responsible for the postnatal health effects of transplacental BVDV infection are not known, the condition bares striking resemblance to developmental immunotoxicities associated with *in utero*

exposure to various compounds including dexamethasone (Dietert et al., 2003), lead (Bunn et al., 2001) and others. The postnatal effects of transplacental infection with BVDV are consistent with the fetal origins of adult disease hypotheses first put forth by Barker (Barker, 1994). Work in the last decade strongly suggests that epigenetic dysregulation is the mechanism underlying the postnatal effects of in utero fetal insults. There is a small body of evidence to suggest that fetal epigenetic dysregulation occurs in transplacental BVDV infections (APPENDIX IV), and it is plausible that it is responsible for the postnatal health effects.

The underlying purpose of the subsequent experiments was to investigate the acute, subacute and chronic stages of PI with BVDV in an attempt to understand: 1) how this disease results in skeletal lesions, 2) whether such lesions lead to impaired structural integrity of long bones, and 3) the nature of the fetal and placental innate immune responses to PI.

CHAPTER II.

BOVINE VIRAL DIARRHEA VIRUS CYCLICALLY IMPAIRS LONG BONE TRABECULAR MODELING IN EXPERIMENTAL PERISISTENTLY INFECTED FETUSES

Introduction

BVDV (genus *Pestivirus*, Family *Flaviviridae*) is taxonomically divided into BVDV1 and BVDV2 genotypes, both of which contain cytopathic (cp) and noncytopathic (ncp) biotypes (Gillespie, 1960; Hamers et al., 2001; Ridpath et al., 1994). The majority of BVDV infections, regardless of infecting strain type, result in asymptomatic infections that largely go undetected. While acute infections can occur with either biotype, infection with a ncp strain of BVDV, regardless of genotype, appears to be a prerequisite for persistent infection (PI) of the fetus (Brownlie et al., 1989; Coria and McClurkin, 1978; Harding et al., 2002).

NcpBVDV, by virtue of its ability to cross the placenta and infect the fetus at any stage of gestation, has been associated with a myriad of different manifestations including early embryonic death, abortion, fetal PI, and congenital abnormalities (Bielefeldt-Ohmann, 1995; Done et al., 1980; Duffell et al., 1984). The fetal consequences of transplacental infection appear to be primarily determined by the age of the fetus at the time of infection, although other factors such as the pathogenicity of the infecting virus strain and the immune and health status of the dam may contribute (Brock, 2003). Transplacental infection of the

fetus by ncpBVDV prior to adaptive immune system development, which occurs during the second and third trimester of gestation, is thought to enable PI and life long viral shedding by the animal due to development of highly virus-specific, T cell tolerance to the infecting strain (Collen and Morrison, 2000).Transplacental infection of the fetus after adaptive immune system development (beyond ~ day 150) results in acute infection, fetal seroconversion to the infecting viral strain, and clearance of the virus (Done et al., 1980). PI animals are of particular epidemiologic significance in that they represent the reservoir of virus in the population and are responsible for perpetuation of the virus through infection of herd mates (Houe, 1999).

There are only a few published investigations of naturally occurring fetal and neonatal skeletal lesions associated with BVDV infection (Nuss et al., 2005; O' Connor, 1993; Scruggs, 1995). A multitude of different terms, from osteopetrosis to growth arrest lines, has been used in the literature to describe the morphologic character of skeletal lesions associated with BVDV infections. Experimentally produced fetal bone lesions were first described by Done et al. (1980) as simple growth arrest lines detected by radiography, but the distribution and histologic character were not described (Done et al., 1980). Another experimental infection, using the same viral strain used herein, noted thickening of the femoral cortices in PI fetuses (Smirnova et al., 2008). In one study, a majority of BVDV positive fetuses had fetal femora with multiple transverse zones of radiodensity in the metaphysis corresponding to growth retardation lattices,

focal radiodensities corresponding to areas of retained secondary spongiosa, and reduced mid-diaphyseal diameter (O' Connor, 1993).

Growth retardation lattices differ from simple growth arrest lines not only in morphologic character but also in the processes responsible for their development (O' Connor, 1993; Thompson, 2007). While both lesions occur in regionally extensive areas parallel to the physis, growth arrest lines are composed of increased bone volume with enhanced trabecular connectivity and result from impaired longitudinal growth of the physis and normal bone formation (Thompson, 2007). In contrast, growth retardation lattices are composed of increased calcified cartilage core volume, typically resulting from impaired resorption of calcified cartilage (Thompson, 2007). Nuss et al. (2005) reported a case of transient benign osteopetrosis in a newborn calf PI with BVDV in which long bone metaphyses contained multiple regularly spaced, thick, transverse bands of radiodensity, which resolved radiographically by 5 months of age (Nuss et al., 2005). Although the term osteopetrosis has been used to describe skeletal lesions associated with BVDV (Nuss et al., 2005; Scruggs, 1995), it is probably more appropriately reserved for genetic diseases which result in diffuse, rather than zonal or cyclic, metaphyseal changes. In the previously mentioned case, BVDV antigen was detected by immunohistochemistry in osteoblasts, osteocytes and other bone marrow hematopoietic cells after necropsy at 13 months (Nuss et al., 2005). Unfortunately the presence or absence of BVDV antigen in osteoclasts was not described.

Thus far, the reported lesions have been largely limited to the long bone metaphyses and have ranged from barely discernible growth arrest lines and growth retardation lattices, to diffuse and zonal retention of secondary and/or primary spongiosa resembling the lesions of genetic osteopetroses of cattle (Done et al., 1980; Nuss et al., 2005; O' Connor, 1993; Scruggs, 1995; Thompson, 2007). The morphogenesis of these lesions and the mechanisms responsible for their development is unclear. Reduced bone and calcified cartilage core resorption would be the direct explanation, but contributions of other potential processes including enhanced bone formation or physeal abnormalities leading to the production of thickened primary spongiosa have not been investigated. Reduced bone resorption due to decreased numbers of osteoclasts, resulting from direct effects of virus on osteoclasts or osteoclast precursor cells as well as secondary effects of viral infection on such cells by production of interleukin 1 (IL-1) inhibitors have been suggested as possible molecular mechanisms (Scruggs, 1995). Reduced osteoclast numbers have been documented in naturally infected calves with skeletal lesions associated with BVDV, however no age-matched controls were available for appropriate comparisons (Scruggs, 1995). Decreased osteoclast numbers have been found in lambs experimentally infected *in utero* with Border disease virus (Caffrey, 1996), a closely related Pestivirus of sheep, further lending support to the contention that these cells or their precursors may be selectively damaged by intrauterine pestiviral infections. Taken collectively most of the previous studies were limited by either uncertainty in the time and course of infection, infection

status (whether subject was persistently or transiently infected) and/or by small numbers of affected animals (Done et al., 1980; Nuss et al., 2005; O' Connor, 1993; Scruggs, 1995).

This study was undertaken to characterize the morphogenesis of long bone lesions over the course of experimentally induced fetal PI with BVDV in an attempt to determine the processes and mechanisms responsible for the development of these lesions.

Materials and Methods

Infection and General Growth Parameters

All animal experiments were approved by Colorado State University's Institutional Animal Care and Use Committee. Forty-six yearling Hereford heifers weighing between 295 and 430 kg were artificially inseminated with semen from a single Angus bull after estrus synchronization. Pregnancy was detected on day 35 and confirmed on day 70 of gestation. All heifers were seronegative for BVDV type 1 and type 2 prior to infection. Heifers were group-housed in outdoor pens. On day 75 of gestation, heifers (n=23) were inoculated intranasally with either 2 ml of α-MEM media containing 4.4 $\log_{10}$TCID50 ncpBVDV type 2 strain 96b2222 (Van Campen et al., 2000), or α-MEM media alone (n=23) to produce PI and control fetuses respectively, as previously described (Smirnova et al., 2008). Maternal infection was confirmed by detection of viral RNA in peripheral blood leukocytes on day 7 post infection by using semi-quantitative real time PCR (qt-RT-PCR) as previously described (Smirnova et al., 2008), and by the presence of

serum neutralizing anti-BVDV2 antibodies on day 28 post infection as previously described (Saliki et al., 1997). Control heifers remained negative for viral RNA and seronegative throughout the study.

Eight fetuses, four infected and four controls, were collected by cesarean section on days 75, 82, 97, 192, and 245 of gestation. Six heifers, (3 infected and 3 controls) received an intravenous injection of 9 mg/kg oxytetracycline (LA-200, Pfizer Animal Health, Exton, PA, USA) on day 175 and again on day 185 of gestation to flurochrome label bone formation for dynamic histomorphometry. Fetuses from these heifers were removed via cesarean section on day 192. Metaphyseal elongation rates for the proximal tibia were calculated from mid-frontal sections of flurochrome-labeled fetuses. These calculations were performed by measuring the length, in four equidistant locations, of the unlabeled spongiosae subjacent to the physis and dividing the average length by the time period (7 days) between administration of the second label and collection. Body, liver, heart, lung, kidney, spleen, thymus, adrenal, and thyroid weights as well as crown-rump lengths and heart girths were recorded. One PI fetus was lost due to abortion on day 230 of gestation.

Radiography

Fetal bones were dissected free of extraneous soft tissues and digital radiographs were produced using a portable X-ray machine set (MinXray, Northbrook, IL, USA) and a digital plate system (Elikin, Carlsbad, CA, USA). Care was taken to precisely align limbs in the same position for these

radiographs. Epiphyseal and mid-diaphyseal widths and physeal to physeal length of the femur, tibia, humerus and radius were obtained from the radiographs, which contained an internal measurement standard, using Imagepro® software (MediaCybernetics, Bethesda, MD, USA). Measured parameters that differed between PI and control fetuses were confirmed by manual measurement with dial calipers.

Histology

Bones were dissected free of soft tissues, fixed in 10% buffered formalin and cut on an ISOMET bone saw (Beuhler, Ltd Lake Bluff, IL, USA) to yield anatomically standardized midfrontal sections of the proximal tibial metaphysis. The sections were decalcified in 5% formic acid (Sigma, St. Louis, MO, USA) over a period of 3-7 days depending on the fetal age, before being routinely processed and paraffin embedded. Five μm thick sections were prepared on a rotary retracting microtome and stained with hematoxylin and eosin. Serial, five μm thick sections were incubated in 0.2 M Tris-HCL, pH 9.0, solution at 37°C for 30 minutes to reactivate acid phosphatases (Liu, 1987), then stained with a commercial kit (Sigma, St. Louis, MO, USA) to detect cells expressing Tartrate-resistant Acid Phosphatase (TRAP). In addition to quantitative histology this approach facilitated qualitative evaluation of osteoclasts for evidence of active resorption in Howship's lacunae and number of nuclei per osteoclast as well as signs of degeneration or apoptosis.

Immunohistochemistry was performed on formalin fixed, non-decalcified,

paraffin embedded sections to avoid potential adverse effects of the decalcifying agent on viral antigen and to exactly duplicate the tissue processing utilized for positive and negative control tissues. Spleen and thymus from day 192 control and PI fetuses served as negative and positive control tissues. The combined effect of small, approximately 1 cm^2, samples of metaphyseal bone and the low degree of mineralization of fetal bone at this location facilitated the production of high quality histologic sections using routine paraffin embedding and sectioning on a rotary microtome utilizing disposable blades. The mouse monoclonal anti-BVDV clone 15C5 (IDEXX Laboratories, Westbrook, Maine, USA) was used as previously described (Ellis, 1998), and staining was visualized with a Vector Elite kit (Vector Laboratories, Burlingame, CA, USA) as per manufacturer's recommendations. Antigen retrieval was performed with 20 μg/ml Proteinase K (Promega, Madison, Wisconsin, USA).

Formalin-fixed, facing sections of tibia that were produced during the initial bone sectioning were embedded in glycol methacrylate as previously described and sectioned on a bone saw (Maruto, Tokyo, Japan) (Huffer, 1994). The resulting non-decalcified semi-thin sections were ground down to 30 μm thickness for assessment of formation parameters. Femoral mid-diaphyseal cross sections were prepared by embedding the sample in Sample- Kwick® (Beuhler, Ltd Lake Bluff, IL, USA) and sectioning on an IsoMet® saw (Beuhler, Ltd Lake Bluff, IL, USA). The resulting sections were ground down to 100 μm thickness.

Histomorphometry

Tibial sections were divided into four zones of interest as illustrated in Figure 1. The zones were designed such that the subphyseal zone would entirely encompass the primary spongiosa, which was found to not exceed 2 mm in length. The subjacent three zones were then determined by dividing the remaining metaphysis equally in thirds.

Histomorphometric analysis of static parameters was performed manually using a modified Mertz grid reticle at a standardized magnification (200x) in a tissue area of 4 mm^2 from the central portion of each zone. Histomorphometric analysis of dynamic parameters was performed on a Nikon E 800 fluorescent microscope (Melville, NY, USA) equipped with an UV filter, using Imagepro® software, in a 15 mm^2 area of interest from the central portion of middle and distal zones. The subphyseal and proximal zones were not analyzed for dynamic parameters due to the complete lack of labeling and predominance of diffuse labeling, respectively. The definition of the parameters evaluated, their corresponding referents, standardized nomenclature, units of measurement and criteria for evaluation, where applicable, are listed below: Bone volume - trabecular bone volume including calcified cartilage cores normalized to tissue volume (BV/TV, %); cartilage volume - longitudinal calcified cartilage core volume normalized to bone volume (Cg.V/BV, %); total bone surface (BS, mm^2); number of osteoclasts (TRAP positive) per mm^2 bone surface (N.Oc/BS, #/ mm^2); osteoclast surface - TRAP positive osteoclast-covered bone surface normalized to bone surface (Oc.S/BS, %); single labeled surface - area of bone surface with

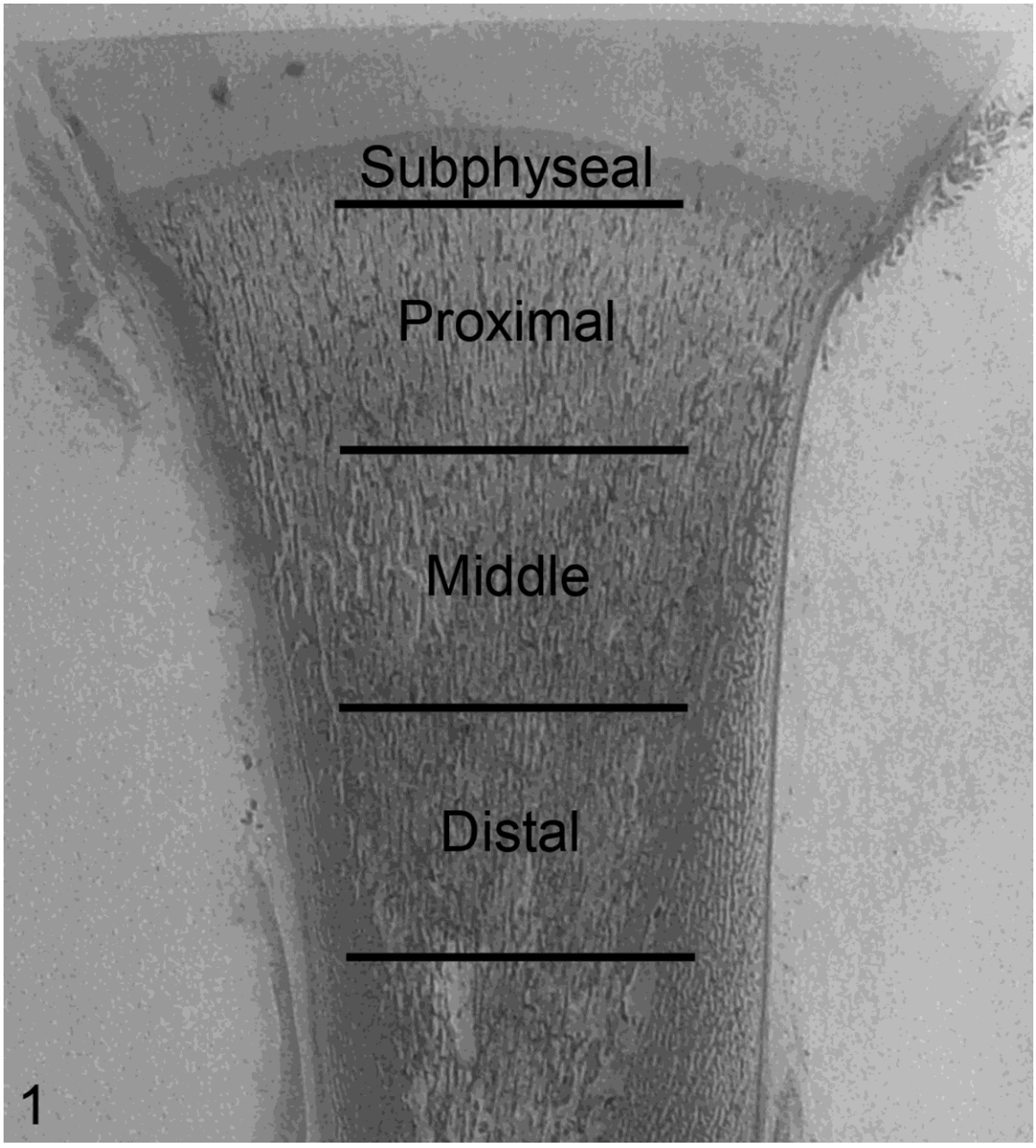

Figure 1. Proximal tibial metaphysis; Bovine fetus, 192 days of gestation. Subdivision of the proximal tibial metaphysis into zones for histomorphometry. The subphyseal zone extends 2 mm distal from the physeal-metaphyseal junction. All other zones are 7 mm in proximal to distal length. (H&E).

a single flurochrome label normalized to bone surface (s.LS/BS, %); double labeled surface - area of bone surface with two labels normalized to bone surface (d.LS/BS, %); mineralizing surface - equal to ½ the area of single labeled surface plus the area of double labeled surface normalized to bone surface (MS/BS, %); mineral apposition rate - average distance between first and second label divided by the number of days in the interlabel period, (MAR, μm/day); and bone formation rate - equal to the mineralizing surface normalized to bone surface multiplied by the mineral apposition rate (MS/BS *MAR, mm^3/mm^2/day).

Femoral mid-diaphyseal apposition rates were determined by averaging the width of non-labeled subperiosteal plexiform bone at five standardized sites and dividing this distance by the time period (7 days) between administration of the second label and collection. Hematopoietic cell density was determined by measuring the proportion of marrow space occupied by such cells. Proximal tibia physeal histomorphometry was performed on decalcified day 192 section to determine whether there were differences between PI and control fetuses in the volume and number of calcified cartilage cores being incorporated into primary spongiosae. The areas occupied by chondrocyte lacunae and by matrix in the hypertrophic zone were determined in a 4 mm^2 area and expressed as a ratio. The number of chondrocyte columns per transverse mm of physeal width was determined along the central most 1 cm aspect of the physis. All bone histomorphometry nomenclature, units, and calculations are consistent with current recommendation for standardization (Parfitt, 1987).

Statistical analysis

Data were compared using Student's t-test or Mann-Whitney test depending on the result of Shapiro-Wilk test for normality. Differences at $P < 0.05$ were considered significant, while differences at $P < 0.10$ are described as tendencies. Data are presented as mean $\pm$ standard deviation.

Results

Infection and General Growth Parameters

Fetal PI was confirmed by qt-RT-PCR for BVDV RNA and immunohistochemical staining for BVDV antigen (Table 1). Fetuses from the PI group on day 82 as well as control fetuses from all collection days were negative for BVDV RNA and antigen. 2 out of 4 PI fetuses on day 89 were positive for BVDV antigen. However, one PI fetus tested positive for BVDV RNA by qtRT-PCR (due to the technical difficulties in sample collection). All PI fetuses from days 97-245 were BVDV positive by both methods.

Crown-rump length, weight, heart girth and major organ weights did not differ between PI and control fetuses on any of the collection days (data not shown). The fetal sex distribution by infection status was: day 192 control (3 male, 4 female), day 192 PI (2 male, 5 female), day 245 control (2 male, 2 female), day 245 PI (3 male, 0 female). There was no statistically significant effect of fetal sex on any of the study parameters reported from day 192 fetuses. The effect of sex on study parameters for day 245 could not be determined due to the lack of female fetuses in the PI group. On days 192 and 245 there was an

enhanced waisting or fluting of the metaphysis in PI femora characterized by similar physeal widths and reduced mid-diaphyseal outer diameter compared to controls (Table 2). This indicated that lateral appositional growth of the physis was not significantly impaired by PI. In mid-diaphyseal cross sections neither cortical thickness nor total cortical area divided by cortical diameter differed between the groups (Table 2). Day 192 PI fetuses had slower rates of periosteal apposition at this site than control fetuses, 23.6 μm/day ± 4.7 versus 35.9 μm/day ± 4.9 respectively.

Table 1. Presence or absence of radiographic lesions within the tibial metaphyses and infection status of PI fetuses.[a]

Gestational age, fetus number	Radiodense transverse bands	Focal radio-densities	qtRT-PCR/IHC for BVDV[b]
89 Days			
1	–	–	+/+
2	–	–	[c]/+
3	–	–	[c] /–
4	–	–	[c] /–
97 Days			
1	–	–	+/+
2	–	–	+/+
3	–	–	+/+

4	–	–	+/+
192 Days			
1	+	–	+/+
2	+	–	+/+
3	+	+	+/+
4	–	+	+/+
5	–	+	+/+
6	–	+	+/+
7	–	–	+/+
245 Days			
1	+	–	+/+
2	+	–	+/+
3	–	–	+/+

[a] Day 82 fetuses from PI group as well as control fetuses from all time points were negative for virus. Controls did not have any radiographic lesions.

[b] qt-RT-PCR for BVDV RNA in umbilical cord blood and BVDV antigen in brain as previously described (Bielefeldt-Ohmann et al., 2012).

[c] Umbilical cord blood was only successfully obtained from 1 fetus at this time point.

Table 2. Femoral dimensions from control and PI fetuses.[a]

Gestational age, group	Number of Fetuses	Mid-diaphyseal outer diameter (mm)	Cortical thickness (mm)	Overall length (mm)	Distal physeal width (mm)
Day 82, Control	4	0.21 ± 0.01	N/A	1.95 ± 0.04	0.64 ± 0.01
Day 82, PI	4	0.19 ± 0.01	N/A	1.90 ± 0.05	0.63 ± 0.01
Day 89, Control	4	0.23 ± 0.01	N/A	2.31 ± 0.03	0.74 ± 0.03
Day 89, PI	4	0.23 ±0.02	N/A	2.28 ± 0.03	0.71 ± 0.02
Day 97, Control	4	0.26 ± 0.01	N/A	2.77 ± 0.10	0.91 ± 0.03
Day 97, PI	4	0.28 ± 0.01	N/A	2.85 ± 0.08	0.94 ± .02
Day 192, Control	7	13.4 ± 0.34	3.51 ± 0.53	109 ± 2.40	34.7 ± 1.29
Day 192, PI	7	12.2 ± 0.50[b]	3.41 ± 0.42	107 ± 2.53	33.6 ± 1.46
Day 245, Control	4	21.9 ± 0.93	3.19 ± 0.74	173 ± 3.95	53.6 ± 0.91
Day 245, PI	3	18.6 ± 0.71[b]	3.4 ± 0.90	170 ± 2.65	54.8 ± 2.44

[a]Mean ± standard deviation (mm). [b]Difference from control ($P < 0.01$). N/A - there is no definition of cortical thickness at days 82-97.

Radiography

Radiographs of the axial skeleton, skull, and limbs were taken at each time of collection. No radiographic abnormalities were detected prior to day 192, after which they were limited to the long bones of the appendicular skeleton. Relative development of secondary and tertiary centers of ossification did not differ between PI and control fetuses. Radiographs of 6 out of 7 day 192 PI fetuses contained metaphyseal lesions. These consisted of focal densities in 4 out of 7 fetuses and multiple, transverse radiodense bands in 3 out of 7 fetuses (Figure 2, 3). Within the metaphysis the distribution of the focal densities appears to be random although they were most frequently identified within the distal femur and proximal tibia metaphyses. Radiographs of day 245 fetal metaphyses had similar bands of alternating radiodensity in 2 out of 3 PI fetuses (not shown). There was marked variation amongst PI fetuses in lesion severity, which ranged from lesions easily appreciable to barely discernible lines. The distribution of such lesions between individuals differed very little. The most commonly affected metaphyses were distal radius, proximal tibia, distal femur, and proximal metacarpal/metatarsal. Radiographic lesions were not observed in the scapula or phalanges.

Metaphyseal elongation rates from day 185 to day 192 did not differ between PI (250 ± 30 μm/day) versus control (310 ± 50 μm/day) fetuses and were utilized to approximate the periods of time between the transverse bands in fetuses, which had easily discernable transverse bands as shown in Figure 3. Acknowledging the non-linear nature of long bone growth during the period of lesion development (day 97-192),

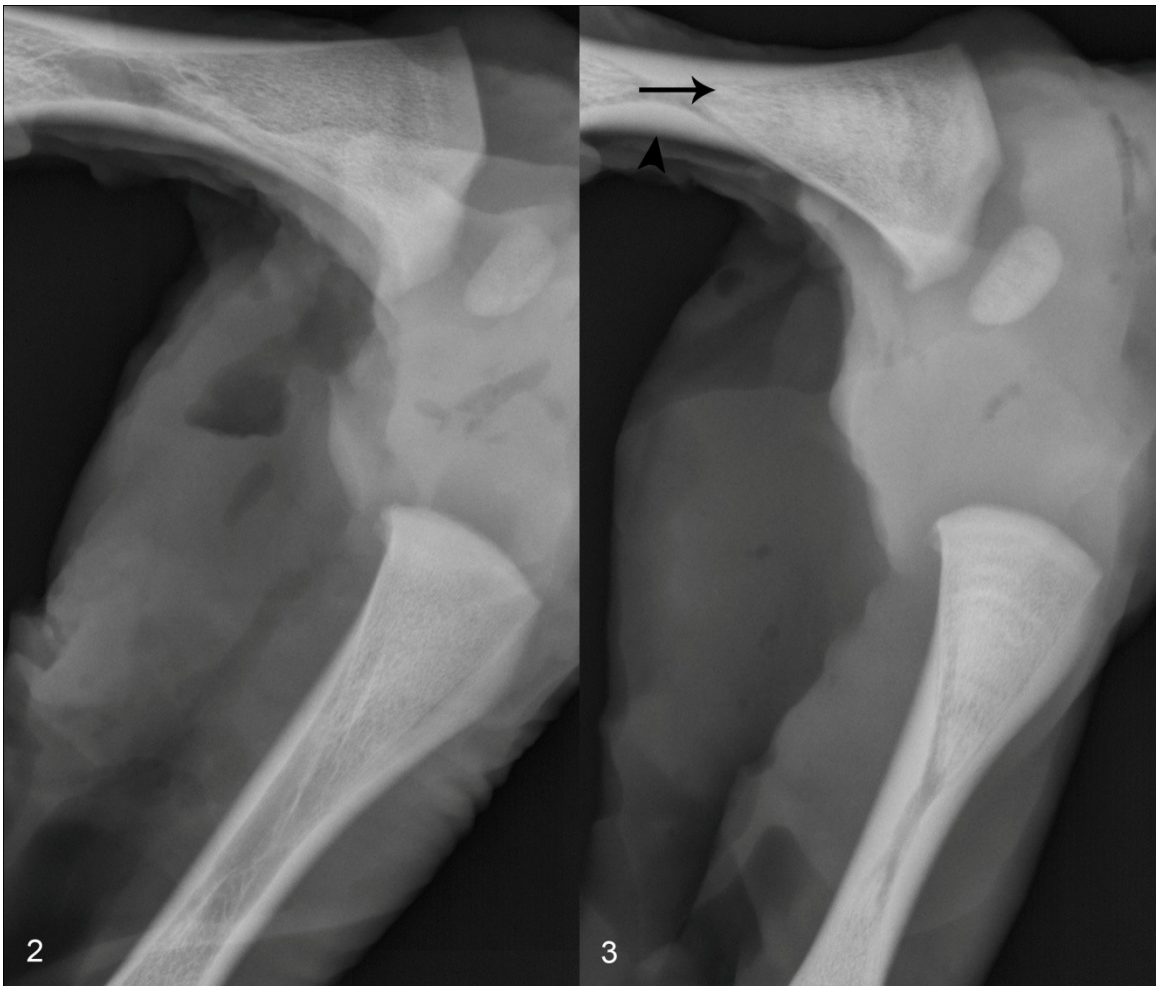

Figure 2. Femur, Tibia; Control bovine fetus, 192 days of gestation. Normal radiographic appearance of femur and tibia in control fetus. (Digital Radiograph).

Figure 3. Femur, Tibia; PI bovine fetus, 192 days of gestation. The distal femoral and proximal tibial metaphyses contain multiple transverse bands of increased radiodensity and focal radiodensity (arrow). Also note the reduced femoral mid-diaphyseal diameter compared to control (Figure 2) (arrowhead). (Digital Radiograph).

bands of radiodensity were on average approximately 3-4 mm in width and would reflect an approximately 15 day period of growth separated by periods of 15 days or greater

between the bands.

Histology and Histomorphometry

Histologic lesions and histomorphometric abnormalities were not detected prior to day 192, although day 97 PI fetuses had similar bone and calcified cartilage volumes, they tended to have fewer TRAP positive osteoclasts (N.Oc/BS, #/mm^2) within the proximal tibia metaphysis this was not statistically significant (data not shown, $P < 0.10$). Overall the histologic lesions in PI fetuses were subtle and characterized by regionally extensive transverse areas of increased trabecular bone volume with increased amounts of longitudinal cartilage core volume and focally extensive areas of increased transverse connectivity between trabeculae (Figure 4-7), the former feature radiographically corresponded to the radiodense transverse bands and the latter to the focal radiodensities. There was no difference in hematopoietic cell density between PI and control fetuses (data not shown). Immunohistochemical staining for BVDV in day 192 fetal bone sections failed to demonstrate any viral antigen within osteoclasts or bone forming cells (data not shown).

Histomorphometric parameters from the proximal tibial metaphyses of day 192 fetuses are detailed by zone in Table 3. Analysis by zone demonstrated increased bone volume within the middle and distal zones of PI tibia as well as increased cartilage core volume within the distal zone. Within the proximal zone, there were decreased numbers of TRAP positive osteoclasts and reduced TRAP positive osteoclast surface (OC.S/BS, %) in PI tibia.

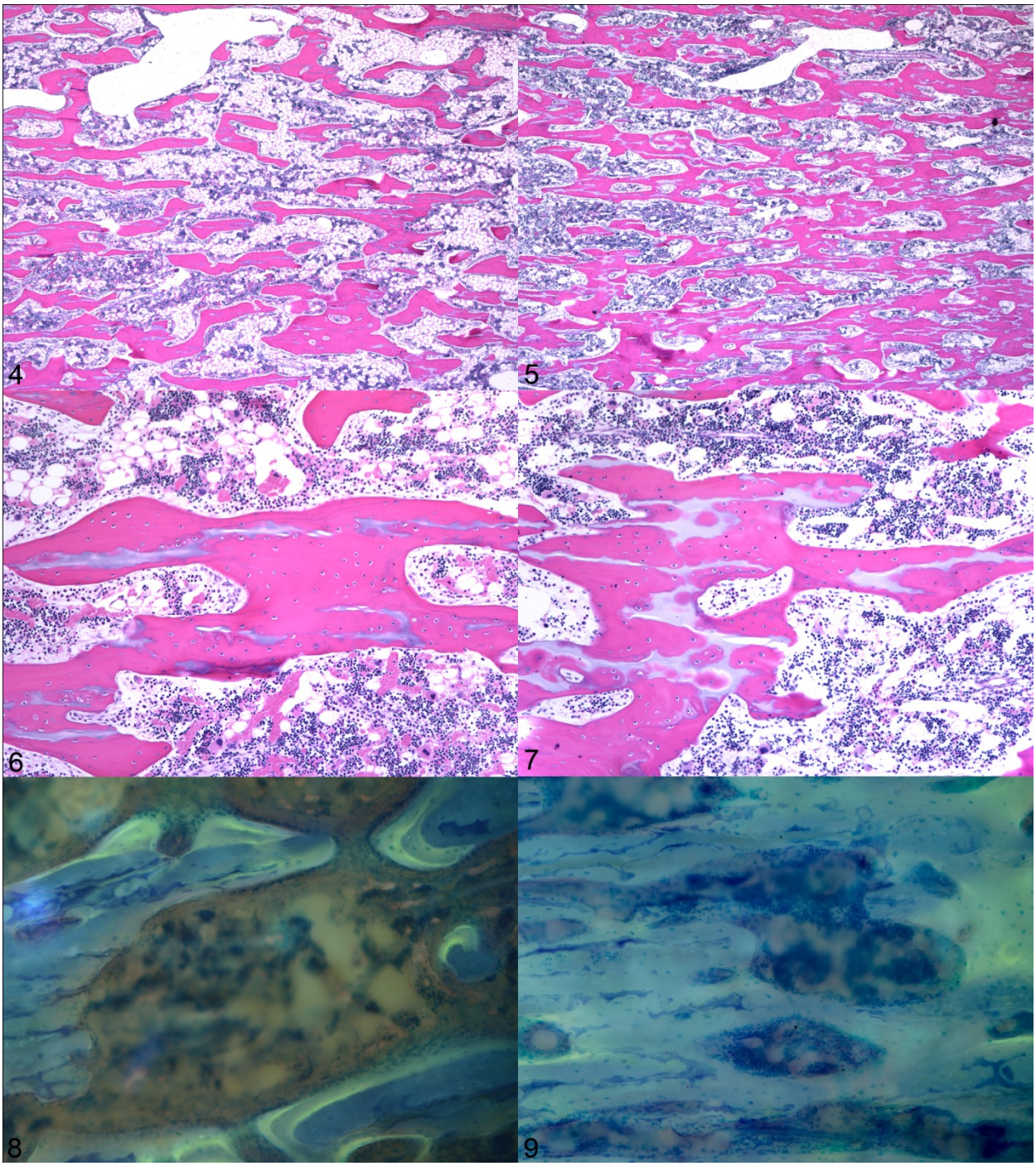

Figure 4. Proximal tibial metaphysis; Control bovine fetus, 192 days of gestation. Normal trabecular bone volume in control fetus. (H&E).

Figure 5. Proximal tibial metaphysis; PI bovine fetus, 192 days of gestation. There is increased volume of trabecular bone compared to control (Figure 4). (H&E).

Figure 6. Higher magnification photomicrograph of Figure 4. Normal volumes of longitudinal cartilage cores and trabecular bone in control fetus. (H&E).

Figure 7. Higher magnification photomicrograph of Figure 5. The volume of longitudinal cartilage cores is increased relative to the volume of trabecular bone compared to control. (H&E).

Figure 8. Proximal tibial metaphysis; Control bovine fetus, 192 days of gestation. Normal flurochrome labeling (thin, single and double greenish-gold lines) in control fetus. (Giemsa stained, oxytetracycline labeled, undecalcified, 30 μm thick ground sections under UV light).

Figure 9. Proximal tibial metaphysis; PI bovine fetus, 192 days of gestation. There is markedly reduced extent of flurochrome labeling (thin, single and double greenish-gold lines) compared to control (Figure 8). (Giemsa stained, oxytetracycline labeled, undecalcified, 30 μm thick ground sections under UV light).

Table 3. Static histomorphometric parameters from proximal tibia metaphysis of day 192 Control and PI fetuses by zone.[a]

Zone	Subphyseal		Proximal		Middle		Distal	
	Control	PI	Control	PI	Control	PI	Control	PI
Bone Volume, BV/TV (%)	25.4 ± 3.4	24.0 ± 2.8	30.4 ± 5.0	28.7 ± 5.8	33.1 ± 6.1	39.9 ± 3.6[b]	34.2 ± 8.2	45.2 ± 10.0[b]
Cartilage Volume, Cg.V/BV(%)	53.2 ± 11.9	54.9 ± 8.4	19.0 ± 4.8	21.3 ± 6.0	14.3 ± 4.7	15.9 ± 4.5	13.3 ± 4.6	21.0 ± 4.0[c]
Number of Osteoclast, N.Oc/BS (#/mm^2)	0.35 ± 0.13	0.34 ± 0.06	0.26 ± 0.09	0.14 ± 0.09[b]	0.10 ± 0.08	0.05 ± 0.05	0.08 ± 0.05	0.04 ± 0.05
Osteoclast Surface, Oc.S/BS (%)	19.6 ± 12.0	11.8 ± 2.8	15.3 ± 6.5	7.0 ± 5.4[b]	4.4 ± 4.5	3.1 ± 3.8	4.0 ± 2.7	2.0 ± 2.7

[a]Mean ± standard deviation (N = 7 Control, N = 7 PI). [b]$P < 0.05$. [c]$P < 0.01$.

Collectively, when all zones were pooled and evaluated as one zone of interest, PI tibia had increased bone volume and cartilage core volume with decreased number of TRAP positive osteoclasts and TRAP positive osteoclast surface. Qualitatively, osteoclasts from PI tibia were present both within deep Howship's lacunae and on crenated surfaces and did not differ in morphologic character or number of nuclei per osteoclast to those from control tibia. Histologic features of degeneration, necrosis, or apoptosis were not identified in osteoclasts or hematopoietic cells at any time point evaluated. In the evaluation of the physis at its junction with the metaphysis there were no differences in the mean number of chondrocyte columns per transverse mm of physeal-metaphyseal junction, 24.4 ± 1.5 versus 23.7 ± 1.0, control versus respectively or chondrocyte lacunar area to matrix area ratios, 1.6 ± 0.4 versus 1.3 ± 0.3, between control and PI fetuses.

Bone formation parameters in the middle and distal zones from the proximal tibial metaphyses of day 192 fetuses are shown in Table 4. The majority of flurochrome labeled bone surface was diffusely labeled, but a considerable amount of discrete single and double labels were present to facilitate analysis (Figure 8,9). Single labeled surface was less within the distal zone as was double labeled surface within the middle zone of PI tibias. Mineralizing surface was less in PI tibia within both zones. There was no difference in mineral apposition rates in either zone. However, bone formation rates were slower within the distal zone of PI tibia. Collectively when the middle and distal zones were pooled and evaluated as one zone of interest there was decreased single labeled surface, double labeled surface, and mineralizing surface in PI fetuses when

Table 4. Dynamic histomorphometric parameters from proximal tibia metaphysis of day 192 fetuses by zone[a].

Zone	Middle		Distal	
	Control	PI	Control	PI
Single Labeled Surface, sL.S/BS (%)	23.2 ± 4.5	20.3 ± 0.9	16.5 ± 1.5	9.6 ± 2.8[b]
Double Labeled Surface, dL.S/BS (%)	9.7 ± 1.7	4.8 ± 1.0[b]	5.5 ± 3.0	1.5 ± 0.7
Mineralizing Surface, MS/BS (%)	21.4 ± 2.8	15.0 ± 1.0[b]	13.7 ± 2.8	6.3 ± 1.9[b]
Mineral Apposition Rate, MAR (μm/day)	0.62 ± 0.12	0.64 ± 0.10	0.66 ± 0.16	0.51 ± 0.14
Bone Formation Rate, BAR ($\mu m^3/\mu m^2$/day)	0.14 ± 0.04	0.10 ± 0.01	0.09 ± 0.03	0.03 ± 0.01[b]

[a]Mean ± standard deviation (N = 3 control and N = 3 PI). [b]P <0.05.

compared to control fetuses. Bone formation rates tended to be slower in PI tibia ($P < 0.10$). There was no difference in mineral apposition rates between the groups.

Discussion

The two major findings that emerged from this study were the negative impact of PI on both tissue level bone formation in trabecular and cortical bone as well as on trabecular modeling. The histomorphometric parameters correlated well with the radiographic findings. The majority of radiodense transverse bands were present within the middle and distal zones where increased bone and cartilage core area were found. The increased radiodensity of these bands was associated with increased volumes ofcalcified cartilage and bone, the former contributing to the radiographic appearance of the bands due to its greater radiodensity relative to immature bone (Eisenstein, 1975).

In order for greater cartilage core volume to be present distally in the metaphysis, cartilage resorption must have been impaired during the initial modeling of these trabeculae. It is hypothesized that in the primary spongiosa a lesser amount of residual intercolumnar cartilage was resorbed before osteoid formation commenced. The alternative possibility is that the increased volume results directly from an increased volume of intercolumnar matrix with a lower lacunar:matrix ratio and less chondrocyte column density in the physis. The physeal morphometry results support the former hypothesis as there was no difference in these parameters between PI and control fetuses at the time of

sample collection. The periodicity of transverse bands certainly suggests a cyclic insult or physiologic alteration that manifests through reduced trabecular modeling of primary spongiosa. The transverse bands reflect a period of approximately 15 days of 'normal' modeling in between periods of approximately 15 days of abnormal modeling. This time period is based on our estimate of metaphyseal elongation rates and the assumption that they are not altered by this process. The reason trabecular modeling resumes normally in between these insults is not known. However, the cyclic nature of the lesions significantly enhances the difficulty of studying the morphogenesis of these lesions, as lesions did not appear within the same region or occur during the same developmental time within all fetuses. For example, a specific metaphyseal zone from a particular PI fetus may contain no bands, when the same zone of another PI contains one or two.

Metaphyseal lesions have been described in association with a variety of different viral infections in growing animals. Growth retardation lattices similar to those found in this study have been described in growing dogs infected with canine distemper virus (Baumgartner, 1995), in cats infected with feline herpesvirus (Hoover, 1971), in sheep infected with border disease virus (Caffrey, 1996), and in pigs which survive acute infections with classical swine fever virus (Thompson, 2007). In contrast to the lesions described in this study, the growth retardation lattices caused by viral infections in other species are typically singular and lack the cyclic nature characterized herein. The pathogenesis of metaphyseal lesions caused by other pestiviruses, border disease virus and

classical swine fever virus, may be similar to those described in this study, while growth retardation lattices due to feline herpesvirus and canine distemper virus infections appear to be due to the direct effect of these viruses on osteoclast resulting in osteoclast necrosis during the acute phase of infection (Baumgartner, 1995; Hoover, 1971).

Abnormal trabecular modeling can result from altered osteoclast production, function, migration and survival, all of which can manifest as similar histomorphometric findings. The morphologic changes do not appear to be due to decreased osteoclast survival as evidenced by the lack of osteoclast apoptosis or necrosis and similar numbers of osteoclast nuclei per osteoclast at all study time points. Osteoclast function appears to be normal in PI fetuses with osteoclasts being found on crenated surface and deep within Howship's lacunae. Likewise osteoclast migration did not appear to be altered, as osteoclasts were present in similar numbers at the leading edge of vascular growth at the physis. Regardless of these observations, the cyclic nature of these lesions would necessitate evaluation of samples from additional time points in the period between day 97 and 192 as well as application of specific assays to determine the cause with any certainty. Reduced numbers of osteoclasts found in the proximal zone of PI tibias are presumably responsible for the abnormal modeling but the reason for this is not clear. Impaired osteoclast differentiation is a possible explanation and investigation of this process may aid in explaining the time course of the cyclic nature of these lesions. It has been well established for some time that the osteoclasts are derived from bone marrow precursor cells of

the monocytic linage (Jotereau; Khan, 1975; Sminia, 1986). Although the time required for generation of functional osteoclasts from permissive precursor cells in the bovine fetus is unknown estimates from *in vitro* experiments in other species suggest that it ranges from 14-21 days for humans and approximately 11 days for mice (Duplomb, 2007; Sivagurunathan, 2005). This time course of development would appear to correlate with the estimated period of 15 days determined in this study.

PI with BVDV may impair osteoclast differentiation either due to a direct effect of viral infection on precursor cells or as a secondary effect as a result of the action of cytokines. Monocytes infected *in vitro* with BVDV have been shown to release an IL-1 inhibitor (Jensen, 1991). Inhibition of IL-1 activity, which positively regulates osteoclastogenesis (Kim, 2009), has been postulated to be responsible for impaired osteoclast differentiation in PI animals (Scruggs, 1995) PI fetuses have been shown to have a chronic moderate IFN-I response (Smirnova et al., 2008), and it is plausible that chronic production of IFN β, a potent negative regulator of osteoclast differentiation (Takayanagi, 2005), negatively impacts osteoclastogenesis.

BVDV is known to infect cells of the innate immune system including, monocytes, macrophages and dendritic cells (Sopp, 1994). Recent studies have demonstrated that BVDV infected monocyte-derived macrophages have significantly impaired functional capacity, as measured by phagocytosis and cytokine production *in vitro (Chase et al., 2004; Peterhans et al., 2003).* Because macrophages and osteoclasts originate from a common precursor cell, both cell

types may be affected by a similar mechanism. Similar to the findings of others (Nuss et al., 2005; Scruggs, 1995), attempts to demonstrate BVDV antigen in osteoclasts by immunohistochemical methods were not successful even though positive control tissues from other organs that were processed in the same manner as the bone sections resulted in positive staining. The reason for this is unclear but may be due to the amount of virus present being below the threshold of detection or absence of viral antigen altogether within osteoclasts.

The second important finding was reduced tissue level bone formation in PI fetuses suggesting a decrease in the extent of osteoblast surface actively involved in bone formation. The cell level parameter of bone formation, mineral apposition rate appeared to be normal, suggesting that PI either impairs recruitment of osteoblasts into active formation or there is cyclic impairment of cell level bone formation not apparent in the intra-labeling period (days 175-185). Other investigators have reported the presence of BVDV antigen in osteoblasts and osteocytes (Nuss et al., 2005), but this was not corroborated in present study. Thus the potential primary effect of ncpBVDV on bone forming cells is uncertain. However, BVDV infection of osteoblasts could impact osteoclastogenesis indirectly through impaired receptor activator for nuclear factor kappa B (RANK) signaling and provide an alternative explanation for the observed effects on both cell types.

One common theme throughout this study was the marked individual variation in parameters measured and lesion severity. Certainly one of the most important contributing factors was the cyclic nature of the lesions, which

inevitably resulted in some PI fetuses demonstrating features of normal modeling while other features of abnormal modeling both within the same anatomic region of the metaphysis. It would appear that this reflects inherent individual biological variation or possibly a complex combination of undetermined factors that may have further contributed to the variation in the degree of lesion severity. This was a consideration in focusing the study on the day 192 fetuses because they possessed the most severe radiographic lesions and a superior sample size when compared to other collection times.

In summary, PI of bovine fetuses with ncpBVDV results in decreased numbers of osteoclasts, which impair trabecular bone modeling in a cyclic fashion. Experiments aimed at clarifying the mechanisms responsible for decreased osteoclast numbers in PI are underway. Additionally, PI impairs tissue level bone formation activity in the trabecular and cortical envelopes. These results may provide one explanation for the growth abnormalities observed in PI cattle. To the authors' knowledge this study provides novel insight as to the time of occurrence of long bone lesion during development in PI, the variable presences and severity of such lesions and their cyclic nature with an estimation of the duration of the period of abnormal modeling. It is also the first study to demonstrate the successful use of in vivo flurochrome labeling of fetal bone, via maternal administration, to document impaired bone formation and periosteal apposition.

CHAPTER III.

THE EFFECTS OF IN UTERO PESTIVIRUS INFECTION ON BONE GEOMETRY, BIOMECHANICAL PROPERTIES AND COMPOSITION OF BOVINE FETAL FEMORA

Introduction

Fetal bone development involves a complex series of processes working in concert to produce substantial longitudinal and appositional growth of the organ in a relatively short period of time. Inherently these conditions enhance the sensitivity of the organ to intrauterine insults, which can lead to abnormal bone growth and may impair neonatal bone function. Viral infections represent unique developmental insults that can result in growth restriction of the fetus and abnormal bone development in domesticated animals and humans (Graham et al., 1970; Smirnova et al., 2008; Williams and Carey, 1966) The effects of such infections on the skeleton remain largely unknown for a majority of the most common viruses with demonstrated ability to cross the placenta and infect the developing fetus. Transplacental infection with human cytomegalovirus and Rubella virus can result in abnormal fetal bone development, characterized by the development of irregular radiodense zones within the metaphyses, and are frequently associated with pathologic fractures in the neonate (Graham et al., 1970; Kopelman et al., 1972; Sacks and Habermann, 1977; Smith and Specht, 1979; Williams and Carey, 1966). To our knowledge the effects of intrauterine

viral infections on the biomechanical properties of fetal bone have not been investigated in any species.

Bovine viral diarrhea virus (BVDV), family *Flaviviridae*, is an important cause of viral disease in cattle and is capable of causing transplacental infection of the fetus. Noncytopathic biotypes of BVDV are characterized by the inability to cause cytopathogenicity in cell culture and able to cause persistent infection (PI) of the fetus. If maternal infection occurs prior to the development of fetal adaptive immunity, the fetus can become PI leading to lifelong viral shedding in the animal. PI with BVDV results in impaired fetal bone development characterized by the development of regularly spaced transverse radiodense bands within long bone metaphyses (Nuss et al., 2005; Webb et al., 2012). The radiodense bands represent growth retardation lattices, which are formed as a result of impaired modeling of primary spongiosa secondary to reduced numbers of osteoclasts, and are similar in morphology to lesions caused by congenital Rubella virus and cytomegalovirus infections in humans (Webb et al., 2012). PI with BVDV also results in impaired tissue level bone growth with one such manifestation being reduced periosteal apposition rates which lead to reduced femoral mid-diaphyseal diameter in affected fetuses (Webb et al., 2012) A reduction in mid-diaphyseal diameter lends a more fluted appearance to the metaphysis of PI long bones because epiphyseal diameter and overall bone length are not significantly affected.

Bone fragility has been previously suspected as the underlying cause of neonatal calf long bone fractures associated with transplacental infection with

BVDV (Constable et al., 1993; Nuss et al., 2005; O'Toole, 2006). Based on these findings it was hypothesized that bones from PI fetuses would have impaired biomechanical properties. This study was undertaken to characterize the biomechanical effects of intrauterine viral infections, specifically PI with BVDV, on fetal femora and determine the architectural and/or compositional factors responsible for any potential differences in mechanical properties.

Materials and Methods

Fetal Infection

All animal experiments were approved by the Colorado State University Animal Care and Use Committee. BVDV-naïve Hereford heifers (n=19), ranging in weight from 295 to 430 kg, were estrus-synchronized and artificially inseminated with BVDV-free semen from a single Angus bull. After confirmation of pregnancy on day 35 of gestation, heifers were inoculated intranasally on day 75 of gestation with either 2 ml of MEM media containing 4.4 $\log_{10}TCID_{50}$ noncytopathic BVDV type 2 strain 96b2222 (Van Campen et al., 2000), or MEM media alone to produce PI and Control fetuses. Six pregnant heifers (n=3 Control, n=3 PI) received intravenous injections of oxytetracycline (9 mg/kg) on days 175 and 185 of gestation to fluorochrome label fetal bone formation. Fetuses from the fluorochrome labeled group were collected via Cesarean section on day 192 of gestation. The remaining non-labeled fetuses were collected via Cesarean section on days 192 (n=4 Control, n=2 PI) and 245 (n=4 Control, n=3 PI) of gestation. Following delivery of the fetus from the uterus, the

fetuses were immediately euthanized with an overdose of sodium pentobarbital. Fetal PI was confirmed by qRT-PCR for viral RNA in fetal blood as previously described (Smirnova et al., 2008).

Following euthanasia, left femora were dissected free of soft tissue with care taken to leave the periosteum intact, then wrapped in saline soaked gauze and frozen for later mechanical testing. Right femora were dissected free of soft tissue and fixed in 10% neutral buffered formalin. The overall length of the left femora from the articular surface of the medial condyle to the articular surface of the femoral head and width of the distal epiphysis at its widest point in the mediolateral plane were recorded. Right femora were then transversely sectioned at the mid-diaphysis and diaphyseal diameter in the medial to lateral and cranial to caudal axis and cortical thickness at five standardized sites were measured with dial calipers. Average mid-diaphyseal diameter divided by overall length and average mid-diaphyseal diameter divided by width at the distal epiphysis were used as indexes of bone geometry. Total cross-sectional area and cortical thickness ratio were calculated, the latter using the following formula: 2 * average cortical thickness/ average diaphyseal diameter as previously described (van Lenthe et al., 2008).

Mechanical Testing

Mechanical testing was performed on a servohydraulic mechanical testing system (858 Mini Bionix II, MTS, Eden Prairie, MN) utilizing a custom-built four-point bending fixture. Femora were thawed at 4°C for 1-2 days and brought to

room temperature immediately before mechanical testing. Since there was no significant difference in length between control and PI femora at either day of collection, standardize fixture settings were used for each collection day. The distance between fixture contacts were as follows: for day 192 fetuses outer contacts were spaced 41 mm apart and inner contacts 22 mm apart, for day 245 fetuses outer contacts were spaced 73 mm apart and inner contacts 48 mm apart. Whole femora were preconditioned by two cycles of loading to 150 N at a crosshead displacement rate of 0.15 mm/second. Femora were then loaded in four-point bending until failure in the cranial to caudal axis at a crosshead displacement rate of 0.15 mm/second. Force and displacement were recorded at 100 Hz with custom software. Strain and stress were calculated from standard beam bending equations for four-point bending of a cylindrical tube: Stress = $\sigma = \frac{Fac}{2I}$, and strain = $\varepsilon = \frac{6cd}{a(3l - 4a)}$, where *a* is the distance between the outer and inner contacts, *c* is equal to one-half femoral diameter, *I* is the area of the moment of inertia, *d* is the displacement and *l* is the distance between the outer contacts (Turner and Burr, 1993). Stiffness was calculated by determining the slope of the linear regression fit of the force displacement curve at three linear segments of the curve, which corresponded to 100-500 N, 500-900 N, and 900-1300 N of force. Elastic modulus was determined by the slope of the linear portion of the stress/strain curve in the same load ranges as for stiffness.

Histomorphometry

Mid-diaphyseal sections of right femora were embedded in an epoxy resin (Sampl-Kwick, Buehler Ltd, Lake Bluff, IL) and cut on a low speed saw (ISOMET saw, Buehler Ltd, Lake Bluff, IL) equipped with a diamond blade to yield 250-400 μm thick sections. The resulting sections were hand ground to 100 ± 20 μm thickness for light microscopic evaluation. Fluorochrome labeled sections were used to determine the portion of the outer cortex containing plexiform bone capable of chelating fluorochrome within the woven bone cores. This proportion, which represents a measure of the amount of newly mineralized bone within the cortex, was determined at four standardized sites by measuring from the endocortical aspect of the first label to the periosteal surface and dividing by cortical thickness (Figure 10).

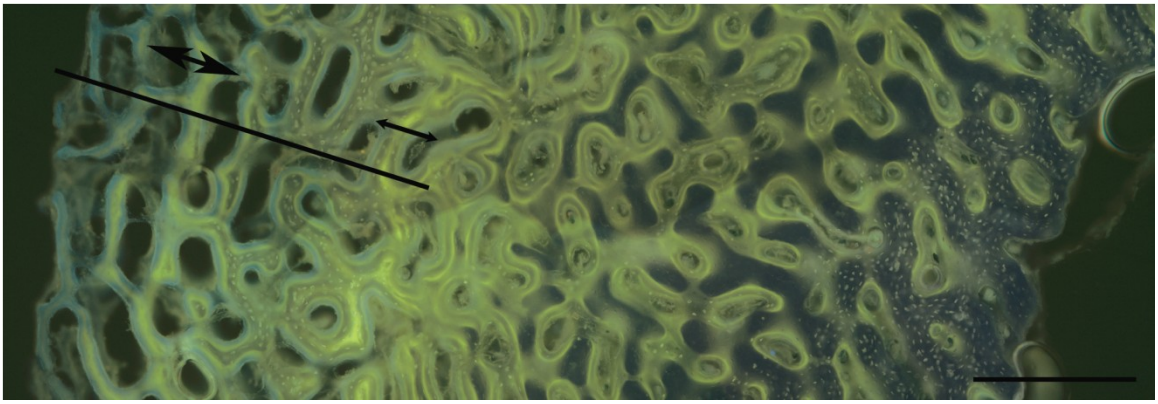

Figure 10. Cross section of femoral cortex from oxytetracycline-labeled day 192 fetus depicting greenish-gold oxytetracycline label within woven bone cores of outer plexiform bone. First label, day 175 of gestation (thin double-headed arrow), second label, day 185 of gestation (thick double-headed arrow), site of measurement for determining portion of newly mineralized cortex (longer line) extends from the periosteal surface to the

endocortical aspect of the first label. Measurement bar = 0.5 mm. Unstained, 100 μm thick section under UV light.

Average plexiform plate separation was determined by averaging the distance from the osteoid surface to the osteoid surface of the adjacent plate for the four outermost plexiform plates at four standardized sites. Cortical porosity was determined using a modified Mertz grid and simple point counting method under 200 x magnification at four anatomically standardized areas of interest, which extended from the periosteum to endocortical surface. The size of the areas of interest inherently varied due to differences in cortical thickness, but was on average 1.1 mm^2 for day 192 fetuses and 1.2 mm^2 for day 245 fetuses.

Ash and Mineral Analysis

Ash and mineral analysis was performed on cortical bone from the left femora (mechanically tested femur) utilizing previously described analytical methods (Norrdin et al., 1977). A transverse section of mid-diaphysis measuring approximately 5 mm in width was ashed and calcium (Ca) and phosphorus (P) content were determined. Tissue volume (cortical cross-sectional area ∗ slice thickness), ash density (g ash/ cm^3 tissue volume ∗ (1 - porosity), apparent density (g ash/cm^3 tissue volume), percent calcium (g Ca/g ash weight), percent phosphorus (g P/g ash weight), and Ca : P molar ratio were calculated for each sample.

Statistical Analysis

Data analysis was performed with SAS statistical software (SAS Institute Inc., Cary, NC) using the General Linear Models procedure. Comparisons were performed with the least square means procedure followed by Student's *t*- test. For mechanical data, linear regression analysis was used to determine the effect of independent variables. All data are presented as mean ± standard deviation and assumptions for use of applicable statistical tests were satisfactorily met. All differences described were significant at the $P < 0.05$ level and tendencies at the $P < 0.10$ level.

Results

All PI fetuses from both days of collection were positive and all Control fetuses were negative for BVDV RNA in blood by qRT-PCR (Bielefeldt-Ohmann et al., 2012). There was no difference in body weight between Control and PI fetuses (Table 5). Fetal sex by day of collection was recorded: day 192 Control (3 males, 4 females), day 192 PI (1 male, 4 females), day 245 Control (2 males, 2 females), day 245 PI (3 males). The long bones of three out of five PI fetuses on day 192 and two out of three PI fetuses on day 245 contained radiographic lesions consisting of focal densities and transverse radiodense bands within metaphyses as previously described (Webb et al., 2012).

Femoral dimensions appear in Table 5. PI fetuses had smaller mid-diaphyseal diameters when compared to Control fetuses. Overall femur length and width at

the distal epiphyses did not differ between PI and Control fetuses, although there was a tendency for overall length to be less in day 192 PI compared to Control fetuses. The two indexes of bone geometry, mid-diaphyseal diameter/length and mid/diaphyseal diameter/width at distal epiphysis, were lower in PI versus Control fetuses on both collection days. This confirmed the gross observation that the bones of PI fetuses have a more accentuated taper from the epiphysis to the diaphysis. Mid-diaphyseal cortical thickness did not differ between PI and Control fetuses, but total cortical cross- sectional area was less in PI fetuses compared to respective groups on day 192. Control and PI fetal femora fromboth days of collection consistently failed between the inner contacts of the testing fixture. The most common fracture configuration was a short oblique fracture located slightly proximal to the mid-diaphysis. There were no differences in fracture configuration or site of fracture between Control and PI fetuses on either day of collection.

Results of the four-point bending test are presented in Table 6. Neither force at failure nor displacement at failure differed between PI and Control fetuses on either day but there was a tendency for force at failure to increase from day 192 to day 245 in the PI group. Displacement at failure increased in both groups from day 192 to day 245. Overall slope of the force versus displacement plot (stiffness) was greater in day 192 fetuses compared to older fetuses (Figure 11 A, $P < 0.01$) even though individual values of stiffness, in different load ranges, only differed with age in Control fetuses at 500-900N of load. When stiffness was plotted against cortical thickness ratio there was

Table 5. Body weight and femoral dimensions of Control and PI fetuses on days 192 and 245 of gestation. (Mean ± standard deviation)

	192 Days		245 Days	
Parameter (units)	Control	PI	Control	PI
Number of fetuses	7	5	4	3
Body weight, (kg)	9.04 ± 0.76	8.01 ±1.08	25.34 ± 0.40	24.83 ±1.80
Femoral length, (cm)	10.94 ± 0.40	10.63 ± 0.27[a]	17.33 ± 0.39	17.00± 0.26
Cranial-caudal mid-diaphyseal diameter, (mm)	13.20 ± 0.31	11.76 ± 0.32[b]	21.48 ± 1.44	18.47 ± 0.91[b]
Medial-lateral mid-diaphyseal diameter, (mm)	13.50 ± 0.43	12.22 ± 0.49[b]	22.28 ± 0.49	18.73 ± 0.51[b]
Mid-diaphyseal diameter/length	0.122 ± 0.004	0.113 ± 0.004[b]	0.126 ± 0.006	0.109 ± 0.004[b]
Mid-diaphyseal diameter / Width at distal epiphysis	0.385 ± 0.014	0.361 ± 0.014[b]	0.408 ± 0.011[c]	0.340 ± 0.007[b,d]
Mid-diaphyseal cortical thickness, (mm)	3.51 ± 0.53	3.44 ± 0.46	3.19 ± 0.74	3.41 ± 0.90

Total cortical cross sectional area, (mm^2)	108.14 ± 13.22	91.97 ± 9.78[b]	184.35 ± 28.04	161.50 ± 38.02
Cortical thickness ratio[e]	0.52 ± 0.07	0.57 ± 0.07	0.29 ± 0.08[c]	0.37 ± 0.07[c]

[a] Tendency for difference from age matched control $P < 0.10$.

[b] Difference from age matched control $P < 0.05$.

[c] Difference from day 192 vs. day 245 of same infection status, $P < 0.05$

[d] Tendency for difference from day 192 vs. day 245 of same infection status $P < 0.10$.

[e] See Materials and Methods for formula.

significant positive correlation (Figure 11 B, $R^2 = 0.49$, $P < 0.01$). After correcting stiffness for bone size, day 192 PI fetuses had greater elastic modulus than respective controls at all load levels examined and day 245 PI fetuses tended to have a higher elastic modulus from 500-900 N and from 900-1300 N loads. Elastic modulus decreased from day 192 to day 245 within both groups. Elastic modulus plotted against cortical thickness ratio demonstrated significant linearcorrelation with an individual distribution similar to that of Figure 11 B (Figure 12 A, $R^2 = 0.48$, $P < 0.001$). Elastic modulus when plotted against mid-diaphyseal diameter/length revealed two populations that appeared to separate based on fetal age and infection status. The resulting regression lines of day 192 fetuses versus day 245 fetuses in this plot differed both in slope and intercept (See Figure 12 B, $P < 0.05$). When force at failure was normalized to bone area, ultimate stress tended to be greater in day 245 PI fetuses compared to age matched controls, but did not differ in day 192 PI fetuses versus day 192 controls. Ultimate stress was lower in both Control and PI fetuses on day 245 when compared to respective groups on day 192 (Table 6), but showed significant linear correlation with cortical thickness ratio (See Figure 12 C, $R^2 = 0.65$, $P < 0.001$). Ultimate stress was lower in both Control and PI fetuses on day 245 when compared to respective groups on day 192 (Table 6), but showed significant linear correlation with cortical thickness ratio (See Figure 12 C, $R^2 = 0.65$, $P < 0.001$).

Table 6. Four-point bending test of femora from Control and PI fetuses on days 192 and 245 of gestation. (Mean ± standard deviation)

	192 Days		245 Days	
Parameter (units)	Control	PI	Control	PI
Displacement at failure, (mm)	4.19 ± 0.36	3.84 ± 0.32	8.6 ± 1.73[a]	10.10 ± 1.58[a]
Force at failure, (N)	2627 ± 890	2126 ± 359	3162 ± 372	3510 ± 1300[b]
Stiffness (N/mm), @ 100-500 N	582 ± 88	574 ± 88	510 ± 44	481 ± 194
Stiffness (N/mm), @ 500-900 N	759 ± 155	800 ± 244	480 ± 96[a]	704 ± 246
Stiffness (N/mm), @ 900-1300 N	837 ± 241	803 ± 177	578 ± 106	705 ± 357
Elastic modulus, (MPa), @ 100-500 N	252.57 ± 42.8	377.92 ± 83.4[c]	141.7 ± 12.9[a]	197.3 ± 64.1[a]
Elastic modulus, (MPa), @ 500-900 N	328.10 ± 66.1	500.54 ± 108.2[c]	133.6 ± 26.7[a]	255.8 ± 76.9[a,b]
Elastic modulus, (MPa), @ 900-1300 N	361.53 ± 106.1	519.36 ± 72.2[c]	160.8 ± 31.3[a]	275.8 ± 96.0[a,b]
Ultimate stress, (MPa)	55.71 ± 16.2	61.07 ± 7.7	26.59 ± 2.5[a]	42.75 ± 12.5[a]

[a] Difference, day 192 vs. day 245 of same infection status, $P < 0.05$.

[b] Tendency for difference from age matched control, $P < 0.10$.

[c] Difference, age matched control $P < 0.01$.

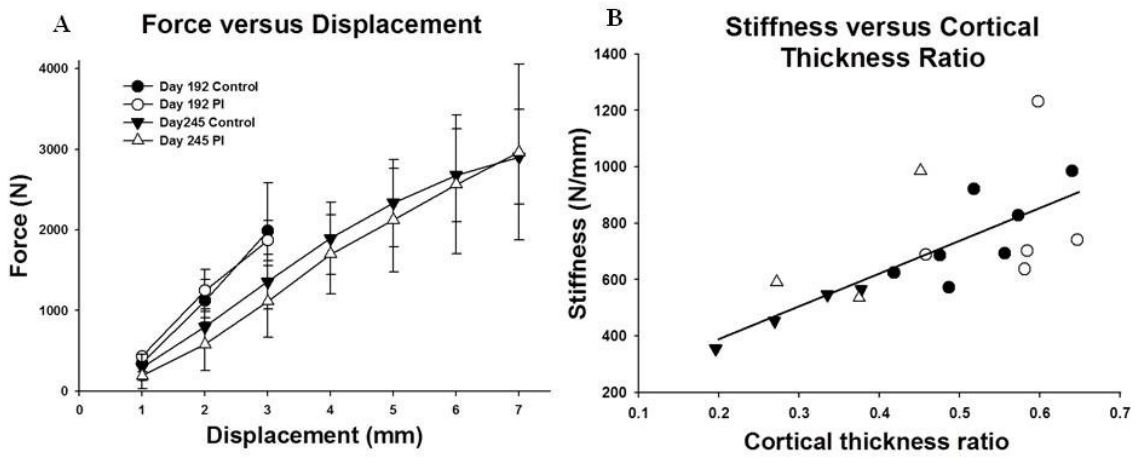

Figure 11. (A) Force versus displacement plot for control and PI fetal femora on days 192 and 245 of gestation. Control and PI femora on day 192 have greater slope (stiffness) when compared to their respective groups on day 245 ($P < 0.01$). (mean $\pm$ standard deviation) (B) Stiffness versus cortical thickness ratio plot for control and PI fetal femora on days 192 and 245 of gestation. There is significant positive linear correlation between stiffness and cortical thickness ratio (R^2 =0 .49, $P < 0.01$).

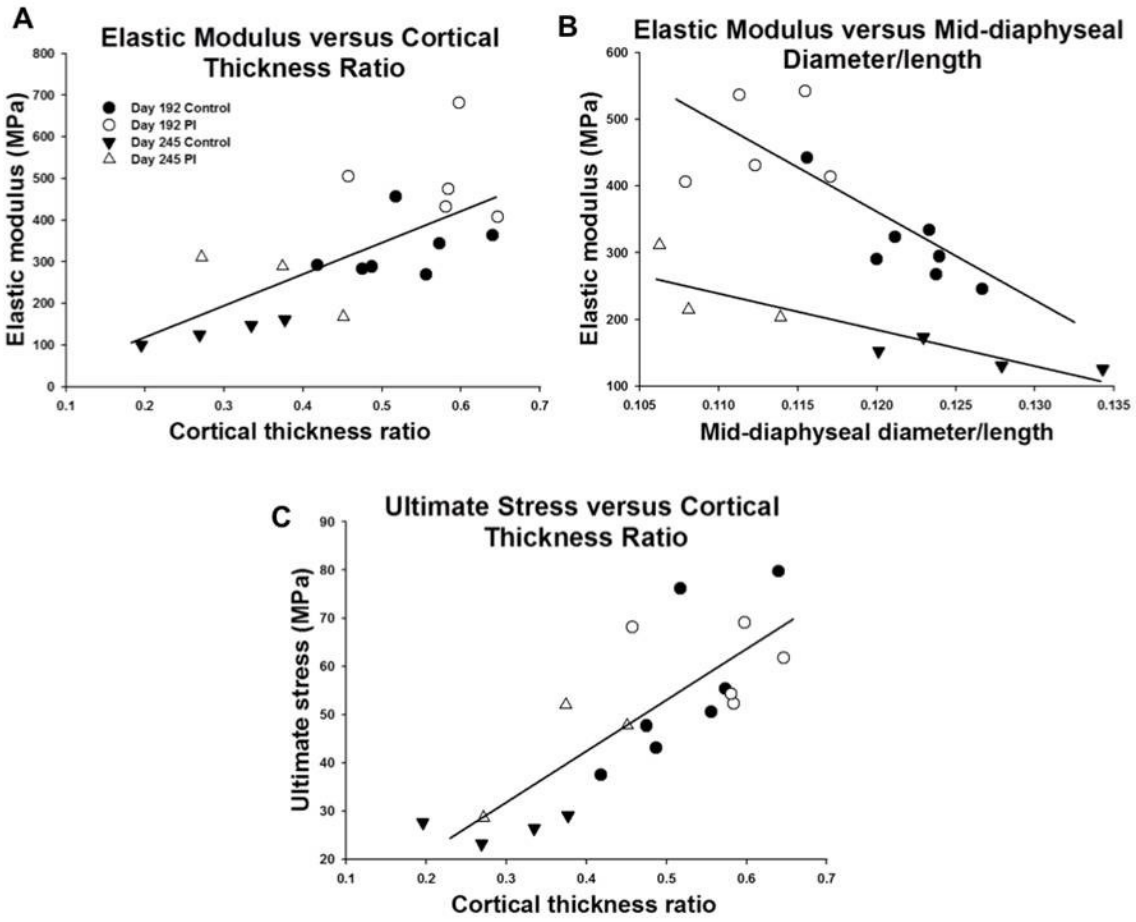

Figure 12. (A) Elastic modulus versus cortical thickness ratio plot for control and PI fetal femora on days 192 and 245 of gestation. There is significant positive linear correlation between elastic modulus and cortical thickness ratio ($R^2 = 0.48$, $P < 0.001$). (B) Elastic modulus versus mid-diaphyseal diameter/length plot for control and PI fetal femora on days 192 and 245 of gestation. The regression lines for day 192 versus day 245 fetuses differ in slope and intercept (both $P < 0.05$). (C) Ultimate stress versus cortical thickness ratio plot for control and PI fetal femora on days 192 and 245 of gestation. There is significant positive linear correlation between ultimate stress and cortical thickness ratio ($R^2 = 0.65$, $P < 0.001$).

Morphometry and compositional data from the femoral mid-diaphyseal cortex appears in Table 7. There was no difference in the percent of fluorochrome labeled cortex between Control and PI fetuses on day 192. PI fetuses on day 192 had shorter average separation of plexiform plates compared to Controls, as did day 245 Control fetuses compared to day 192 Control fetuses. Cortical porosity was less in PI fetuses on both days 192 and 245 when compared to respective age controls, but did not change from day 192 to day 245 in either group. There was no significant linear correlation between porosity and elastic modulus nor ultimate stress, or between average separation of plexiform plates and elastic modulus or ultimate stress.

There was no difference in apparent density, ash density, percent calcium, percent phosphorus, or Ca:P molar ratio between PI and Control fetuses on either day of collection or between fetuses from day 192 compared to day 245.

Discussion

The first objective of this study was to determine if *in utero* infection with BVDV impaired the biomechanical properties of fetal femora. Elastic modulus increased as a result of PI but decreased in older fetuses (Table 6.) Ultimate stress also decreased in older fetuses. A plot of ultimate stress versus elastic modulus showed good linear correlation (data not shown), suggesting that the values are proportionally in line with previous studies (Currey, 1999). Collectively these results suggest that the strength and elastic modulus of fetal bone decreases in

Table 7. Morphometry and Compositional data from the femoral cortex of Control and PI fetuses on days 192 and 245 of gestation. (Mean ± standard deviation)

	192 Days		245 Days	
Parameter (units)	Control	PI	Control	PI
Labeled cortex, (%)[a]	36.1 ± 8.8	36.2 ± 20.6	N/F	N/F
Plexiform plate separation, (μm)[a]	139 ± 11	124 ± 10[b]	118 ± 8[c]	114 ± 15
Porosity, (%)	34.2 ± 4.9	26.8 ± 3.7[b]	30.0 ± 1.7	25.6 ± 1.3[b]
Apparent density, (g/cm^3)[a]	1.00 ± 0.09	1.02 ± 0.06	0.96 ± 0.06	1.13 ± 0.21
Ash density, (g/cm^3)[a]	1.04 ± 0.11	0.94 ± 0.09	0.91 ± 0.04	1.03 ± 0.20
Calcium, (%)	24.1 ± 1.4	25.1 ± 1.4	27.5 ± 6.2	24.6 ± 0.4
Phosphorus, (%)	11.0 ± 1.8	11.4 ± 2.0	12.0 ± 0.5	11.8 ± 0.5
Ca:P (M/M)	1.74 ± 0.37	1.74 ± 0.32	1.78 ± 0.45	1.62 ± 0.04

[a] See Materials and Methods for formulae.

[b] Difference from age matched control $P < 0.05$.

[c] Difference from day 192 vs. day 245 of same infection status, $P < 0.01$.

N/F – not flurochrome labeled.

the third trimester of gestation and that PI with BVDV results in increased elastic modulus.

Major architectural and compositional determinants of elastic modulus were evaluated in an attempt to determine the cause of increased elastic modulus in PI fetuses and to gain an understanding of why both strength and

elastic modulus decreased with age. Because fetal cortical bone is more heterogeneous in architecture and in degree of mineralization than cortical bone of skeletally mature animals, oxytetracycline labeling was used to evaluate variations in anatomic distribution of bone with varying degrees of mineralization. The percent of labeled cortex which represents the portion of bone, which is still in the process of mineralization and able to chelate oxytetracycline label did not differ between PI and Control fetuses. Significant differences in average separation of plexiform plates and porosity were found between PI and Control fetuses. There was no difference in ash or mineral composition between any of the groups. These findings demonstrate that there were no significant quantitative differences in cortical mineralization between PI and Control fetuses. All of these factors failed to correlate statistically with elastic modulus and thus explain the observed difference. Furthermore, there were no significant differences in these factors to explain the differences in biomechanical properties between day 192 and day 245 fetuses. While it is reasonable to presume that each of these factors do make small contributions to material properties, the sample size of this study was not large enough to provide sufficient statistical power in a more complex statistical model that would enable these lesser contributions to be defined.

The only significant gross morphologic difference between PI and Control fetuses in this study was mid-diaphyseal diameter. Cortical thickness, cortical thickness ratio, overall bone length and width of the distal physis did not differ. The cause of impaired femoral periosteal apposition rates (Webb et al., 2012),

and thus reduced diameter, in PI fetuses is unknown, but the fact that cell level osteoblastic bone formation is reportedly normal in these fetuses suggests that there is defective recruitment or differentiation of osteoblasts into active bone forming cells (Webb et al., 2012).

As our samples differed significantly in diameter we investigated the relationship of bone geometry and biomechanical parameters, which were found to differ. Unexpectedly, there was a profound effect of cortical geometry on elastic modulus, with cortical thickness ratio accounting for approximately 49% of the difference in elastic modulus that was observed between the groups. Differences in elastic modulus between day 192 and day 245 fetuses were largely explained by differences in bone geometry (mid-diaphyseal diameter) (regression analysis not shown), although there appears to be a disproportionate effect on modulus in day 192 versus day 245 fetuses as described by the differences in regression line slope and intercept between fetal age (Figure 12 B). Cortical geometry (cortical thickness ratio) accounted for approximately 65% of the difference in decreased ultimate stress in day 245 fetuses (Figure 12 C)

The idea that cortical geometry can have significant influence on area normalized biomechanical parameters such as elastic modulus is not a novel contention and has been described by others (Akhter et al., 2004; Silva et al., 2004; van Lenthe et al., 2008). One study evaluating the effect of cortical thickness ratio on elastic modulus values as calculated by beam theory equations in three-point bending found that elastic modulus was disproportionally affected by differences in bone geometry (van Lenthe et al., 2008). The

specimens tested in this study differed significantly in cortical thickness ratio which was similar to that observed between day 192 versus day 245 fetuses tested herein. However we demonstrated differences in elastic modulus between PI versus Control which had similar cortical thickness ratios and differed only in mid-diaphyseal diameter. These results suggest that differences in cortical diameter can have a similar affect on modulus values even when cortical thickness ratios are similar.

At least in humans, cattle and some strains of mice, bone geometry changes with age such that the mid-diaphyseal diameter increases to a much greater degree than cortical thickness (Land and Schoenau, 2008; Silva et al., 2002). Compared to calculation of elastic modulus by different methods such as finite element analysis modeling, calculation by classical beam theory has been found to significantly underestimate modulus values (van Lenthe et al., 2008). These observations seem to apply to the values for elastic modulus obtained in this study as they were considerably less than published values for fetal bone from cattle and deer in which somewhat different methodology was used (Currey and Pond, 1989; Garnero et al., 2006). The nature of fetal bone may have contributed to this discrepancy as plexiform bone is an orthotropic material, whose mechanical properties vary with the direction in which they are tested (Turner and Burr, 1993).

Use of beam theory equations for calculation of stress and strain requires that many assumptions be made (Loveless, 1966; Westwater, 1949). Whilst these assumptions are commonly made but rarely satisfied completely in testing

bone, one must carefully consider the resultant error and determine whether it is of an acceptable level (Draper and Goodship, 2003). The results of this study suggest that the error from using classical beam equations is not acceptable when testing samples which vary in diameter, and confirm previous observations concerning comparisons of samples which vary in cortical thickness ratio (van Lenthe et al., 2008). It is unclear in these cases which assumptions for use of classical beam theory equations are invalid. Some authors contend that the error is attributable to use of calculated values for strain rather than direct measurement of strain using strain gauges or extensometers (Turner and Burr, 1993). The relationships between bone geometry and both ultimate stress and elastic modulus identified in this study suggest that neither calculation can be performed with an acceptable degree of error when comparing specimens differing in diameter, cortical thickness ratio or both.

Even though the results of the present study did not demonstrate a statistically significant correlation between porosity and elastic modulus, it is unlikely that porosity is not a contributing factor given the well established relationship which has been determined in mature bovine cortical bone (Schaffler and Burr, 1988). Decreased porosity, as measured in the PI fetuses, included reduced average plexiform plate separation, which was only present in day 192 fetuses. Our evaluation of determinants of biomechanical properties in fetal bone were by no means conclusive as other parameters such as the extent of Type I collagen cross-linking have been found to be important as well (Garnero et al., 2006).

To our knowledge this study represents the first investigation of the effects of *in utero* viral infection on biomechanical properties of fetal bone and demonstration of the effect of reduced femoral mid-diaphyseal diameter on elastic modulus as calculated by classic beam theory. Although *in utero* infection with BVDV results in fetal femora with higher elastic modulus, the difference was largely accounted for by decreased periosteal appositional bone formation (Webb et al., 2012), and decreased mid-diaphyseal diameter rather than difference in the inherent biomechanical properties of PI fetal bone. Similarly, the decreased ultimate stress in day 245 fetuses was largely do to differences in bone geometry. The results of this study also suggest that inherent biomechanical properties of fetal cortical bone may exhibit a different relationship with important determinants of the biomechanical properties of bone such as porosity.

CHAPTER IV.

DEVELOPMENT OF THE TYPE I INTERFERON RESPONSE IN FETUSES FOLLOWING IN UTERO INFECTION WITH BOVINE VIRAL DIARRHEA VIRUS

Introduction

Infection with BVDV, a pestivirus in the family *Flaviviridae,* leads to significant economic losses for cattle producers worldwide (Moerman et al., 1994; Valle et al., 2005). BVDV, small enveloped viruses with a single-stranded, positive-sense RNA genome of ~12.5 kb, are classified into two biotypes – cytopathic (cp) and non-cytopathic (ncp) - based on their lytic activity in cell culture (Gillespie, 1961). Both cp and ncp BVDV strains are able to cause acute infection in immunocompetent animals resulting in varying clinical manifestations ranging from mild subclinical disease to severe systemic disease and reproductive failure, including embryonic death, abortion and stillbirth (Brownlie et al., 1989; Murray, 1990). While both cp and ncp BVDV viruses are able to cross the placenta and infect the fetus, only ncp BVDV strains have the ability to cause persistent infection in fetuses infected during the first 150 days of gestation due to the insufficient development of the fetal immune system (Bielefeldt-Ohmann, 1995; Brownlie et al., 1989; Harding et al., 2002; McClurkin et al., 1984). Infection with BVDV in late gestation (after day 150) results in a transient infection that is cleared by the dam and fetus because adaptive immune

systems are sufficiently developed in both to mount an immune response to the infecting virus (Done et al., 1980; Goyal, 2005).

Ncp BVDV strains that are able to establish fetal persistent infection in early gestation provide excellent models for studying not only the feto-placental immune response to chronic viral infection, but also the effects of such infections on fetal development. We have shown previously that persistent infection adversely affects fetal growth (Smirnova et al., 2008) and development of multiple organs, including the brain (Bielefeldt-Ohmann et al., 2012; Bielefeldt-Ohmann et al., 2008; Done et al., 1980) and bone (Webb et al., 2012). Persistent infection with BVDV also alters fetal antiviral immune responses (Hansen et al., 2010; Shoemaker et al., 2009), and may alter maternal immune function through down regulation of CXCR4/CXCL12 and T cell receptor pathways in blood cells (Smirnova et al., 2009). Establishment of fetal persistent infection involves complex interactions between the maternal, fetal, and placental immune responses.

Cattle have an epitheliochorial placenta comprised of placentomes - the organs of nutrient exchange composed of a fetal and maternal component, the cotyledon and the caruncle, respectively (Bjorkman, 1957; Igwebuike, 2006)The microanatomic arrangement of epitheliochorial placentation precludes transplacental delivery of large maternal proteins such as immunoglobulins to the fetus (reviewed in (Chucri et al., 2010; Halliday, 1978). The unique physiologic and anatomic characteristics of the ruminant placenta enables concurrent studies of the immune responses of the fetus, placenta, and dam in a way that allows

individual contributions as well as cause-effect relationships to be ascertained. Previously BVDV was shown to spread to and replicate in placenta of cows either acutely or persistently infected (PI) with BVDV (Fredriksen et al., 1999; Swasdipan et al., 2002). Binucleate trophoblast cells are one of the major reservoirs for the virus replication in placenta (Fredriksen et al., 1999) and are thought to play a role in the secondary spread of the virus from fetus to the dam (Swasdipan et al., 2002). The complexity of the processes taking place at the maternal-fetal interface during establishment and maintenance of fetal persistent infection requires a thorough and comprehensive approach.

The first mechanism of antiviral defense is an innate immune response mediated by the induction of type I interferon (IFN), a family of proteins that includes, but is not limited to, IFN-τ, IFN-α, and IFN-β. IFN-τ plays an important role in maternal recognition of pregnancy in ruminants and is produced in large amounts during early gestation (reviewed in (Spencer and Bazer, 2004; Spencer, 1996). Despite the ability of IFN-τ to upregulate IFN type I pathways, its role in the regulation of BVDV replication in placenta has not been studied extensively (Swasdipan et al., 2002). Likewise, there are no detailed studies in the literature pertaining to the production of IFN-α or IFN-β in virally infected bovine placenta.

Virus must be recognized by host cells in order for an innate immune response to be induced. Toll-like receptors (TLRs) on the cellular membranes of immune cells along with RNA helicases in the cytosol serve as sensors for viral RNA (Kang et al., 2002; Yoneyama et al., 2004). Retinoic acid inducible gene I (RIG-I) and melanoma differentiation-associated gene 5 (MDA5) are RNA

helicases, which are able to detect the presence of double stranded RNA (dsRNA) in the cell cytoplasm(Kato et al., 2006). These RNA helicases function as cytoplasmic pattern recognition receptors (PRRs), which detect the presence of pathogens by binding the pathogen-associated molecular patterns (PAMPs) within the cell and inducing the innate immune response through activation of the IFN type I cascade (Kato et al., 2006; Yoneyama et al., 2004). We have previously demonstrated robust up-regulation of both RIG-I and MDA5 in blood of pregnant heifers and fetuses transiently infected with ncp BVDV, while moderate up-regulation of RIG-I and MDA5 was also detected in PI fetuses at day 190 of gestation, 115 days post maternal infection (dpmi) with ncp BVDV and in PI yearling steers (Shoemaker et al., 2009; Smirnova et al., 2008). However, it is not known how early in gestation nor how soon after infection of the fetus with BVDV these PRRs can be activated.

Induction of the type I IFN pathway leads to up-regulation of IFN stimulated genes (ISGs). Our previous study demonstrated up-regulation of multiple ISGs, including myxovirus resistance factor 2 (MX2), oligoadenylate synthetase 1 (OAS-1), and ISG15, in PI fetuses and steers (Shoemaker et al., 2009). ISG15 is considered a prominent marker for the cascade of events induced by the type I IFNs in innate immune responses (Haas, 1987; Lenschow, 2007), and for these reasons it has been chosen as a marker of ISGs up-regulation in the present study.

The current experiments were designed to delineate timing of the development of the innate immune response, in particular, the up-regulation of

PRRs, ISGs, and IFN-α and IFN-β, in fetuses and placenta during establishment of persistent infection with ncp BVDV. It was hypothesized that: i) chronic stimulation of innate immune responses occurs following viral infection of the fetus; ii) placental production of the type I IFN contributes to up-regulation of ISGs in PI fetuses. The presented data summarize our findings.

Materials and methods

Animals

The Animal Care and Use Committee at Colorado State University approved all animal experiments using cattle. Forty-six weaned BVDV-naïve Hereford heifers were purchased from a source that did not vaccinate for BVDV and were transported to the Animal Reproduction and Biotechnology Laboratory at Colorado State University. Upon arrival all heifers were confirmed to be seronegative to BVDV1 and BVDV2 by using standard serum neutralization assay and BVDV-antigen-free in an ear-notch extracts-based BVDV antigen-capture ELISA as described previously (Smirnova et al., 2008). Repeated serum neutralization assay for BVDV antibodies was performed one week prior to BVDV inoculation to confirm naïve status.

At ~ 12 months of age estrous cycles of the heifers were synchronized and heifers were artificially inseminated with BVDV-free semen. Pregnancy was confirmed with ultrasound examination on day 32 and later on day 70 of gestation.

In vivo infection with BVDV and fetal collections

The experimental design is depicted in Figure 13.

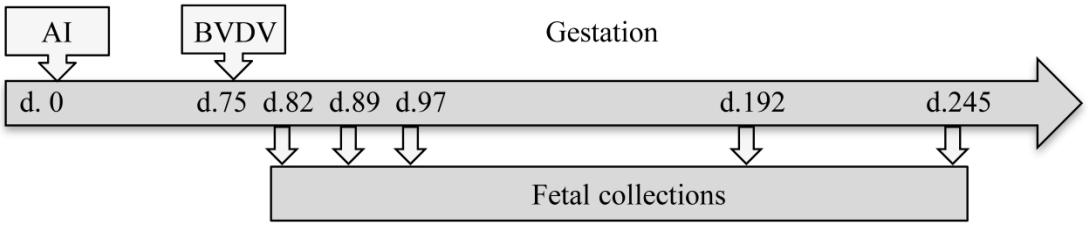

Figure 13. Experimental design. Estrous cycles were synchronized and heifers were artificially inseminated (AI) on day 0. Pregnant heifers were infected intranasally with ncp BVDV type 2 viral strain on day 75 of gestation to generate PI fetuses or kept BVDV-naïve to generate control, uninfected fetuses. Fetal collections were performed through Cesarean section on days 82, 89, 97, 192, and 245 of gestation.

Prior to BVDV infection pregnant heifers were randomly assigned to two experimental groups - control and infected (n=23/group), which were kept separated in isolated pens. In order to generate PI fetuses, pregnant heifers of the infected group were inoculated with ncp BVDV2 strain 96B2222 (Van Campen et al., 2000) on day 75 of gestation. Each heifer received intranasal inoculation of a 2 ml aliquot of the virus stock aliquot 4.4 $\log_{10}$ $TCID_{50}$/ml (PI group) as described previously (Smirnova et al., 2008) or a sham inoculation with 2 ml of culture media (control group). Control heifers were kept away from the infected group and remained BVDV-free throughout the experiment. Blood samples for serology and RNA using Tri-reagent BD for blood derivatives (Sigma, USA) were collected from heifers on days 75, 78, 82, 85, 89, 97, 103,

115 during acute infection and seroconversion, and every two weeks thereafter, until day 245. Fetuses were collected by Cesarean section on days 82, 89, 97, 192 and 245 (n=4 control/4 PI fetuses for day 82, 89 and 97; n=7 control/7 PI fetuses for the day 192; n=4 control/3 PI fetuses for the day 245 group). The latter group had only three PI fetuses due to the abortion of one fetus prior to the Cesarean section for reasons unrelated to the experimental infection. Fetal umbilical cord blood for RNA, serum and plasma, and fetal tissues for RNA and protein analysis were collected following Cesarean section and either preserved with Tri-reagent BD or snap-frozen in liquid nitrogen. Placentomes were collected at Cesarean section, and cotyledonary and caruncular parts were manually separated by gentle traction and snap-frozen in liquid nitrogen.

Virus neutralization assay for BVDV antibodies

Serum of heifers was tested for presence of antibodies against BVDV1 and BVDV2 in bovine turbinate cells in 96-well plate format as described previously (Carbrey, 1973; Smirnova et al., 2008). Briefly, serum samples were complement- deactivated (30 min at 56° C) prior to 1 h incubation with cytopathic virus (Singer strain was used as BVDV type 1 and 125c as BVDV type 2) at 37° C and 5%CO2. After incubation bovine turbinate cells were added to each well, plates were incubated at 37° C and 5%CO2 for 3 days, and then examined for cytopathic effects of the test virus. Virus neutralizing titers for each serum sample were determined as the reciprocal of the highest dilution at which virus was completely neutralized. Titers lower than two were considered negative.

Analysis of gene expression by qRT-PCR

Detection of BVDV RNA was performed as previously described (Smirnova et al., 2008). Briefly, total RNA was extracted from samples of the umbilical cord blood preserved with Tri-reagent BD for blood derivatives (Sigma, USA) or from frozen caruncular and cotyledonary tissue using Trizol (Sigma, USA) according to manufacturer's protocols. Extracted RNA was purified using the RNeasy MinElute Cleanup kit (Qiagen, USA) and used for cDNA synthesis with the iScript cDNA synthesis kit (Bio-Rad, USA). Semi-quantitative real time PCR (qRT-PCR) was performed in a 384-well plate format on the LightCycler480 (Roche, Basel, Switzerland) with IQ SYBR green Supermix (Bio-Rad, USA). Upon completion of qRT-PCR amplification melting curve analysis was performed to assess the quality of amplification; all amplicons were sequenced to confirm their match to the target genes. The qRT-PCR results were analyzed with the Comparative C_t (ΔC_t) method and presented as $2^{-\Delta Ct}$. Primers for BVDV were designed to target the conserved region of the 5'UTR sequence, nucleotides 190-376. Glyceraldehyde-3-phosphate dehydrogenase (GAPDH) mRNA was used as an endogenous control for data normalization. All primer sequences used for qRT-PCR are listed in Table 8.

Table 8. qRT-PCR primer sequences.

Target gene	*Accession number*	*Primer sequences*
GAPDH	DQ403066	F: TGACCCCTTCATTGACCTTC
		R: CGTTCTCTGCCTTGACTGTG
BVDV	GU395547.1	F: TCGTCAATGGTTCGACACTC
		R: CCGCATGGGTTAAGATGTG
ISG15	NM_174366	F:GGTATCCGAGCTGAAGCAGTT
		R: CCTCCCTGCTGTCAAGGT
RIG-I	DQ471980	F: ACGTGCCAGAACAAATCAGA
		R: TCTGGTTGAACCCTGACTGA
MDA5	XM_615590	F: TGGGACTAACAGCTTCACCA
		R: ACTGCATCAAGATTGGCACA
IFN-α	Z46508	F: TCTCTGTGCTCCATGAGGTG
		R: TAGCTTGACCAGGAGGCTCT
IFN-β	M15477.1	F: GATGCCTGAGGAGATGAAGA
		R: GGTGAGAATGCCGAAGATGT

Statistical analysis

Statistical analysis of qRT-PCR data was performed using Student's *t*-test. Differences with the $P < 0.05$ were considered statistically significant. Data are presented as mean ± standard error (SE).

Results

Viremia in blood of fetuses and their dams

BVDV RNA in blood of infected heifers peaked on days 7 and 10 after BVDV inoculation (day 82 and day 85 of gestation, respectively) using qRT-PCR

(Fig. 14). Viral RNA was at a barely detectable concentration 14 dpmi with BVDV (day 89 of gestation), and was cleared from blood by 22 days after inoculation of the virus (day 97 of gestation). Seroconversion following BVDV infection of the heifers was confirmed at 28 dpmi (day 103 of gestation) using standard serum neutralization assay (data not shown). All control heifers remained free of virus throughout the experiment.

BVDV RNA was not detected in blood of PI fetuses collected on day 82 of gestation (7 dpmi with BVDV). Due to the difficulties in obtaining blood samples in early gestational fetuses, blood was collected only from one PI fetus on day 89 of gestation. Viral RNA was detected in blood of this fetus, indicating that BVDV virus was able to reach the fetus by 14 dpmi. High concentrations of BVDV RNA were detected in all fetuses of the PI group collected on days 97 and 192, and in 2 out of 3 fetuses collected on day 245 of gestation. One fetus from the day 245 group had very low concentration of BVDV RNA, at the limit level of detection despite widespread virus antigen expression in tissues, detected by immunohistochemistry (Bielefeldt-Ohmann et al., 2012). The reason why this fetus has very little viral RNA within the blood is unknown. The greatest BVDV RNA concentration in fetal blood was detected on day 97 of gestation (22 dpmi with BVDV), with significant decrease in BVDV RNA by days 192 and 245 ($P<0.01$; fold reduction between days 97 and 192 - 4.89, days97 and 245 - 13.1). All control fetuses were confirmed to be BVDV-negative at the time of fetal collections.

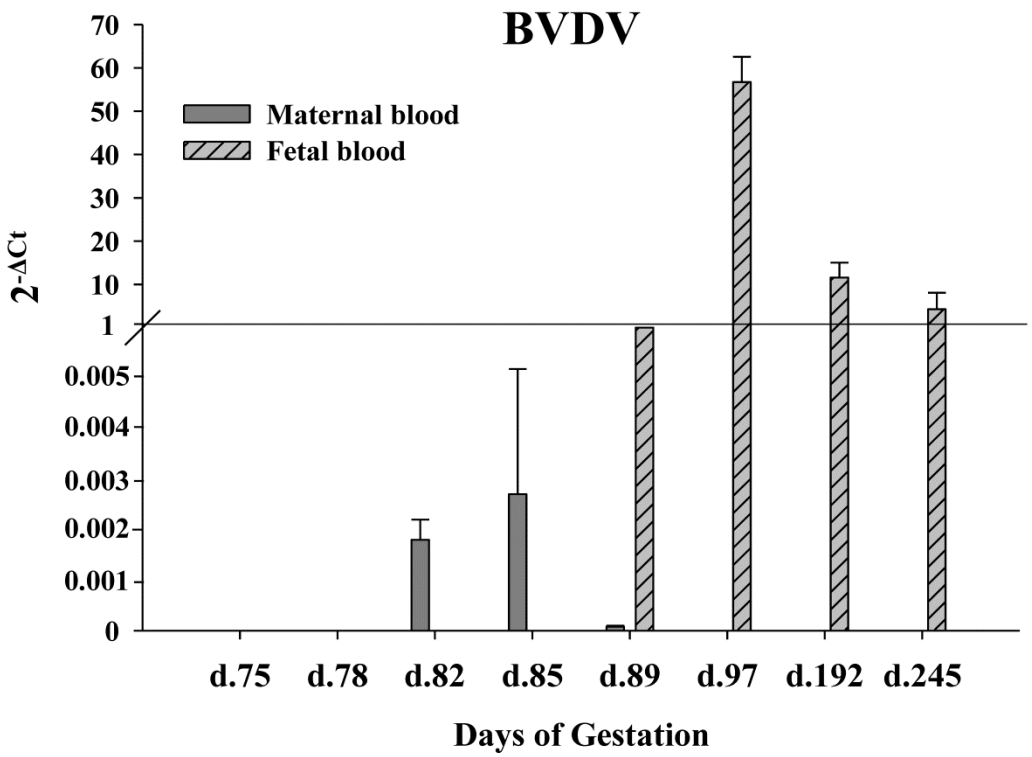

Figure 14. BVDV RNA in maternal and fetal blood (qRT-PCR). Peak of viremia in maternal blood was detected on days 82 and 85 of gestation. BVDV RNA was first detected in fetal blood 14 days after maternal BVDV inoculation (day 89 of gestation), and at all later time points (days 97, 192, and 245). Please note the difference in scale above and below horizontal line at y=1. Data are represented as mean ± SE.

Expression of type I IFN pathway in blood of pregnant heifers and their fetuses

Detection of *ISG15* mRNA was used as an indicator of type I IFN pathway up-regulation in qRT-PCR performed on blood of fetuses and their dams. A robust 53.4-fold increase ($P<0.001$) in *ISG15* mRNA concentration was present in whole blood of BVDV infected pregnant heifers 3 days post BVDV infection (day 78 of gestation), which significantly declined by 7 dpmi (day 82 of gestation;

P<0.001) and returned to baseline by 10 dpmi (day 85 of gestation; Fig. 15, A). *ISG15* mRNA concentrations remained unchanged at the baseline level in blood of control heifers at all time points tested. No difference in *ISG15* mRNA concentration was detected in blood of control and PI fetuses collected 7 dpmi (day 82 of gestation; Fig. 15, B). However, increase of *ISG15* mRNA concentration was detected in blood of the PI fetuses collected at later time points - days 89, 97, and 192 (14, 22 and 117 dpmi, respectively), when compared to the control uninfected fetuses. While average *ISG15* mRNA concentration in blood of PI fetuses on day 245 of gestation remained high, the difference was not statistically significant.

The concentrations of mRNA for cytosolic sensors – *MDA5* and *RIG-I* - in fetal blood are shown in Fig. 15, C and Fig. 15, D, respectively. *RIG-I* mRNA concentration increased significantly in PI fetuses versus control fetuses as early day 82. *RIG-I* mRNA concentration in blood of PI fetuses increased gradually over the course of fetal infection and was significantly higher on day 97 compared to day 82, and on day 192 when compared to day 97. Due to the high individual variation, the difference in *RIG-I* mRNA concentration between PI and control fetuses on day 245 was not significant, even though there was a trend for the average concentration in the PI group to be higher then in the control group (P=0.06). *MDA5* mRNA concentration showed a possible tendency to increase in blood of day 89 PI fetus, was significantly higher in blood of day 97 PI fetuses

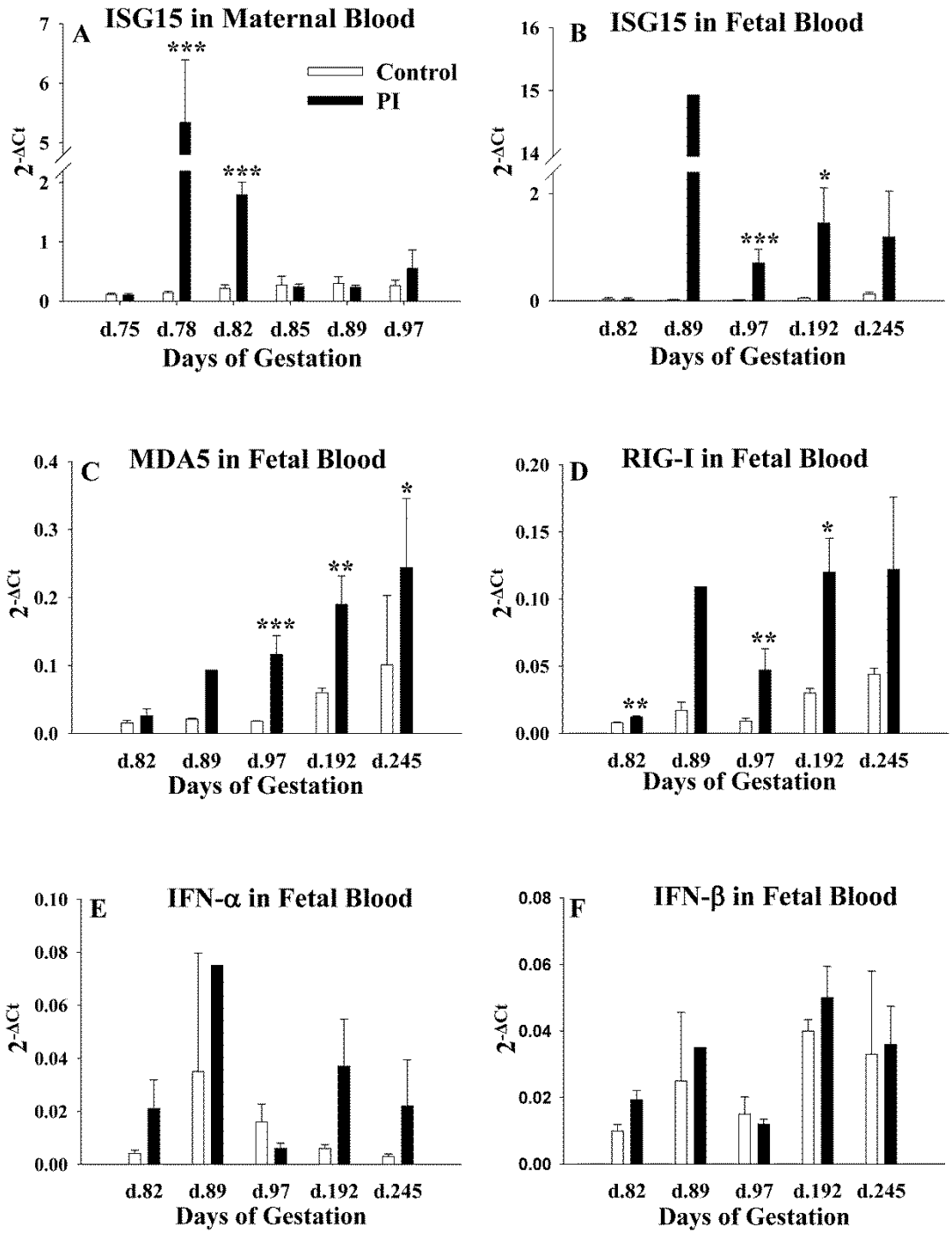

Figure 15. Amplification of type I IFN pathway genes in fetal and maternal blood (qRT-PCR). A, *ISG15* mRNA in blood of pregnant heifers during acute stage of infection; B-F – fetal blood: B, *ISG15* mRNA; C, *MDA5* mRNA; D, *RIG-I* mRNA; E, *IFN-*α mRNA; F,

IFN-β mRNA. Data are represented as mean ± SE. * - P<0.05, ** - P<0.01, *** - P< 0.001.

(P<0.001), and remained significantly higher in PI group compared to control group through days 192 and 245 of gestation. Both *IFN-α* and *IFN-β* mRNA were detected in very low concentrations in fetal blood, however, concentrations did not differ in PI compared to control fetuses (Fig. 15, E and F).

Expression of IFNs and ISGs in caruncle and cotyledon

qRT-PCR was performed on caruncle and cotyledon tissues for BVDV RNA, *IFN-α*, *IFN-β*, and *ISG15* mRNA on three selected time points representing the course of the establishing fetal persistent infection – days 89, 97, and 192 of gestation (Fig. 16). BVDV RNA was detected at similar concentrations in both cotyledon and caruncle tissue samples at each time point tested in PI group, while no viral RNA was amplified from cotyledons and caruncles of the control group (data not shown). No differences were found for *IFN-α* and *IFN-β* mRNA concentrations in caruncle between the control and PI groups on any of the days of gestation tested (Fig. 16, A and C). However, significant increase in *ISG15* mRNA concentration was found in caruncles of the PI vs. control group (Fig. 16, E) on days 97 and 192 (2.6-fold and 4.13-fold, respectively).

No differences in *IFN-α*, *IFN-β*, and *ISG15* mRNA concentrations were detected in cotyledons on days 89 and 97 of gestation when PI fetuses were compared to controls (Fig. 16, B, D and F, respectively). However, mRNA

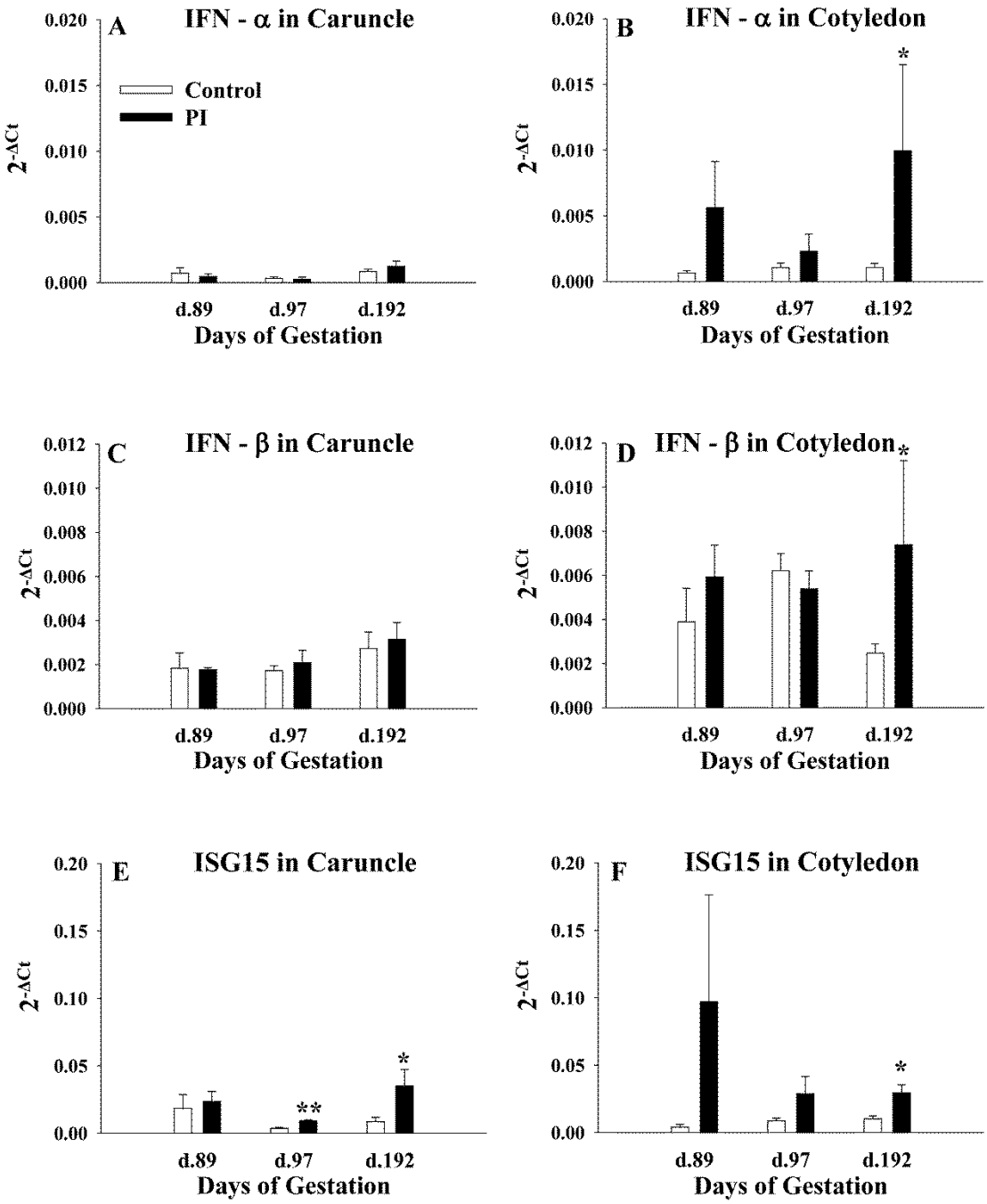

Figure 16. Amplification of *IFN-α, IFN-β, and ISG15* mRNA in caruncle and cotyledon (qRT-PCR). A significant increase in *IFN-α*, *IFN-β*, and *ISG15* mRNA was detected in cotyledons of the PI fetuses on day 192 of gestation. Only *ISG15* mRNA concentrations increased on days 97 and 192 in caruncle. Caruncle: A, *IFN-α* mRNA; C, *IFN-β* mRNA;

E, *ISG15* mRNA. Cotyledon: B, *IFN-α* mRNA; D, *IFN-β* mRNA; F, *ISG15* mRNA. Data are represented as mean $\pm$ SE. * - P<0.05, ** - P<0.01.

concentrations for all three genes were significantly higher on day 192 in PI compared to the control group: 9.3-fold for *IFN-α* mRNA, 3.0-fold for *IFN-β* mRNA, and 2.9-fold for *ISG15* mRNA (P<0.05).

Discussion

Studies of transplacental viral infections present challenges due to the complexity of the processes occurring during the establishment of infection and the contribution of multiple factors of maternal and feto-placental immune responses affecting viral spread and replication. In order for the virus to successfully infect the fetus it has to replicate in maternal blood and tissues, reach and cross the placenta before maternal immune response clears the virus in the dam. The time course required to establish sufficient maternal infection and to spread to the fetal blood likely accounts for the delay in fetal viremia. In the experimental model described herein, maternal viremia was detected 7 days after BVDV inoculation, reproducing findings of a related previous study (Smirnova et al., 2008). Fetuses, collected at the peak of maternal viremia (7 dpmi) did not have any detectable BVDV RNA or antigen. BVDV RNA in fetal blood was detected later, namely, 14 days after BVDV inoculation of their dams, at the time when virus was almost cleared from the maternal blood circulation. Detection of BVDV RNA in fetal blood coincides with the first detection of BVDV

antigen in the brain of two fetuses collected at 14 dpmi as described in a previous publication (Bielefeldt-Ohmann et al., 2012). This finding indicates that fetal viremia and subsequent viral dissemination to the brain of infected fetuses occur between 7 and 14 dpmi. Other studies have described a 72-hour interval for the spread of the virus to fetal tissues(Swasdipan et al., 2002; Tsuboi et al., 2011). The time needed for the virus to reach the ruminant fetus can depend on the species, virulence of the virus isolate, stage of gestation at the time of infection, infectious viral dose, and route of infection. The study, described by Swasdipan et al. (2002), was performed with a sheep model using intranasal inoculation, while the study of Tsuboi et al. (2011) used intravenous inoculation in cows. Both studies used different virus isolates than herein and maternal challenge took place in the first month of the gestation: much earlier than in our model.

In the present experiment BVDV was cleared from maternal blood by 22 dpmi with BVDV, which coincided with the peak of BVDV RNA concentration in the fetal blood. Comparison of the BVDV RNA concentrations in maternal and fetal blood at the peaks of viremia (day 82 and day 97, respectively) revealed striking, ~30,000-fold increase in fetuses compared to dams. The difference in the competence of the immune system between adults and their fetuses in early gestation, as well as the ability of BVDV to replicate more efficiently in fetal cells, might explain the much higher levels of BVDV in fetal blood. Inability of the fetus at early gestation to develop an adequate adaptive immune response is thought to be the key factor allowing the development of fetal persistent infection

(Peterhans et al., 2003; Potgieter, 1995). Surprisingly, BVDV RNA concentrations decreased significantly between day 97 and day 192 (~5-fold) and day 245 (~13-fold) collected fetuses. As noted in the Results, one of the three day 245 PI fetuses had barely detectable BVDV RNA concentration, although viral antigen was detected in the brain (Bielefeldt-Ohmann et al., 2012) and liver (Morarie S. E., unpublished data) of this fetus.

We have previously demonstrated a transient robust increase of *ISG15* mRNA concentration in blood of pregnant heifers infected with the same strain of ncp BVDV as early as 3 dpmi (Smirnova et al., 2008), which is prior to the establishment of detectable viremia. The same drastic, but short-term (3-7 dpmi), ISG15 up-regulation was detected in blood of infected heifers in the current experiment. In contrast, the increase in I*SG15* mRNA concentration in fetal blood coincided with fetal viremia, 14 days after maternal inoculation with BVDV. *ISG15* mRNA concentration remained increased for almost the whole duration of experiment (until at least day 192), indicating that the factor responsible for the induction of ISGs persists in the PI fetuses. Increased expression of *ISG15* mRNA was also detected in fetal spleen and bone marrow (data not shown), and ISG15 protein up-regulation was found in fetal brains with immunohistochemistry starting at 14 dpmi (Bielefeldt-Ohmann et al., 2012).

The ability of ncp BVDV viruses to evade the innate immune response and failure to induce type I IFN pathway through inhibition of IFN regulatory factors 3 and 7 has been described (Baigent et al., 2004; Baigent et al., 2002; Schweizer et al., 2006). However, the ncp BVDV strain used in our experiments induces

strong antiviral activity in blood of infected animals and robust up-regulation of ISGs in blood and tissues (Bielefeldt-Ohmann et al., 2012; Shoemaker et al., 2009; Smirnova et al., 2008). The rapidly developing chronic up-regulation of ISGs in the PI fetuses in our model demonstrates an ability to provide at least partial control over viral replication in the PI fetuses, leading to the decreased viremia in fetuses later in infection/gestation. One fetus, collected at day 245, with very low levels of BVDV RNA in the blood, also had concentrations of *ISG15*, *RIG-I*, and *MDA5* mRNA, comparable with concentrations in blood from control uninfected fetuses.

The innate immune response is triggered by the recognition of pathogen-associated molecular patterns such as viral dsRNA (Saito and Gale, 2007). RNA helicases RIG-I and MDA5 serve as pattern recognition receptors responsible for detection of pathogen's nucleic acids and induction of the type I IFN cascade (Kang et al., 2002; Yoneyama et al., 2004). RIG-I, shown to play a key role in recognition of RNA viruses, specifically and preferentially associates with the copy-back defective interfering RNA particles produced during viral replication (Baum and Garcia-Sastre, 2011). Very rapid increase of *RIG-I* mRNA concentration in PI fetuses might indicate that not only RIG-I is present in early gestation, but also is able to detect very low number of viral particles and trigger the type I IFN pathway, precluding fetal viremia. This is the first report demonstrating that RNA helicases RIG-I and MDA5 can be induced in bovine fetuses as early as the first trimester, thus contributing to the induction of the innate immune response to BVDV infection.

Despite significant up-regulation of RIG-I, MDA5, and ISG15 in fetal blood and other tissues, there was no difference in the mRNA concentrations of *IFN-*α or *IFN-*β in blood of PI fetuses and control uninfected fetuses at any time point examined. *IFN-*α and *IFN-*β mRNAs were also present in fetal spleen and bone marrow, but their concentration did not differ when compared to healthy control fetuses (data not shown). We have previously demonstrated low antiviral activity in blood of only 1 out of 6 PI fetuses in the previous study (Smirnova et al., 2008). Two questions surface based on the findings: what is causing up-regulation of ISGs in fetuses during the establishment of PI and which tissues produce these ISGs?

High antiviral activity was detected previously in the blood of pregnant heifers 7 dpmi with ncp BVDV (Smirnova et al., 2008). The type I IFNs found in the maternal blood during the acute phase of maternal infection could potentially induce ISGs in the fetuses collected during the first 2 weeks after maternal BVDV inoculation if IFNs are able to cross the bovine placenta. We have shown that *in vitro* treatment of naïve peripheral blood mononuclear cells (PBMC) with uterine vein serum collected at day 82 surgeries (7 dpmi) is able to upregulate *RIG-I* and *ISG15* mRNAs (Weiner et al., 2012). Uterine vein serum collected 3 weeks after maternal infection (following seroconversion) was not able to cause up-regulation of ISGs in naïve PBMC. To our knowledge there is no clear information in the literature that proves the ability of IFNs or lack thereof to cross the bovine placenta. Thus the mechanism leading to the induction of fetal ISGs in establishing persistent infection remains unanswered.

Another potential source of IFNs is the placenta itself. It has been shown that trophoblast cells in human placenta are able to produce type I IFNs when stimulated by Sendai virus infection (Aboagye-Mathiesen et al., 1991). High levels of *IFN-α* in placenta during pregnancy are thought to protect the fetus from intrauterine herpes simplex virus infection (Zdravkovic et al., 1997). To evaluate the possibility of placental IFN production we analyzed both *IFN-α* and *IFN-β* mRNA concentration in caruncles and cotyledons on days 97, 192, and 245 of gestation. Both *IFN-α* and *IFN-β* mRNAs were present in low concentration in bovine placenta of BVDV naïve heifers, (caruncular (maternal) and cotyledonary (fetal) tissues). While BVDV RNA was present and *ISG15* mRNA was upregulated in caruncles and cotyledons of the placentome, only cotyledons had higher concentrations of *IFN-α* and *IFN-β* mRNA in fetuses during the established fetal PI (117 dpmi). These data combined with the absence of *IFN-α* and *IFN-β* mRNA up-regulation in fetal blood, bone marrow and spleen suggest that at least during later gestation the cotyledon might be a source of the type I IFN production contributing to the chronic up-regulation of ISGs in PI fetuses. While cotyledon might be the source of the type I IFN secretion, which leads to up-regulation of ISGs in the fetal tissues, it does not explain why fetal cells appear incapable of up-regulating type I IFN expression in response to BVDV, when virus is present both in the placenta and fetus. Additional studies focused on elucidating potential reasons for the phenomenon are needed.

The presented data provide novel insights into the intriguing complex phenomenon of establishment of transplacental persistent infection with BVDV.

Significant questions such as, why fetal tissues are unable to produce the type I IFNs in response to BVDV infection in contrast to placenta, have arisen from this study. Further studies are therefore required to elucidate the complex interactions between the virus and maternal and feto-placental immune responses.

In summary, it is concluded that fetuses respond to the early gestational ncp BVDV infection with the induction of the type I IFN pathway, resulting in chronic ISGs up-regulation. The placenta, more specifically, the cotyledon, might be responsible for the production of IFNs and thus up-regulation of fetal ISGs. The innate immune response of the fetus may be partially effective in curtailing viral replication, but is not able to eliminate the virus without contribution from the mature adaptive immune response.

CHAPTER V.

CONCLUSIONS

These studies investigated the morphogenesis of fetal skeletal lesions, biomechanical effects of PI on the developing skeleton and temporal development of the innate immune responses to PI. The experimental model utilized for this work was unique in that fetuses were collected at multiple time points both within the acute and chronic stages of PI.

The major findings that emerged from examining the morphogenesis of fetal skeletal lesions were the cyclic nature (approximately 15 days) of the growth retardation lattices, which arise secondary to decreased osteoclast numbers, and impaired tissue level bone formation. Radiographically apparent skeletal lesions were not documented until day 192 of gestation (117 days post maternal inoculation), although there were tendencies for both trabecular bone volume to be increased and osteoclast numbers to be decreased on day 97 of gestation (22 days post maternal inoculation). Fetal viremia peaks some time between days 97 and 192, most likely closer to day 97, which coincides with the initial lesions in some day 97 fetuses. With increasing fetal age, bone lesion severity increases, while the level of viremia decreases. This observation along with the absence of viral antigen or cytopathic lesions within osteoclasts suggests that BVDV does not directly affect osteoclasts.

The reduced tissue level bone formation was an unexpected finding that

could result from impaired osteoblast differentiation, proliferation, activation or recruitment. In states of reduced bone resorption, such as in PI fetus, impaired bone formation appears to be common due to the extensive cross-talk and regulatory control by osteoclasts and osteoblasts over one another (Martin and Sims, 2005). C-fos deficient mice, which develop severe osteopetrosis secondary to impaired osteoclast differentiation have impaired bone formation rates (Grigoriadis et al., 1994). C-fos and its osteoclast specific transcriptional target, fos like antigen 1, are downregulated in the bone marrow of PI fetuses and may indicate that osteoclast differentiation is impaired (APPENDIX IV). Attempts to determine whether a soluble factor within the serum, such as IFN-I, was present and capable of impairing osteoclast differentiation in vitro were fraught with high inter/intra assay variations but revealed no major differences. The cause of reduced osteoclast numbers was not definitively identified. The cause of the cyclic nature of the metaphyseal lesions was not extensively investigated although a cyclic impairment of osteoclast differentiation seems most probably based on the collective data. Serial collection of bone marrow or fetal blood samples during the time course of lesion development may lend additional information with respect to effects on other cell types and potential mechanisms underlying this unique feature.

Congenital BVDV infections has been associated with neonatal longbone fractures (reviewed in CHAPTER III), however mechanical testing of fetal femora on day 192 and 245 did not reveal any significant reduction in bone material properties, nor composition. An unexpected finding of the mechanical testing

experiment was the marked effect of cortical geometry on area normalized mechanical parameters. Mechanical testing of beams machined from cortical bone would have alleviated any effect of cortical geometry and been a better experimental approach to determine whether inherent biomechanical properties of long bones were compromised by PI. The mild nature of bone lesions obtained may have been an important contributor to the lack of observed biomechanical effects as the lesions were less severe than those obtained during previous infections with the same viral strain and dose (Smirnova et al., 2008). The reason for the latter is not clear but presumably is related to differences in host or environmental factors.

Examination of the temporal development of the innate immune response not only revealed interesting findings, but also gave rise to additional questions. Upregulation of IFN-α and IFN-β mRNA concentrations in the cotyledon of PI fetus in the absence of detectable upregulation of these genes in fetal tissues was the most significant finding. This finding lead to the question of why PI fetuses are unable to upregulate IFN-α and IFN-β when they are: 1) physiologically able to produce IFN-I and 2) respond to type I IFN with massive upregulation of ISGs in all tissues evaluated. There are approximately a dozen manuscripts describing inhibition of type I IFN production by BVDV nonstructural proteins (reviewed in CHAPTER IV), but this virus-interferon regulatory factor interaction does not fully explain the discrepancy between type I IFN production in the two tissues knowing that virus is present in both locations (fetal tissues, cotyledon). It seems plausible that the epigenetic dysregulation documented in

PI fetuses (APPENDIX) may have a role in silencing fetal type I IFN production ,but not placental type I IFN production as there are marked differences in epigenetic regulation of gene expression between the fetus and placenta (Chapman, 1984; Rossant, 1986). Expression of IFN-α and IFN-β genes do not appear to be regulated by methylation of DNA cytosine residues as the promotor regions of these genes lack classical CpG islands. This observation certainly does not discount the possible effect of other epigenetic mechanisms (reviewed in APPENDIX VI) exerting control on type I IFN gene expression nor the effects of such mechanisms on other genes that regulate type I IFN expression. Although the experimental model that was used for these experiments enables one to investigate the temporal aspects of PI by collecting fetuses during different time point during the course of infection, its single limitation is the low numbers of animals at each collection points compounded with marked individual variation in fetal response to PI manifesting as variation in lesion severity. The individual variations in fetal response to PI continues to be a source of intrigue and underscores not only the complexity of the model used but also how little we know about the effects of fetal, placental and maternal (host) factors on the outcome of transplacental infection with BVDV.

REFERENCES

Aboagye-Mathiesen, G., Toth, F.D., Juhl, C., Norskov-Lauritsen, N., Petersen, P.M., Zachar, V. and Ebbesen, P. (1991) Characterization of Sendai virus-induced human placental trophoblast interferons. Journal of General Virology 72 (Pt 8), 1871-6.

Akhter, M.P., Fan, Z. and Rho, J.Y. (2004) Bone Intrinsic Material Properties in Three Inbred Mouse Strains. Calcified Tissue International 75(5), 416-420.

Baigent, S.J., Goodbourn, S. and McCauley, J.W. (2004) Differential activation of interferon regulatory factors-3 and -7 by non-cytopathogenic and cytopathogenic bovine viral diarrhoea virus. Veterinary Immunology Immunopathology 100(3-4), 135-44.

Baigent, S.J., Zhang, G., Fray, M.D., Flick-Smith, H., Goodbourn, S. and McCauley, J.W. (2002) Inhibition of beta interferon transcription by noncytopathogenic bovine viral diarrhea virus is through an interferon regulatory factor 3-dependent mechanism. Journal Virology 76(18), 8979-88.

Barker, D.J.P. (1994) The fetal origins of adult disease. Fetal and Maternal Medicine Review 6, 71-80.

Baum, A. and Garcia-Sastre, A. (2011) Differential recognition of viral RNA by RIG-I. Virulence 2(2), 166-9.

Baumgartner, W., Boyce, R. W., Weisbrode, S. E., Alldinger, S., Axtthelm, M. K., Krakowka, S. (1995) Histologic and immunocytochemical characterization

of canine distemper-associated metaphyseal bone lesions in young dogs following experimental infection. Veterinary Pathology 32, 702-709.

Bielefeldt-Ohmann, H. (1995) The pathologies of bovine viral diarrhea virus infection. A window on the pathogenesis. Veterinary Clinics of North America: Food Animal Practice 11(3), 447-76.

Bielefeldt-Ohmann, H., Smirnova, N.P., Tolnay, A.E., Webb, B.T., Antoniazzi, A.Q., van Campen, H. and Hansen, T.R. (2012) Neuro-invasion by a 'Trojan Horse' strategy and vasculopathy during intrauterine flavivirus infection. Internation Journal of Experimental Patholology 93(1), 24-33.

Bielefeldt-Ohmann, H., Tolnay, A.E., Reisenhauer, C.E., Hansen, T.R., Smirnova, N. and Van Campen, H. (2008) Transplacental infection with non-cytopathic bovine viral diarrhoea virus types 1b and 2: viral spread and molecular neuropathology. Journal of Comparative Pathology 138(2-3), 72-85.

Bjorkman, N., Bloom, G. (1957) On the fine structure of the foetal-maternal junction in the bovine placentome. Zeitschrift fur Zellforsch Mikroskopisch-Anatomische 45(6), 649-659.

Brock, K.V. (2003) The persistence of bovine viral diarrhea virus. Biologicals 31(2), 133-5.

Brock, K.V. (2004) The many faces of bovine viral diarrhea virus. Veterinary Clinics of North America: Food Animal Practice 20, 1-3.

Brown, T.T., Scott, F. W., de Lahunta, A. (1975) Pathogenetic studies of infection of the boviine fetus with bovine viral diarrhea virus. II. Ocular lesions. Veterinary Pathology 12(5-6), 394-404.

Brownlie, J., Clarke, M.C. and Howard, C.J. (1989) Experimental infection of cattle in early pregnancy with a cytopathic strain of bovine virus diarrhoea virus. Research in Veterinary Science 46(3), 307-11.

Brownlie, J., Hooper, L.B., Thompson, I. and Collins, M.E. (1998) Maternal recognition of foetal infection with bovine virus diarrhoea virus (BVDV)—the bovine pestivirus. Clinical and Diagnostic Virology 10(2–3), 141-150.

Brownlie, J.C., M. C., Howard, C. J. (1984) Experimental production of fatal mucosal disease in cattle. Veterinary Record 114, 535-536.

Bunn, T.L., Parsons, P.J., Kao, E. and Dietert, R.R. (2001) Gender-based profiles of developmental immunotoxiicty to lead in the rat: assessment in juveniles and adults. Journal of Toxicology and Environmental Health, Part A 64(3), 223-240.

Caffrey, J.F.D., A. M., Donnelly, W.J. C., Sheahan, B. J., Atkins, G. J. (1996) Morphometric analysis of growth retardation in fetal lambs following experimental infection of pregnant ewes with Border Disease virus. Research in Veterinary Science 62(3), 245-248.

Caraso, A.P.E., Kendrick, J. W., Kennedy, P. C. (1971) Response of the bovine fetus to bovine viral diarrhea-mucosal disease virus. American Journal of Veterinary Research 32, 1543-1562.

Carbrey, E.A., Downing, D. R., Snyder, M. L., Wessman, S. J., Gustafson, G. A. (1973) Microtiter and automated serologic techniques for diagnostic virology. Proceedings of the Annual Meeting of the United States Animal Health Associatation 77, 553-562.

Chapman, V., Forrester, L., Sandrod, J., Hastie, N. (1984) Cell lineage-specific undermethylation of mouse repetitive DNA. Nature 307, 284-286.

Chase, C.C., Elmowalid, G. and Yousif, A.A. (2004) The immune response to bovine viral diarrhea virus: a constantly changing picture. Veterinary Clinics of North America: Food Animal Practice 20(1), 95-114.

Childs, T. (1946) X Disease of Cattle- Saskatchewan. Canadian Journal of Compative Medicine and Veterinary Science 10(11), 316-319.

Chucri, T.M., Monteiro, J.M., Lima, A.R., Salvadori, M.L., Kfoury, J.R., Jr. and Miglino, M.A. (2010) A review of immune transfer by the placenta. Journal of Reproductive Immunology 87(1-2), 14-20.

Cleveland, R. and Liu, Y. (1996) CD4 Expression by erythroid precursor cells in human bone marrow. Blood 87(6), 2275-2282.

Collen, T. and Morrison, W.I. (2000) CD4(+) T-cell responses to bovine viral diarrhoea virus in cattle. Virus Research 67(1), 67-80.

Collins, M.E., Desport, M., Brownlie, J. (1999) Bovine viral diarrhea quasispecies during persistent infection. Virology 259, 85-98.

Constable, P., Hull, B., Wicks, J. and Myer, W. (1993) Femoral and tibial fractures in a newborn calf after transplacental infection with bovine viral diarrhoea virus. Veterinary Record 132(15), 383-385.

Coria, M.F. and McClurkin, A.W. (1978) Specific immune tolerance in an apparently healthy bull persistently infected with bovine viral diarrhea virus. Journal of the American Veterinary Medical Association 172(4), 449-51.

Currey, J.D. (1999) What determines the bending strength of compact bone? Journal of Experimental Biology 202(18), 2495-2503.

Currey, J.D. and Pond, C.M. (1989) Mechanical properties of very young bone in the axis deer (Axis axis) and humans. Journal of Zoology 218(1), 59-67.

Dietert, R.R., Lee, J.-E., Olsen, J., Fitch, K. and Marsh, J.A. (2003) Developmental immunotoxicity of dexamethasone: comparison of fetal versus adult exposures. Toxicology 194(1–2), 163-176.

Done, J.T., Terlecki, S., Richardson, C., Harkness, J.W., Sands, J.J., Patterson, D.S., Sweasey, D., Shaw, I.G., Winkler, C.E. and Duffell, S.J. (1980) Bovine virus diarrhoea-mucosal disease virus: pathogenicity for the fetal calf following maternal infection. Veterinary Record 106(23), 473-9.

Dow, C.J., W. F. H., Mcintyre, K. (1960) A disease of cattle in Britain resembling the virus diarrhoea-mucosal disease complex. Veterinary Record 68, 620-623.

Draper, E.R.C. and Goodship, A.E. (2003) A novel technique for four-point bending of small bone samples with semi-automatic analysis. Journal of Biomechanics 36(10), 1497-1502.

Duffell, S.J., Sharp, M.W., Winkler, C.E., Terlecki, S., Richardson, C., Done, J.T., Roeder, P.L. and Hebert, C.N. (1984) Bovine virus diarrhoea-mucosal

disease virus-induced fetopathy in cattle: Efficacy of prophylactic maternal pre-exposure. Veterinary Record 114(23), 558-61.

Duplomb, L.D., M., Jourdon, P., Heymann, D. (2007) Concise review: embryonic stem cells: A new tool to study osteoblast and osteoclast differentiation. Stem Cells 25, 544-552.

Eisenstein, R., Kawanoue, S. (1975) The lead line in bone - A lesion apparently due to chondroclastic indigestion. American Journal of Pathology 80, 309-316.

Ellis, J.A., West, K. H., Cortese, V. S., Myers, S. L. Carman, S., Martin, K. M., Haines, D. M. (1998) Lesions and distribution of viral antigen following an experimental infection of young seronegative calves with virulent bovine viral diarrhea virus type II. Canadian Journal of Veterinary Research 62, 161-169.

Espinasse, J., Parodi, A.L., Constantin, A., Viso, M., Lava, A. (1986) Hyena disease in cattle: A review. Veterinary Record 118, 328-330.

Fray, M.D., Paton, D.J. and Alenius, S. (2000a) The effects of bovine viral diarrhoea virus on cattle reproduction in relation to disease control. Anim Reprod Sci 60-61, 615-27.

Fray, M.D., Supple, E.A., Morrison, W.I. and Charleston, B. (2000b) Germinal centre localization of bovine viral diarrhoea virus in persistently infected animals. Journal of General Virology 81(7), 1669-1673.

Fredriksen, B., Press, C.M., Loken, T. and Odegaard, S.A. (1999) Distribution of viral antigen in uterus, placenta and foetus of cattle persistently infected with bovine virus diarrhoea virus. Veterinary Microbiology 64(2-3), 109-22.

Fredriksen, B., Press, C. M., Sandvik, T., Odegaard, S. A., Loken, T. (1999) Dection of viral antigen in placenta and fetus of cattle of acutely infected with bovine viral diarrhea virus. Veterinary Pathology 36, 267-275.

Garnero, P., Borel, O., Gineyts, E., Duboeuf, F., Solberg, H., Bouxsein, M.L., Christiansen, C. and Delmas, P.D. (2006) Extracellular post-translational modifications of collagen are major determinants of biomechanical properties of fetal bovine cortical bone. Bone 38(3), 300-309.

Gillespie, J., Baker, J., McEntee, K. (1960) A cytopathogeneic strain of virus diarrhea virus. Cornell Veterinarian 50, 73-79.

Gillespie, J.H., Coggins, L., Thompson, J., Baker, J. A. (1961) Comparison of neutralization tests of strains of virus isolated from virus diarrhea and mucosal disease. Cornell Veterinarian(51), 155-159.

Goyal, S.M., Ridpath J.F. (2005) Bovine viral diarrhea virus. diagnosis, management, and control., 261 pp. first ed. Trans. 0-8138-0478-7, edited by R.J.F. Goyal S.M. Blackwell Publishing, Ames, Iowa, USA.

Graham, C.B., Thal, A. and Wassum, C.S. (1970) Rubella-like bone changes in congenital cytomegalic inclusion disease. Radiology 94(1), 39-43.

Grigoriadis, A., Wang, Z., Cecchini, M., Hofstetter, W., Felix, R., Fleisch, H. and Wagner, E. (1994) c-Fos: a key regulator of osteoclast-macrophage lineage determination and bone remodeling. Science 266(5184), 443-448.

Gunn, G.J., Stott, A.W. and Humphry, R.W. (2004) Modelling and costing BVD outbreaks in beef herds. Veterinary Journal 167(2), 143-9.

Haas, A.L., Ahrens, P. Bright, P. M., Ankel, H. (1987) Interferon induces a 15 kilodalton protein exhibiting marked homology to ubiquitin. Journal of Biologic Chemistry 262(23), 11315-11323.

Halliday, R. (1978) Immunity and health in young lambs. Veterinary Record 103(22), 489-492.

Hamers, C., Dehan, P., Couvreur, B., Letellier, C., Kerkhofs, P. and Pastoret, P.P. (2001) Diversity among bovine pestiviruses. Veterinary Journal 161(2), 112-22.

Hansen, T.R., Smirnova, N.P., Van Campen, H., Shoemaker, M.L., Ptitsyn, A.A. and Bielefeldt-Ohmann, H. (2010) Maternal and fetal response to fetal persistent infection with bovine viral diarrhea virus. American Journal of Reproductive Immunology 64(4), 295-306.

Harding, M.J., Cao, X., Shams, H., Johnson, A.F., Vassilev, V.B., Gil, L.H., Wheeler, D.W., Haines, D., Sibert, G.J., Nelson, L.D., Campos, M. and Donis, R.O. (2002) Role of bovine viral diarrhea virus biotype in the establishment of fetal infections. American Journal of Veterinary Research 63(10), 1455-63.

Hirbe, A.C., Rubin, J., Uluçkan, Ö., Morgan, E.A., Eagleton, M.C., Prior, J.L., Piwnica-Worms, D. and Weilbaecher, K.N. (2007) Disruption of CXCR4 enhances osteoclastogenesis and tumor growth in bone. Proceedings of the National Academy of Sciences 104(35), 14062-14067.

Hoover, E.A., Griesemer, R. A. (1971) Bone lesions produced by feline herpesvirus. Laboratory Investigation 25, 457-464.

Houe, H. (1993) Survivorship of animals persistently infected with bovine virus diarrhoea virus (BVDV). Preventive Veterinary Medicine 15(4), 275-283.

Houe, H. (1999) Epidemiological features and economical importance of bovine virus diarrhoea virus (BVDV) infections. Veterinary Microbiology 64(2-3), 89-107.

Huffer, W.E., Ruegg, P., Zhu, J. M. Lepoff, R. B. (1994) Semiautomated methods for cancellous bone histomorphoemtry using a general purpose video image analysis system. Journal of Microscopy 173, 53-66.

Igwebuike, U.M. (2006) Trophoblast cells of ruminant placentas--A minireview. Animal Reproductive Science 93(3-4), 185-98.

Jensen, J., Schultz, R. D. (1991) Effect of infection by bovine viral diarrhea virus (BVDV) in vitro on interleukin-1 activity of bovine monocytes. Veterinary Immunology Immunopathology 29, 251-265.

Jotereau, F.V., Le Douarin, N. M. The developmental relationship between osteocytes and osteoclast: a study using quail-chick nuclear markers in endochondral ossification. Developmental Biology 63, 255-265.

Kaariainen, L., Ranki, M. (1984) Inhibition of cell functions by RNA-virus infections. Annual Review of Microbiology 38, 91-109.

Kahrs, R. (1968) The relationship of bovine viral diarrhea-mucosal disease to abortion in cattle. Journal of the American Veterinary Medical Asssociation 153, 1652-1655.

Kahrs, R.F. (1973) Effects of bovine viral diarrhea on the developing fetus. Journal of the American Veterinary Medical Asssociation 163, 877-878.

Kang, D.C., Gopalkrishnan, R.V., Wu, Q., Jankowsky, E., Pyle, A.M. and Fisher, P.B. (2002) mda-5: An interferon-inducible putative RNA helicase with double-stranded RNA-dependent ATPase activity and melanoma growth-suppressive properties. Proceedings of the National Academy of Sciences 99(2), 637-42.

Kato, H., Takeuchi, O., Sato, S., Yoneyama, M., Yamamoto, M., Matsui, K., Uematsu, S., Jung, A., Kawai, T., Ishii, K.J., Yamaguchi, O., Otsu, K., Tsujimura, T., Koh, C.S., Reis e Sousa, C., Matsuura, Y., Fujita, T. and Akira, S. (2006) Differential roles of MDA5 and RIG-I helicases in the recognition of RNA viruses. Nature 441(7089), 101-5.

Kelling, C.L. (2007) Viral diseases of the fetus. Virology Papers 1(1), paper 127.

Kendrick, J.W. (1971) Bovine viral diarrhea-mucosal diseases virus infection in pregnant cows. American Journal of Veterinary Research 32, 533-544.

Khan, A.J., Simmons, D. J. (1975) Investigation of the cell lineage in bone using a chimera of chick and quail embryonic tissue. Nature 258, 325-327.

Kim, J.H., Jin, H. M., Kim, K., Song, I., Youn, B. U. Matsuo, K., Kim, N. (2009) The mechanisms of osteoclast differentiation induced by IL-1. Journal of Immunology 183, 1862-1870.

Kopelman, A.E., Minnefor, A.B. and Halsted, C.C. (1972) Osteomalacia and spontaneous fractures in twins with congenital cytomegalic inclusion disease. Journal of Pediatrics 81(1), 101-5.

Lamm, C.G., Broaddus, C.C. and Holyoak, G.R. (2009) Distribution of bovine viral diarrhea virus antigen in aborted fetal and neonatal goats by immunohistochemistry. Veterinary Pathology 46(1), 54-58.

Land, C. and Schoenau, E. (2008) Fetal and postnatal bone development: reviewing the role of mechanical stimuli and nutrition. Best practice & research. Clinical endocrinology & metabolism 22(1), 107-118.

Larsson, B., Jacobsson, S. O., Bengtsson, B. (1991) Congentical curly haircoat as a symptoms of persistent infection with bovine virus diarrhoea virus in calves. Archives of Virology Supplement 3, 143-148.

Leiser, R. and Kaufmann, P. (1994) Placental structure: in a comparative aspect. Experimental and Clinical Endocrinology and Diabetes 102(3), 122-34.

Leiser, R., Krebs, C., Klisch, K., Ebert, B., Dantzer, V., Schuler, G. and Hoffmann, B. (1997) Fetal villosity and microvasculature of the bovine placentome in the second half of gestation. Journal of Anatomy 191 (Pt 4), 517-27.

Leiss, B., Frey, H-R., Kittsteiner, H., Baumann, F., Neumann, W. (1974) Beobachtungen und Utersuchungenuber die (mucosal disease) des Rindes. Dtsch Tieraerztl Wochenschr 81, 477-500.

Lenschow, D.J., Lai, C., Frias-Staheli, N., Giannakopoulos, N. V., Lutz, A., Wolff, T., Osiak, A., Levine, B., Schmidt, R. E. Garcia-Sastre, A., Leib, D. A., Pekosz, A., Knobelock, K. P., Horak, I., Virgin, H. W. T. (2007) INF-stimulated gene 15 functions as a critical antiviral molecule agaist

influenza, herpes, and Sindbis viruses. Proceedings of the National Academy of Sciences 104(4), 1371-1376.

Liu, C.C., Sherrard, D. J., Maloney, N. A., Howard G. A. (1987) Reactivation of inhibited bone acid phosphatase and its significance in bone histomorphometry. Journal of Histochemistry and Cytochemistry 35, 1355-1367.

Loneragan, G.H., Thomson, D.U., Montgomery, D.L., Mason, G.L. and Larson, R.L. (2005) Prevalence, outcome, and health consequences associated with persistent infection with bovine viral diarrhea virus in feedlot cattle. Journal of the American Veterinary Medical Asssociation 226(4), 595-601.

Loveless, H.S. (1966) Flexural Tests.In: Schmitz, J. V. (Ed), Testing of Polymers. Interscivence Publishers, London 2, 321-347.

Malmquist, W.A. (1968) Bovein viral diarrhea-mucosal disease: etiology, pathogenesis and applied immunity. Journal of the American Veterinary Medical Asssociation 152, 763-768.

Martin, T.J. and Sims, N.A. (2005) Osteoclast-derived activity in the coupling of bone formation to resorption. Trends in Molecular Medicine 11(2), 76-81.

McClurkin, A.W., Littledike, E.T., Cutlip, R.C., Frank, G.H., Coria, M.F. and Bolin, S.R. (1984) Production of cattle immunotolerant to bovine viral diarrhea virus. Canadian Journal of Compative Medicine 48(2), 156-61.

Mengeling, W.L., Van Der Naaten, M. J. (1988) Prepartion of embryonic spleen cell cultures. Journal of Tissue and Culture Methods 11(3), 135-139.

Meyers, G., Tautz, N., Stark, R., Brownlie, J., Dubovi, E.J., Collett, M.S. and Thiel, H.-J. (1992) Rearrangement of viral sequences in cytopathogenic pestiviruses. Virology 191(1), 368-386.

Meyers, G. and Thiel, H.-J. (1996) Molecular characterization of pestiviruses. In: F.A.M. Karl Maramorosch and J.S. Aaron (Eds), Advances in Virus Research, pp. 53-118. Vol. Volume 47. Academic Press.

Moerman, A., Straver, P.J., de Jong, M.C., Quak, J., Baanvinger, T. and van Oirschot, J.T. (1994) Clinical consequences of a bovine virus diarrhoea virus infection in a dairy herd: a longitudinal study. Veterinary Quarterly 16(2), 115-9.

Montgomery, D.L., Van Olphen, A., Van Campen, H., Hansen, T. R. (2008) The fetal brain in bovine diarrhea virus-infected calves: lesions, distribution, and cellular heterogeneity of viral antigen at 190 days gestation. Veterinary Pathology 45, 288-296.

Muñoz-Zanzi, C.A., Hietala, S.K., Thurmond, M.C. and Johnson, W.O. (2003) Quantification, risk factors, and health impact of natural congenital infection with bovine viral diarrhea virus in dairy calves. American Journal of Veterinary Research 64(3), 358-365.

Muñoz-Zanzi, C.A., Thurmond, M.C. and Hietala, S.K. (2004) Effect of bovine viral diarrhea virus infection on fertility of dairy heifers. Theriogenology 61(6), 1085-1099.

Murray, R.D. (1990) A field investigation of causes of abortion in dairy cattle. Veterinary Record 127(22), 543-7.

Nicholson, G.C., Malakellis, M., Collier, F. M., Cameron, P. U., Holloway, W. R., Gough, T. J., Gregorio-King, C., Kirdland, M. A., Myers, D. E. (2000) Induction fo osteoclast from CD14-positive human peripheral blood mononuclear cells by receptor activator of nuclear factor Kappa B ligand (RANKL). Clinical Science 99, 133-140.

Norrdin, R.W., Phemister, R.D., Jaenke, R.S. and Lo Presti, C.A. (1977) Density and composition of trabecular and cortical bone in perinatally irradiated beagles with chronic renal failure. Calcified Tissue Research 24(1), 99-104.

Nuss, K., Spiess, A., Hilbe, M., Sterr, K., Reiser, M. and Matis, U. (2005) Transient benign osteopetrosis in a calf persistently infected with bovine virus diarrhoea virus. Veterinary and Comparative Orthopaedics and Traumatology 18(2), 100-4.

O' Connor, B.P., Doige, C. E. (1993) Abnormal modelling of trabecular bone in calves. Canadian Journal Veterinary Research 57, 25-32.

O'Toole, D. (2006) Osteopetrosis with long bone fractures in neonatal calves persistently infected with nc BVDV. In proceedings of the 49th Annual Meeting of the AAVLD, Minneapolis, Minnesota.

Olafson, P., McCallum, A. and Fox, F. (1946) An apparently new transmissible disease of cattle (BVD). Cornell Veterinarian 36, 205-213.

Parfitt, A.A., Drezner, M. K., Glorieux, F. H., Kanis, J. A., Malluche, H., Meunier, P. J., Ott, Sm. M., Recker, R. R. (1987) Bone histomorphometry:

standardization of nomenclature, symbols and units. Journal of Bone and Mineral Research 2, 595-610.

Parsonson, I.M., O'Halloran, M. L., Zee, Y. C., Snowdan, W. A. (1979) The effects of bovine viral diarrhoea-mucosal disease virus on the ovine fetus. Veterinary Microbiology 4(279-292).

Peterhans, E., Jungi, T.W. and Schweizer, M. (2003) BVDV and innate immunity. Biologicals 31(2), 107-12.

Potgieter, L.N. (1995) Immunology of bovine viral diarrhea virus. Veterinary Clinics of North America: Food Animal Practice 11(3), 501-20.

Ramsey, F.K., Chivers, W. H. . (1953) Mucosal disease of cattle. North American Veterinarian 34, 629-633.

Ridpath, J. (2010) The contribution of infections with bovine viral diarrhea viruses to bovine respiratory disease. Veterinary Clinics of North America: Food Animal Practice 26(2), 335-348.

Ridpath, J.F., Bolin, S.R. and Dubovi, E.J. (1994) Segregation of bovine viral diarrhea virus into genotypes. Virology 205(1), 66-74.

Ritchlin, C.T., Haas-Smith, S.A., Li, P., Hicks, D.G. and Schwarz, E.M. (2003) Mechanisms of TNF-α– and RANKL-mediated osteoclastogenesis and bone resorption in psoriatic arthritis. The Journal of Clinical Investigation 111(6), 821-831.

Rohrer, F. (1921) Der Index der Korperfulle als MaB des Ernahrungszustandes (The index of corpulence as a measure of nutritional state. Munch Med Wochensch 68(580-582).

Rossant, J., Sandford, J. P., Chapman, V. M., Andrews, G. K. (1986) Undermethylation of structural gene sequences in extraembryonic lineages of the mouse. Developmental Biology 117, 567-573.

Sacks, R. and Habermann, E.T. (1977) Pathological fracture in congenital rubella. A case report. Journal of Bone and Joint Surgery 59(4), 557-9.

Saito, T. and Gale, M., Jr. (2007) Principles of intracellular viral recognition. Current Opinion in Immunology 19(1), 17-23.

Saliki, J.T., Fulton, R.W., Hull, S.R. and Dubovi, E.J. (1997) Microtiter virus isolation and enzyme immunoassays for detection of bovine viral diarrhea virus in cattle serum. Journal of Clinical Microbiology 35(4), 803-7.

Schaffler, M.B. and Burr, D.B. (1988) Stiffness of compact bone: Effects of porosity and density. Journal of Biomechanics 21(1), 13-16.

Schweizer, M., Matzener, P., Pfaffen, G., Stalder, H. and Peterhans, E. (2006) "Self" and "nonself" manipulation of interferon defense during persistent infection: bovine viral diarrhea virus resists alpha/beta interferon without blocking antiviral activity against unrelated viruses replicating in its host cells. Journal of Virology 80(14), 6926-35.

Schweizer, M. and Peterhans, E. (2001) Noncytopathic Bovine Viral Diarrhea Virus Inhibits Double-Stranded RNA-Induced Apoptosis and Interferon Synthesis. Journal of Virology 75(10), 4692-4698.

Scruggs, D.W., Fleming, S. A., Maslin, W. R., Grace, A. W. (1995) Osteopetrosis, anemia, thrombocytopenia and marrow necrosis is beef calves naturally

infected with bovine virus diarrhea virus. Journal of Veterinary Diagnostic Investigation 7, 555-559.

Shoemaker, M.L., Smirnova, N.P., Bielefeldt-Ohmann, H., Austin, K.J., van Olphen, A., Clapper, J.A. and Hansen, T.R. (2009) Differential expression of the type I interferon pathway during persistent and transient bovine viral diarrhea virus infection. Journal of Interferon and Cytokine Research 29(1), 23-35.

Silva, M.J., Brodt, M.D. and Ettner, S.L. (2002) Long bones from the senescence accelerated mouse SAMP6 have increased size but reduced whole-bone strength and resistance to fracture. Journal of Bone and Mineral Research 17(9), 1597-1603.

Silva, M.J., Brodt, M.D., Fan, Z. and Rho, J.-Y. (2004) Nanoindentation and whole-bone bending estimates of material properties in bones from the senescence accelerated mouse SAMP6. Journal of Biomechanics 37(11), 1639-1646.

Sivagurunathan, S., Muir, M. M., Brennan, T. C., Seale, J. P., Mason, R. S. (2005) Influence of glucocorticoids on human osteoclast generation and activity. Journal of Bone and Mineral Research 20, 390-398.

Sminia, T., Dijkstra, C. D. (1986) The origin of osteoclast: an immunohistochemical study on macrophages and osteoclast in embryonic rat bone. Calcified Tissue International 39, 263-266.

Smirnova, N.P., Bielefeldt-Ohmann, H., Van Campen, H., Austin, K.J., Han, H., Montgomery, D.L., Shoemaker, M.L., van Olphen, A.L. and Hansen, T.R.

(2008) Acute non-cytopathic bovine viral diarrhea virus infection induces pronounced type I interferon response in pregnant cows and fetuses. Virus Research 132(1-2), 49-58.

Smirnova, N.P., Ptitsyn, A.A., Austin, K.J., Bielefeldt-Ohmann, H., Van Campen, H., Han, H., van Olphen, A.L. and Hansen, T.R. (2009) Persistent fetal infection with bovine viral diarrhea virus differentially affects maternal blood cell signal transduction pathways. Physiologic Genomics 36(3), 129-39.

Smith, R.K. and Specht, E.E. (1979) Osseous lesions and pathologic fractures in congenital cytomegalic inclusion disease: report of a case. Clinical Orthopaedics and Related Research(144), 280-3.

Snowdon, W.A., Parsonson, I. M., Broun, M. L. (1975) The reaction of pregnant ewes to inoculation with mucosal disease virus of bovine origin. Journal of Comparative Pathology 85, 241-251.

Sopp, P., Hooper, L. B., Clarke, M. C., Howard, C. J., Brownlie, J. (1994) Dectection of bovine viral diarrhoea virus p80 protein in subpopulations of bovine leukocytes. Journal of General Virology 75, 1189-1194.

Spencer, T.E. and Bazer, F.W. (2004) Conceptus signals for establishment and maintenance of pregnancy. Reproductive Biology and Endocrinology 2, 49.

Spencer, T.E., Bazer, F. W. (1996) Ovine interferon tau suppresses transcription of the estrogen receptor and oxytocin receptor genes in the ovine endometrium. Endocrinology 137(3), 1144-1147.

Swasdipan, S., McGowan, M., Phillips, N. and Bielefeldt-Ohmann, H. (2002) Pathogenesis of transplacental virus infection: pestivirus replication in the placenta and fetus following respiratory infection. Microbial Pathogenesis 32(2), 49-60.

Takayanagi, H., Sato, K., Takaoka, A., Taniguchi, T. (2005) Interplay between interferon and other ctokin systems in bone metabolism. Immunology Reviews 208, 181-193.

Thompson, K. (2007) Bones and Joints In: Jubb, Kennedy and Palmer's Pathology of Domestic Animals. Saunders Elsevier Philidelphia ed Maxie, M.G. 1(5th ed.), 66-67.

Thompson, R.G., Savan, M. (1963) Studies on virus diarrhea and mucosal disease of cattle. Canadian Journal of Compative Medicine and Veterinary Science 27(9), 207-214.

Tran, P.T., Bender, M. A. (1960) Factor affecting survival of mouse bone marrow cells during freezing and thawing in glycerol. Journal of Applied Physiology 15(5), 939-942.

Tsuboi, T., Osawa, T., Kimura, K., Kubo, M. and Haritani, M. (2011) Experimental infection of early pregnant cows with bovine viral diarrhea virus: transmission of virus to the reproductive tract and conceptus. Research in Veterinary Science 90(1), 174-8.

Turner, C.H. and Burr, D.B. (1993) Basic biomechanical measurements of bone: A tutorial. Bone 14(4), 595-608.

Underdahl, N.R., Grace, O. D., Hoerlein, A. B. (1957) Cultivation in tissue-culture of cytopathogenic agent from bovine mucosal disease. Proceedings of the Society of Experimental Biology and Medicine 94(795-797).

Valle, P.S., Skjerve, E., Martin, S.W., Larssen, R.B., Osteras, O. and Nyberg, O. (2005) Ten years of bovine virus diarrhoea virus (BVDV) control in Norway: a cost-benefit analysis. Preventive Veterinary Medicine 72(1-2), 189-207; discussion 215-9.

Van Campen, H., Vorpahl, P., Huzurbazar, S., Edwards, J. and Cavender, J. (2000) A case report: evidence for type 2 bovine viral diarrhea virus (BVDV)-associated disease in beef herds vaccinated with a modified-live type 1 BVDV vaccine. Journal of Veterinary Diagnostic Investigation 12(3), 263-5.

van Lenthe, G.H., Voide, R., Boyd, S.K. and Müller, R. (2008) Tissue modulus calculated from beam theory is biased by bone size and geometry: Implications for the use of three-point bending tests to determine bone tissue modulus. Bone 43(4), 717-723.

Wang, Y. and Leung, F.C.C. (2004) An evaluation of new criteria for CpG islands in the human genome as gene markers. Bioinformatics 20(7), 1170-1177.

Webb, B.T., Norrdin, R.W., Smirnova, N.P., Van Campen, H., Weiner, C.M., Antoniazzi, A.Q., Bielefeldt-Ohmann, H. and Hansen, T.R. (2012) Bovine viral diarrhea virus cyclically impairs long bone trabecular modeling in experimental persistently infected fetuses. Veterinary Pathology DOI: 10.1177/0300985812436746.

Weiner, C.M., Smirnova, N.P., Webb, B.T., Van Campen, H. and Hansen, T.R. (2012) Interferon stimulated genes, CXCR4 and immune cell responses in peripheral blood mononuclear cells infected with bovine viral diarrhea virus. Research in Veterinary Science DOI: 10.1016/j.rvsc.2012.01.011.

Welsh, M.D., Adair, B.M. and Foster, J.C. (1995) Effect of BVD virus infection on alveolar macrophage functions. Veterinary Immunology Immunopathology 46(3–4), 195-210.

Westwater, J.W. (1949) Flexural Testing of Plastic Materials. Proceeding of the American Society of Testing Materials 49, 1092-1118.

Whitmore, H.L., Zemjanis, R., Olson, J. (1981) Effect of bovine viral diarrhea virus on conception in cattle. Journal of the American Veterinary Medical Asssociation 178, 1065-1067.

Williams, H.J. and Carey, L.S. (1966) Rubella embryopathy. Roentgenologic features. American Journal of Roentgenology, Radium Therapy, and Nuclear Medicine 97(1), 92-9.

Yoneyama, M., Kikuchi, M., Natsukawa, T., Shinobu, N., Imaizumi, T., Miyagishi, M., Taira, K., Akira, S. and Fujita, T. (2004) The RNA helicase RIG-I has an essential function in double-stranded RNA-induced innate antiviral responses. Nature Immunology 5(7), 730-7.

Zdravkovic, M., Knudsen, H.J., Liu, X., Hager, H., Zachar, V., Aboagye-Mathiesen, G. and Ebbesen, P. (1997) High interferon alpha levels in placenta, maternal, and cord blood suggest a protective effect against

intrauterine herpes simplex virus infection. Journal of Medical Virology 51(3), 210-3.

Zhang, G., Aldridge, S., Clarke, M.C. and McCauley, J.W. (1996) Cell death induced by cytopathic bovine viral diarrhoea virus is mediated by apoptosis. Journal of General Virology 77(8), 1677-1681.

APPENDIX I

FETAL GROWTH

Introduction

A previous experimental infection documented generalized growth restriction in day 190 fetuses PI with BVDV (Smirnova et al., 2008). To this end, fetal size, weight, select organ weight and long bone size were measured at each collection time to determine the temporal nature and scope of growth and developmental impairment in PI fetuses.

Materials and Methods

On each day of collection (Days of gestation 82, 89, 97, 192, 245) crown-rump length, heart girth, body weight, liver weight, adrenal and thyroid/parathyroid weight were determined. Ponderal Index as calculated using the following formula: Weight/Crown-Rump length^3) x 100 (Rohrer, 1921). Skeletal growth parameters are presented in Table 2 (CHAPTER II), Table 5 (CHAPTER III), and Table 10 (APPENDIX II)

Results

There were no differences between PI and Control fetal growth parameters on any day of collection.

Discussion

PI fetuses in this study were not growth restricted nor did they have impaired organ development that manifest as altered organ weights. The reason why PI did not lead to growth restriction similar to the previous study (Smirnova et al., 2008) is unclear. PI fetuses may have been more mildly affected than those of the previous as marked of femoral cortical thickening, which was identified in PI fetuses in the previous study (Smirnova et al., 2008), was not seen in all PI fetuses studied herein. Other potential confounding factors include unequal sex distribution between PI and Control groups. The use of sexed semen in future experiments may be of benefit in eliminating the effect of sex.

Table 9. General growth parameters of PI and Control fetuses (Mean ± standard deviation)

Gestational age (days)	Infection status	Number/Sex	Crown-Rump length (cm)	Heart Girth (cm)	Body weight (kg)	Rohrers Ponderal Index[a]
82	Control	4/Male	14.8 ± 0.7	10.7 ± 0.5	0.12 ± 0.01	3.86 ± 0.46
82	PI	3/Male, 1/Female	14.6 ± 0.5	10.1 ± 0.2	0.11 ± 0.01	3.58 ± 0.55
89	Control	4/Male	17.3 ± 0.5	12.2 ± 0.4	0.19 ± 0.02	3.70 ± 0.18
89	PI	2/Male, 1/Female	15.8 ± 0.4	11.7 ± 0.5	0.17 ± 0.02	4.22 ± 0.20
97	Control	4/Female	20.3 ± 0.7	14.0 ± 0.7	0.30 ± 0.03	3.57 ± 0.21
97	PI	3/Male, 1/Female	21.3 ± 1.0	14.6 ± 0.9	0.34 ± 0.06	3.51 ± 0.24
192	Control	3/Male, 4/Female	64.6 ± 3.5	44.4 ± 1.5	9.04 ± 0.76	3.39 ± 0.55
192	PI	2/Male, 5/Female	63.8 ± 1.7	42.8 ± 1.9	8.15 ± 0.99	3.13 ± 0.24
245	Control	2/Male, 2/Female	90.3 ± 1.0	63.5 ± 1.3	25.34 ± 0.40	3.45 ± 0.16
245	PI	3/Male	89.7 ± 2.3	61.7 ± 1.2	24.83 ± 1.80	3.47 ± 0.54

Table 9. cont.

Gestational age (days)	Infection status	Liver weight (g)	Adrenal weight (mg)	Thyroid/Parathyroid weight (mg)
82	Control	4.37 ± 1.58	77 ± 3	71 ± 2
82	PI	4.07 ± 0.15	72 ± 2	70 ± 3
89	Control	8.23 ± 1.48	95 ± 17	80 ± 12
89	PI	7.27 ± 0.82	104 ± 14	81 ± 16
97	Control	11.10 ± 1.12	124 ± 43	129 ± 23
97	PI	13.99 ± 1.59	139 ± 9	158 ± 19
192	Control	267.14 ± 44.24	1131 ±295	3470 ± 498
192	PI	260.71 ± 57.33	988 ± 260	3570 ± 426
245	Control	542.50 ± 15.00	2296 ± 380	8997 ± 2103
245	PI	533.34 ± 57.74	2099 ± 242	8559 ± 1915

[a] equal to (Weight/Crown-Rump length^3) x 100 (Rohrer, 1921).

APPENDIX II

RIB MORPHOMETRY

Introduction

Impaired bone resorption would most severely affect those individual bones having the highest rates of growth or most extensive osseous drift. Rib growth occurs by both endochondral ossification and intramembranous ossification. Endochondral ossification is responsible for the majority of longitudinal growth, which primarily occurs in the physis at the costochondral junction. The bone that is formed by this process is woven bone, which is deposited on calcified cartilage cores (primary bone). During rib growth, in order to accommodate the growth of thoracic cavity organs and outward drift, primary bone must be resorbed on the periosteal surface of the medial cortex and the endocortical surface of the lateral cortex. Meanwhile bone formed by intramembranous ossification, is deposited on the endocortical surface of the medial cortex and the periosteal surface of the lateral cortex. Due to impaired bone resorption secondary to reduced osteoclast numbers (Webb et al., 2012) in PI fetuses it was hypothesized that ribs from PI fetuses would have greater proportions of primary bone as well as cartilage core volumes and these proportion may differ between the medial and lateral cortices if osseous drift was significantly affected.

Material and Methods

Ribs from Day 192 fetuses were selected based on the increased number of fetuses and the greater severity of metaphyseal lesion than other collection days. The entire right 8th rib was collected at fetal necropsy and measured from the head to the costochondral junction (straight line). Based on these measurements, precise mid-rib cross-sections were cut with a band saw and decalcified as previously described (Webb et al., 2012). Medial and lateral cortical thicknesses (width, mm), medial and lateral bone volume (BV/TV, %), bone volume of original woven bone (primary bone) (1° BV, %), and cartilage core volume (Cg.V/BV, %) were determined.

Results

The results of the morphometry appear in Table 10. Both the medial and lateral rib cortices from PI fetuses had higher Cg.V than Controls. All other parameters assessed did not differ between Control and PI fetuses although overall length of PI ribs tended to be less than controls but was not statistically significant.

Discussion

Collectively, increased Cg.V in the face of similar1° BV suggests that PI with BVDV primarily affected rib growth through impaired modeling of primary spongiosa during initial endochondral ossification rather than affecting the modeling during osseous drift in which case 1° BV would be expected to be

Table 10. Morphometric analysis of 8th rib cross sections from day 192 PI and Control fetuses. (Mean ± standard deviation)

Infection Status	Length (mm)	Medial Cortex				Lateral Cortex			
		Width (mm)	BV (%)	Cg.V (%)	1°BV (%)	Width (mm)	BV (%)	Cg.V (%)	1° BV (%)
Control	101 ± 2.9	0.59 ± 0.12	94.9 ± 1.3	1.45 ± 0.5	13.5 ± 0.8	0.71 ± 0.09	87.7 ± 8.4	0.3 ± 0.3	15.4 ± 3.6
PI	97 ± 2.7[a]	0.55 ± 0.13	91.2 ± 4.2	2.6 ± 0.7[b]	12.3 ± 5.7	0.71 ± 0.12	84.6 ± 5.0	3.9 ± 1.6[b]	17.5 ± 3.7

[a] Tendency for difference from Control ($P < 0.07$)

[b] Difference from Control ($P < 0.5$)

increased. The most likely reason why osseous drift was not affected in the PI fetuses might be impaired bone formation, which was documented in both the tibia and femur (CHAPTER II). Thus, when bone formation and resorptive processes are both impaired proportionately no net changes in bone composition would be expected during osseous drift.

APPENDIX III

FETAL BONE MARROW FLOW CYTOMETRY

Introduction

This experiment was performed to test the hypothesis that PI with BVDV results in decreased numbers of CD14 positive cells (osteoclast-macrophage precursors) within the bone marrow.

Materials and Methods

Bone marrow cells were isolated from the marrow cavity of fetal long bones by flushing with α-MEM media to dislodge the cells. Cell viability was assessed prior to immunostaining with trypan blue. The cells were then strained to remove any bone spicules and other tissue debris. Red blood cells were lysed with a solution of NH_4Cl (0.15M), $KHCO_3$ (10mM), Na_2EDTA (0.1mM) and cells were removed by centrifugation at 1,200rmp for 10 minutes. The cells were then incubated with antibody for 30 minutes at room temperature followed by rinsing twice with phosphate buffered saline (pH 7.4). Cells were analyzed on a CyAn flow cytometer (Beckman-Coulter, Miami, FL)

Table 11. Antibodies used for bone marrow flow cytometry.

Antibody[a]	Cell specificity	Clone	Working dilution
Anti-CD4- FITC conjugated	T cells, erythroid precursors	1658	1:100
Anti-CD8- FITC conjugated	T cells	837F	1:100
Anti-CD14- FITC conjugated	Monocyte/ macrophage	2678F	1:100
Anti-CD21- FITC conjugated	B cells	1424F	1:100
Anti-CD45- APC conjugated	All leukocyte	2220	1:100
Anti-WC-1- FITC conjugated	Gamma/ delta T cells	838F	1:100

[a] All antibodies from ABD-serotec, Raleigh, NC.

Results

The results of flow cytometry staining appear in Table 12. Overall a small percentage of cells stained double positive for the cell markers used. There were significantly reduced numbers of $CD4^{+}/CD45^{-}$ cells in PI bone marrow when compared to controls. There were no differences in the percentage of other cell populations between PI and Control animals.

Table 12. Flow cytometry of bone marrow from day 192 PI and Control fetuses. (Mean ± standard deviation)

Infection Status	Percent of Histogram				
	CD4+/CD45+	CD8+/CD45+	CD14+/CD45+	CD21+/CD45+	WC-1+/CD45+
Control	0.70 ± 0.39	0.68 ± 0.41	0.84 ± 0.83	0.43 ± 0.16	0.54 ± 0.42
PI	0.78 ± 0.38	0.77 ± 0.39	0.81 ± 0.64	0.44 ± 0.41	0.35 ± 0.18
	Percent of Histogram				
	CD4+/CD45-	CD8+/CD45-	CD14+/CD45-	CD21+/CD45-	WC-1+/CD45-
Control	49.5 ± 4.8	47.7 ± 8.0	12.3 ± 2.7	14.3 ± 13.7	1.8 ± 1.3
PI	35.3 ± 5.8[a]	31.8 ± 5.2	9.7 ± 2.6	6.6 ± 6.5	4.7 ± 5.3

[a] Difference from Control ($P < 0.05$)

Discussion

Two significant limitations of this experiment include the low number of viable cells at the time of cytometry and the small percentage of cells that stained positively for the markers. The results did not support the hypothesis that CD14+/CD45+ cells would be present at lower numbers in the PI bone marrow. It is however difficult to draw definitive conclusion on this finding because the percentage of cells is so low and near the limit of detection of this assay. The considerable percentage of CD4+/CD45– cells, which were decreased in PI bone marrow, likely reflect staining of erythroid precursor cells as they have been shown to have this immunophenotype in human bone marrow (Cleveland and Liu, 1996). This may suggest that erythropoeisis is impaired in PI fetuses. The concurrent high numbers of CD8+/CD45- cells is assumed to be associated with nonspecific binding of CD8 antibody.

APPENDIX IV.

IN VITRO OSTEOCLAST ASSAYS

Introduction

Osteoclast numbers tended to be reduced in day 97 PI fetal tibia and were reduced in day 192 PI fetal tibia which lead to abnormal trabecular modeling as previously described in Chapter II (Webb et al., 2012). The absence of histologic features of necrosis or apoptosis within mature osteoclasts of days 82, 89, 97 and 192 fetuses suggests that osteoclast proliferation and/or differentiation may be affected by PI. However, minor alteration in osteoclast function or survival could significantly affect overall osteoclastic resorption, especially in states of decreased osteoclast density as described above. Reduced numbers of osteoclasts could potentially result from either impaired proliferation of precursor cells or impaired differentiation of precursor cells into mature osteoclast. This series of experiments was conducted to assess osteoclast differentiation and resorptive functions in PI fetuses and test the hypothesis that there is a soluble factor, present in PI fetal serum, which impairs osteoclast precursor proliferation or differentiation. Functional assays were also performed to assess for functional impairment that was not apparent in histologic sections.

Materials and Methods

Experiment I

Bone marrow cells were collected by the following procedures: The marrow cavity of fetal long bones was flushed with α-MEM media to dislodge cells. The cells were then strained to remove bone spicules and other tissue debris. The cells were counted, viability determined by trypan blue staining, and frozen in α-MEM media with 20% FBS and 20% DMSO as previously described (Mengeling, 1988). The cells were thawed quickly in α-MEM media with 15% glycerol which has been shown to be optimal for thawing bone marrow cells (Tran, 1960). PI and Control fetal bone marrow cells were cultured at 4 x 10^5 cells/well in 24 well plates in Phenol-free α-MEM media with 10% FBS (harvested from either PI or control fetuses, virus-free) and 2 mM L-glutamine for 24, 48, and 72 hours.

Experiment II

Differentiation Assay

Peripheral blood mononuclear cells (PBMC) from a yearling angus bull calf were isolated as previously described (Weiner et al., 2012). In summary this method uses Histopaque 1077® (Sigma Aldrich, St Luis, MO) solution to separate PMBC from red blood cells and granulocytes based on cellular density. The isolated PBMC were counted and viability determined. Cells were plated on 200μm thick dentine discs in 24 well plates (5 x 10^5 cells/well containing Phenol-free α-MEM media with 10% FBS, harvested from either PI or control fetuses

(virus-free), 25 mM Hepes, 1% solution of penicillin, gentamicin and Amphotericin B and 35 nM of recombinant human receptor activator for nuclear Kappa B ligand (RANKL) and 50 nM of recombinant human macrophage colony stimulating factor (M-CSF). Fetal serum was heat inactivated at 56 degrees Celsius for 30 minutes. All media was sterilized by filtration (0.2 μm pore size). The dentine discs were produced by embedding bovine incisors in an epoxy resin (Sample- Kwick®, Beuhler, Ltd Lake Bluff, IL, USA) and cutting cross section on an diamond blade saw (Isomet saw®, Beuhler, Ltd Lake Bluff, IL, USA) followed by hand grinding to 100 μm thickness. The discs were sterilized in 70% ethanol. After two hours of culture non-adherent cells (lymphocytes) were removed and media was replaced. Media was replaced every three days thereafter. Cultures were terminated at day 0 (2 hours after initial plating), day 4, and day 8 at which time the media was removed and discs were fixed with citrate buffered acetone and stained with a commercial enzyme histochemical kit for Tartrate-resistant Acid Phosphatase (TRAP) (Sigma Aldrich, St Luis, MO).

Pit resorption assay

TRAP staining discs were sonicated for 30 seconds in DI water and stained with a 0.1% aqueous solution of toluidine blue with sodium borate for 30 seconds to visualize resorption pits.

Results

Experiment I

The viability of previously frozen bone marrow cells was poor (less than 10% viable cells) so an alternative approach detailed in Experiment II was employed.

Experiment II

Representative photomicrographs of TRAP stained dentine discs are presented in Figure 17. TRAP positive osteoclast-like cells were first observed after 3 days of culture. Extending the culture length out to 14 days did not result in significant increases in TRAP positive osteoclast-like cell numbers, rather after day 8 of culture osteoclast-like cells increased in size and gained additional nuclei (Qualitative evaluation). There was no discernible difference between cultures treated with PI serum versus Control serum and a high degree of intra/inter-assay variation was noticed.

Conclusions

The most significant pitfall in this assay was the extreme intra-assay variation in the number of TRAP positive osteoclasts-like cell numbers such that meaningful data resultant from quantitating these cells could not be produced. A potential reason for this may be related to the scarcity of permissible cells in peripheral blood. While the percentage of PBMC capable of efficiently differentiating into osteoclasts in cattle are unknown such cells are exceedingly

rare (< 0.01%) in peripheral blood of humans (Ritchlin et al., 2003) and even when plating 500,000 cells per well the exact number of precursor cells was unknown. This type of variation appears to be a common problem when using PBMC rather than selectively enriched cell populations, such as CD14+ cells, for differentiation assays (Nicholson, 2000). Utilizing fluorescent antibody cell sorting to produce an enriched population of osteoclast precursors would likely lend more consistent results. Although the pit resorption assay was standardized in this series of experiments it was not completed due to the poor results obtained from the differentiation assays.

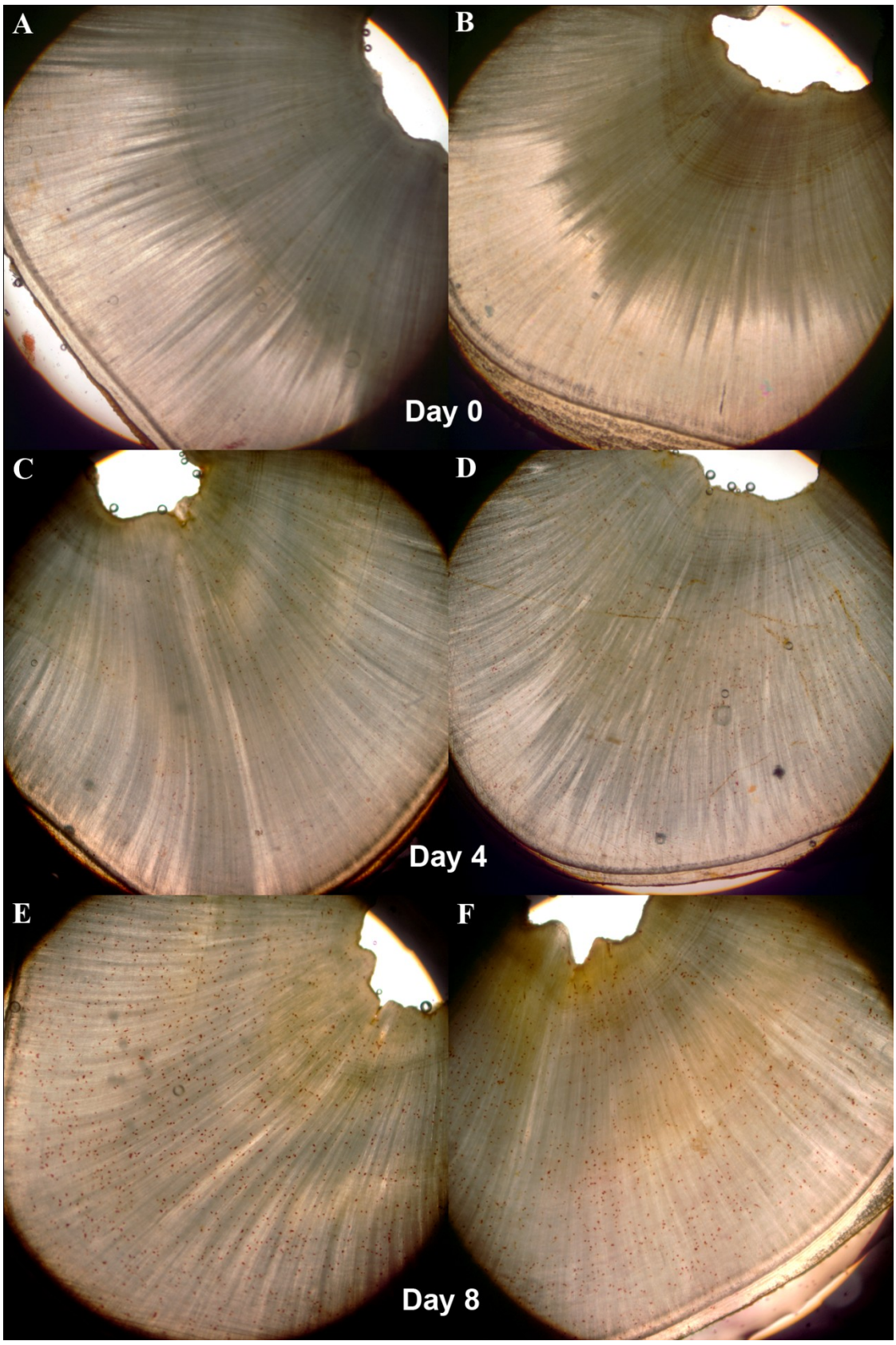
A
B
Day 0
C
D
Day 4
E
F
Day 8

Figure 17. Photomicrographs of dentine discs stained for TRAP from days 0, 4, and 8 osteoclast-like cell cultures. Numerous TRAP positive osteoclast-like cells can be seen (pinpoint red dots) on the surface of both Control (C and E) and PI (D and F) discs. Osteoclast-like cells are noticeably larger in cultures from day 8 (E and F). Disc A and B are devoid of osteoclast-like cells. Original magnification 20X, unstained 100 μm thick sections.

APPENDIX V.

FETAL BONE MARROW GENE EXPRESSION

Introduction

The mRNA expression of molecular mediators of osteoclast differentiation were evaluated by qRT-PCR in bone marrow. mRNA expression of receptor/ligands, intermediate mediators in signal transduction pathways and the transcriptional targets of such pathways were evaluated. It was hypothesized that if osteoclast differentiation was impaired in PI fetuses there would be down regulation of mRNA transcripts of either receptor/ligands, transcription factors activated by these pathways, transcriptional targets of these pathways or up regulation of negative regulators (inhibitors).

Materials and Methods

Spicules of distal femur metaphyseal bone marrow were obtained at fetal necropsy, placed in Tri-Reagent (Sigma Aldrich, St Louis, MO), and snap frozen in liquid nitrogen until analysis. Total bone marrow mRNA was isolated with Tri-Reagent and purified with RNeasy MinElute Cleanup Kit (Quiagen, Valencia, CA) as previously described (Smirnova et al., 2008). Target genes and corresponding primer sequences appear in Table 13. Primer sequences for GAPDH, RIG-I, ISG15, IFN-α and IFN-β appear in Table 8 (CHAPTER IV.).

Table 13. qRT-PCR primer sequences

Target Gene	Accession number	Primer sequence
Calcitonin Receptor	NM_001101107.1	F: TTTCACCCCTGAGAAAATGC R: AACACGCATGAAAATCACCA
TNFSF11 (RANKL)	NM_001205770.1	F: GCTCCATGAAAACACGGATT R: CTGCACAGCTGCTTGAAAAG
FOSL1	NM_001205985.1	F: TTTCCCTGCTCATTTGATCC R: GTCTTGTCTGGAGGGATGGA
CSF-1 Receptor	NM_001075403.2	F: GACTGCGTCTACACCGTTCA R: ACCAGGATACCAGGGTAGGG
TNFARSF11A (RANK)	XM_002697844.1	F: GCTGCTCTTCATGTCTGTGG R: ACCCAGTGCCACAAATTAGC
IL-1R1	NM_001206735	F: GCTGAAGTGGAGGATTCAGG R: TAGGCTCATGCTGCACAAAC
IL-1R2	NM_001046210.1	F: CATGACGTATGCCCACAAAG R: GGGGAGAGATGATCACAGGA
MITF	NM_001001150.1	F: TGAGTCGGATCATCAAGCAG R: TGTGAGATCCAGGGTTGTTG
NFAT1c	NM_001166615.1	F: CTTTCTGCAGGACTCCAAGG R: TCGGCTTACACAGGTCTCCT
c-fos	AY322482.1	F: CGTCTTCCTTCGTCTTCACC R: AGTCAGAGGAAGGCTCGTTG

TRAF6	NM_001034661.1	F: AGATTGGCAACTTTGGGATG R: ACAGGTTGTAGCCGGGTTTG
IL-1α	NM_174092.1	F: GGATTCTCCAGGCAAGAACA R: GAGTCGGACATGACTGAGCA
IL-1β	NM_174093.1	F: CAGTGCCTACGCACATGTCT R: GGAGGACGTTTCGAAGATGA
CSF-1	NM_174026.1	F: AGAGCTTTGAGTCGCCAGAG R: ACGTCTTCCATCCCAGTGAC
TANK	NM_001192264.1	F: GAGACTGTGTGCCAGGATCA R: TATGGGGTCAATTCCCTGAA
TNFRSF11B (OPG)	NM_001098056.1	F: AACTGGCTCAGTGTCCTGGT R: CTCGTGAGTTGTGTCGCTGT
CXCR4	NM_174301.2	F: AAGGCTCAGAAGCGCAAG R: GAGTCGATGCTGATCCCAAT
CD14	NM_174008.1	F: CTCAGCGTGCTTGATCTCAG R: AAGGGATTTCCGTCCAGAGT

Results

Genes found to be differentially expressed in PI fetal bone marrow appear in Table 14. The most significant finding of this experiment was down-regulation of both c-fos and its transcriptional target in osteoclast precursor cells, Fosl1. Up-regulation of the ISGs, ISG15 and RIG-I and CD14, which may also be

stimulated by interferon, were identified. CXCR4 was downregulated in PI bone marrow as well but the significance of this, if any, in context of decreased osteoclastogenesis in PI is uncertain as this factor has been shown to negatively regulated osteoclastogenesis (Hirbe et al., 2007).

Table 14. Differential expression of genes associated with osteoclast differentiation in the bone marrow of day 192 PI.[a]

Gene	mRNA fold change versus control	Gene functions
c-fos	- 2.6	Transcription factor activated by RANK/RANKL pathway
Fosl1	- 2.0	Transcriptional Target of c-fos in osteoclast precursors
CXCR4	-1.7	Chemotaxis and other immune functions as reviewed in (Smirnova et al., 2009)
RIG-I	+ 11.7	Cytosolic RNA sensor (ISG)
ISG15	+ 152.9	Anti-viral activity
CD14	+ 3.3	LPS receptor expressed on monocytes/osteoclast precursor cells (ISG)

[a] $P < 0.05$

Conclusion

Down-regulation of the transcriptional target of c-fos, FosL1, suggests that either levels of diphosphorylated (activated) c-fos are decreased or Fosl1 transcription is being depressed via another mechanism. Western blot analysis of bone marrow protein extracts for diphosphorylated c-fos and Fosl1 are necessary to determine whether reduced levels of activated transcription factor are truly present and having an effect (decreased Fosl1 protein) on the protein level. These experiment are currently underway. However, regardless of the outcome of these planned experiments it will remain to be determined whether these changes are physiologically relevant. A cause and effect relationship between decreases in c-fos and Fosl1 and impaired osteoclast differentiation, in PI fetuses, would need additional investigation to be firmly established.

APPENDIX VI.

FETAL SPLEEN AND BONE MARROW DNA METHYLATION

Introduction

This series of experiments were undertaken in an attempt to gain understanding of two phenomena that occur following transplacental infections with BVDV. As described in CHAPTER IV, PI fetuses appear to be unable to induce the expression IFN-α or IFN-β in response to PI but are able to respond to IFN as evidenced by a profound type I IFN response (ISG up regulation). In contrast, cotyledons from PI fetuses appear to be able to induce both IFN-α or IFN-β. BVDV as well as other pestiviruses, such as Classical Swine Fever Virus, have been shown to directly modulate the activity of interferon regulatory factors 3 and 7 (Baigent et al., 2004; Baigent et al., 2002; Schweizer et al., 2006) and thus ablate type I IFN production, this mechanism is insufficient to explain the difference in type I IFN production as virus is present in similar amounts in both the cotyledons and fetal tissues. Thus it was hypothesized that type I IFN production may be silenced by epigenetic mechanisms in the fetus but not the placenta. The second phenomenon that occurs following transplacental infection with BVDV is increased susceptibility to pathogens in postnatal life. Increased susceptibility to pathogens is well documented in PI cattle but epidemiologic evidence suggests that a similar increase in susceptibility to pathogens occurs in fetuses transiently infected with BVDV during late gestation (Muñoz-Zanzi et al.,

2004). This suggests that the presence of the virus cannot completely account for immunosuppression and increased susceptibility to pathogens; rather transplacental infection during a critical period may result in developmental immune deficits. Epigenetic mechanisms controlling gene expression include DNA methylation, DNA hydroxymethylation, histone deacetylation, and micro-RNA. It was hypothesized that transplacental infection results in epigenetic modification of the fetal genome and the epigenetic modification may result in silencing of genes essential for normal immune function.

Materials and Methods

Experiment I - Global DNA methylation

Genomic DNA was extracted from days 82, 89, 97, 192, and 245 PI and Control fetuses day 190 PI, TI, and control fetal spleen using GeneElute, mammalian genomic miniprep kit (Sigma Aldrich, St. Louis, MO). The latter day 190 spleen samples were derived from a previous study(Smirnova et al., 2008) using the same viral strain with maternal inoculation on day 75 (PI) and day 175 (TI). DNA was evaluated for quality and quantitated on a Nanodrop spectrophometer (Thermo Scientific, Wilmington, DE). Total genomic 5-methylcytosine and 5-hydroxymethylcytosine content were determined by a commercial colorimetric ELISA, MethylFlash (Epigentek, Farmingdale, NY).

Experiment II – Locus specific methylation

Genes downregulated (CXCR4, c-fos), within the bone marrow of day 192 PI fetuses, which were identified in previous experiments in addition to genes

which were expected to be up regulated but were not (IFN-α, IFN-β) were evaluated for the presence of cytosine paired to guanine (CpG) islands within their promotors regions. Promotor sequences were identified using Ensembl Genome Browser (www.ensembl.org) and a 3000 base pair region upstream from the start codon was evaluated for the presence of CpG islands by using the criteria previously described (Wang and Leung, 2004). Genes found to contain CpG islands within their promotors and meeting the published criteria were evaluated by Methylation Sensitive Endonuclease Restriction–PCR (MSRE-PCR) to determine the extent of 5-methycytosine modifications at specific loci. Primers were designed to amplify a region containing no less than three restriction sites. Primer sequences appear in Table 15. MSRE-PCR was performed with OneStep qMethyl kit (Zymo Research, Irvine, CA). This kit contains a mixture of MSREs and is a real-time PCR assay. The assay is performed by comparing the differences in amplification (delta Ct) between two reactions; a reference reaction which does not containing MSREs and a test reaction that contains MSREs. If the locus of interested is unmethylated, digestion occurs, little product is amplified in the PCR reaction. In contrast, if the locus is methylated there is robust amplification of the product.

Results

Experiment I

The results appear in Figures 18,19 and 20. There was no difference in DNA hydroxymethylation content between PI and Control fetuses at days 97, 192

and 245 of gestation (data not shown).

Table 15. Primer sequences for MSRE-PCR

Target Gene	Ensembl number	Primer sequence
c-fos	ENSBTAG00000004322	F: CAGGGACCTGTGTCTCTGC R: CCTAGCCTCCTGCTCAGATG
CXCR4	ENSBTAG00000001060	F: TTTCCTGGGTCAGCAATACC R: CAACTTGGGAAAGCAGGATG

A

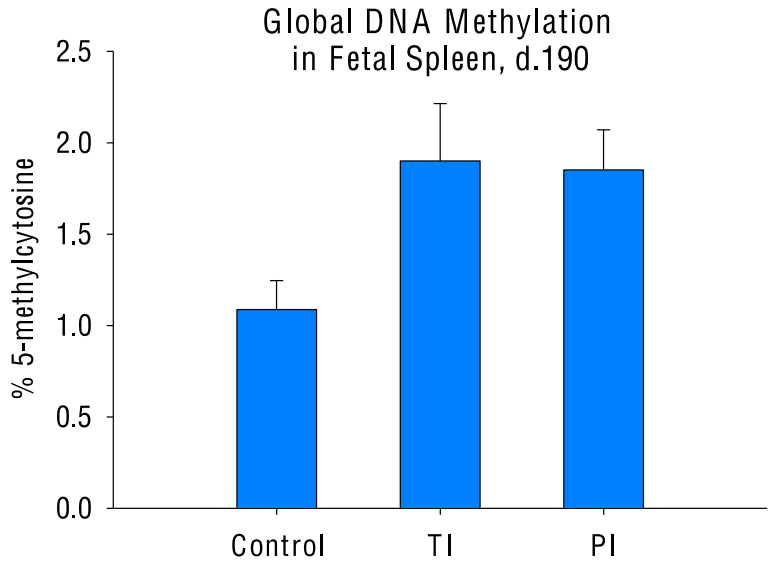

B

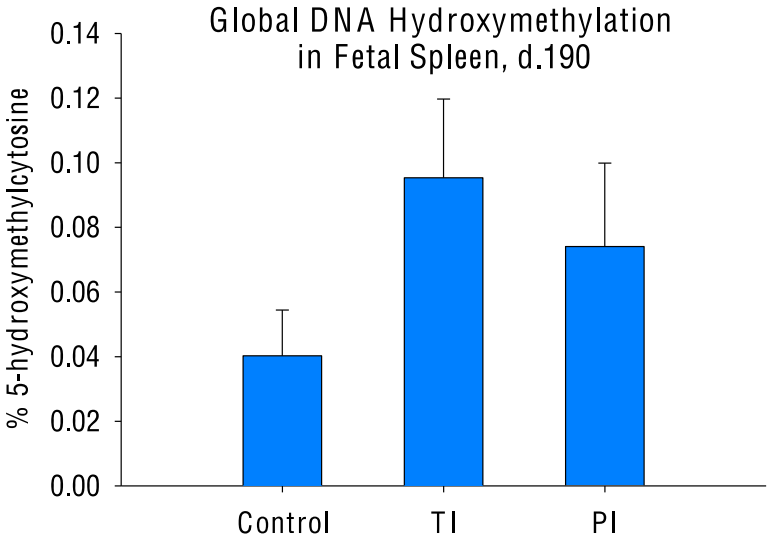

Figure 18. Global DNA 5-methylcytosine and 5-hydroxymethylcytosine content from spleen of Day 190 PI, TI (transiently infected), and Control fetuses. (A) Global DNA methylation is increased in PI fetuses ($P < 0.05$) and tends to be increased in TI fetuses ($P < 0.06$) when compared to controls. (B) Global hydroxymethylation is increased in TI

fetuses (P < 0.05.)

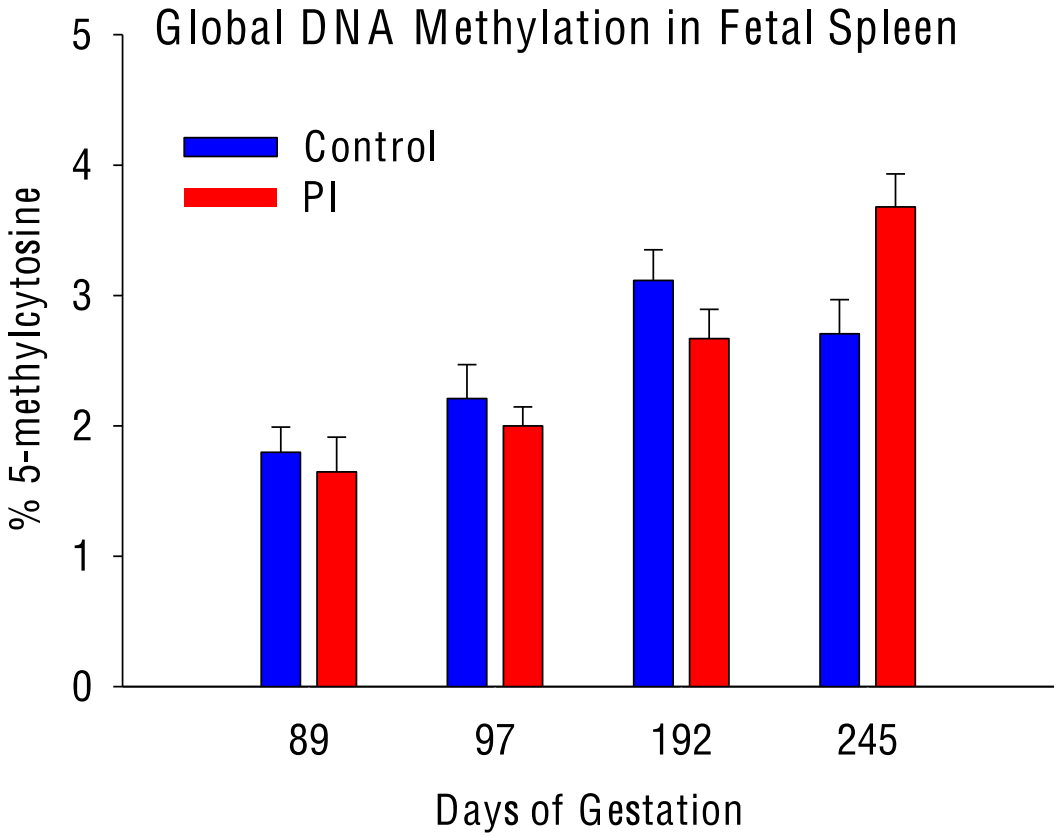

Figure 19. Global DNA methylation in PI and Control fetal spleens from days 89, 97, 192, and 245 of gestation. There is a greater concentration of 5-methylcytosine in PI fetuses on Day 245 when compared to Controls (P < 0.05)

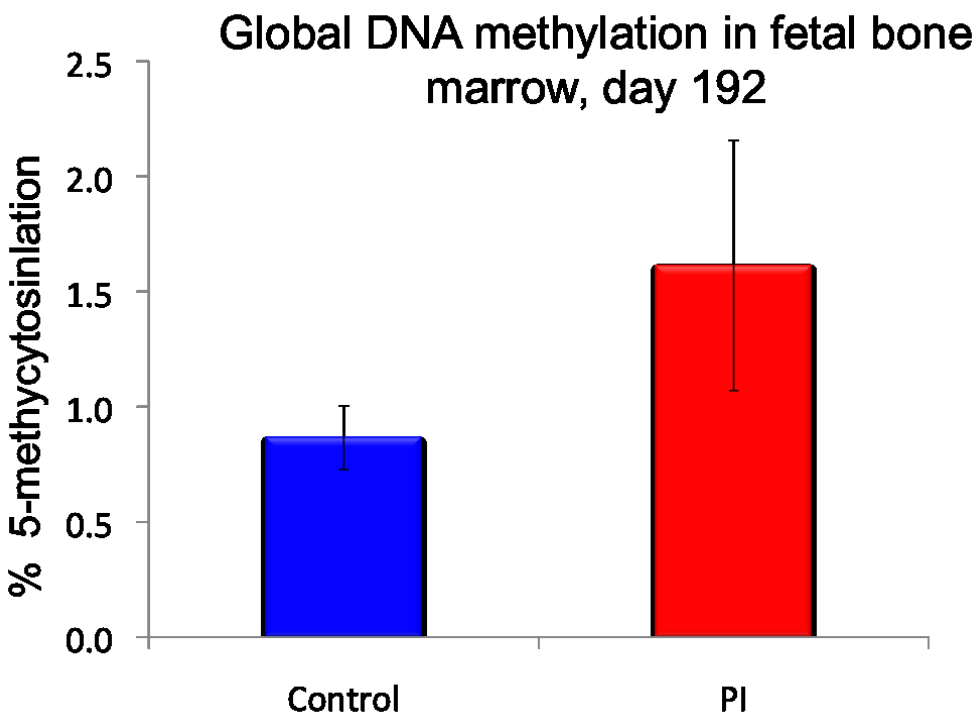

Figure 20. Global DNA methylation of fetal bone marrow from day 192 of gestation. There is no difference between 5-methylcytosine concentration in PI and Control fetuses.

Experiment II

The results of locus specific DNA methylation analysis are presented in Table 16. There were no differences between PI and Control fetuses on Day 190 in the percent of DNA methylation within the CXCR4 and c-fos promotors. CXCR4 appears to be hypomethylated when compared to c-fos, suggesting that transcription of the latter gene may be silenced in a majority of bone marrow cells by this mechanism.

Table 16. Percent methylation of CXCR4 and c-fos in bone marrow of day 192 PI and Control fetuses.

Infection status	Percent methylation at locus	
	CXCR4	c-fos
Control	2.8 ± 2.6	86.7 ± 16.7
PI	2.8 ± 1.6	71.4 ± 23.4

Conclusion

In experiment I, PI fetuses on day 190 had global hypermethylation of spleen DNA, which may be associated with either silencing of genes or differences in populations of cells that have different degrees of methylation. Interestingly, TI fetal spleen DNA tended to have a similar degree of global hypermethylation and hyperhydroxymethylation as PI fetal spleen DNA, however, because these fetuses were in the acute stage of BVDV infection, it is difficult to interpret the significance of these findings. It is uncertain why day 192 PI fetuses in current experiment did not mirror the hypermethylation of DNA present in the day 190 PI fetuses from the previous experiment. Rather, hypermethylation of global spleen DNA was not observed in the current experiment until day 245. One potential reason as stated previously in APPENDIX I is that fetuses from the current experiment were less severely affected than those from the previous experiment. Cell lineage specific assessment of DNA methylation would be required to determine the significance, if any, of these findings. Although c-fos

transcription appears to be regulated by DNA methylation, no effect of PI was observed on the degree of methylation suggesting that downregulation of this gene in PI may occur through alternate mechanisms.

LIST OF ABBREVIATIONS

BVDV - bovine viral diarrhea virus;

cp -cytopathic;

dpmi – days post maternal infection;

dsRNA – double-stranded RNA;

IFN - interferon;

IFN-I – type one interferon;

ISG - interferon stimulated gene;

RIGI – retinoic acid inducible gene 1;

MDA5 - melanoma differentiation-associated protein 5;

ncp - noncytopathic;

PAMP – pathogen associated molecular pattern;

PI – persistently infected;

qRT-PCR - Semi-quantitative real time polymerase chain reaction